American Urogynecologic Society Prolapse Consensus Conference Summary Report

Nazema Y. Siddiqui, MD, MHSc,† W. Thomas Gregory, MD,*‡ Victoria L. Handa, MD,*§ John O.L. DeLancey, MD,*‖ Holly E. Richter, MD,*¶ Pamela Moalli, MD, PhD,*,** Matthew D. Barber, MD, MHS,*† Samantha Pulliam, MD,*†† Anthony G. Visco, MD,*† Marianna Alperin, MD,*‡‡ Carlos Medina, MD,*§§ Matthew O. Fraser, PhD,*‖‖ and Catherine S. Bradley, MD, MSCE*¶¶*

Objectives: The 2016 American Urogynecologic Society Prolapse Consensus Conference brought together thought leaders in the field of pelvic organ prolapse (POP). The goal was to identify critical areas of need for future research. This article summarizes the findings.

Methods: Prior to the conference, 5 major focus areas were identified. Focus areas were explored over the 2-day conference. Clinicians, clinical and basic science researchers, and representatives from government agencies, industry, patient advocacy groups, and the public convened to identify the major gaps in knowledge in each of these focus areas.

Results: The 5 major topics were as follows: (1) mechanistic research on pelvic supportive structures and how these are altered with pregnancy, delivery, and aging; (2) novel prostheses or implants that address pathophysiology and provide mechanical support; (3) large-scale community-based research; (4) clinical trials to optimize outcomes after POP surgery; and (5) evidence-based quality measures for POP outcomes. Key recommendations were made for each topic.

Conclusions: Critical gaps in our knowledge were identified. These limit scientific discovery across all 5 topic areas. Further scientific progress would be advanced by (1) developing a standardized group of POP outcomes and quality measures for large trials and community-based research, (2) creating specimen biorepositories that are integrated with robust clinical data, and (3) developing collaborative teams with expertise from a variety of disciplines, convened to tackle our most challenging and complex scientific questions.

Key Words: AUGS, consensus report, prolapse research

(*Female Pelvic Med Reconstr Surg* 2018;00: 00–00)

The American Urogynecologic Society (AUGS) supports the advancement of knowledge regarding all aspects of female pelvic medicine, the dissemination of related scientific discoveries, and the training of health care professionals and researchers in this field. In this spirit, the 2016 AUGS Prolapse Consensus Conference brought together thought leaders in the field, including clinicians, clinical and basic science researchers, and representatives from government agencies, industry, patient advocacy groups, and the public. The goal of the conference was to identify critical areas of need for future research.

Prior to the conference, the AUGS scientific community completed a Web-based survey to identify the highest priority research questions pertaining to pathophysiology and treatments of pelvic organ prolapse (POP). A total of 15 separate items were evaluated using a modified Delphi approach,[1] and ultimately 5 major focus areas were identified:

1. mechanistic research on pelvic supportive structures and how these are altered with pregnancy, delivery, and aging;
2. novel prostheses or implants that address pathophysiology and provide mechanical support;
3. large-scale community-based research;
4. clinical trials to optimize outcomes after POP surgery; and
5. evidence-based quality measures for POP outcomes.

Over a 2-day consensus meeting, these 5 topic areas were explored. The goal was to combine scientific, industry, funding agency, and patient perspectives to identify the major gaps in knowledge in each of these topic areas. Here we summarize the results of this interactive conference.

Mechanistic Research on Pelvic Supportive Structures and How These Are Altered With Pregnancy, Delivery, and Aging

The anatomical failure rate after POP surgery is as high as 25%, even when criterion-standard surgical procedures are used.[2] This suggests great opportunity for improvement; simply comparing existing operations is not likely to substantially advance our treatment of POP. Thus, an improved understanding of the mechanisms responsible for POP (and how they relate to operative failure) is needed. Although several major knowledge gaps were identified at the conference, we focus on 4 important and broadly defined issues that require urgent attention in future studies.

In the last 30 years, scientists have built upon the discoveries of prior generations, which had focused on remarkably detailed anatomic characterization of the female pelvis. In recent decades, scientists have applied new tools including neurophysiology, imaging (ultrasound and magnetic resonance imaging), cell biology, and molecular genetics to study the biology of pelvic connective tissue and muscle. Despite these efforts, we still do not understand the basic mechanisms that lead to the development of POP.

Individual groups of investigators have been using biomechanical principles to compare women with and without POP. However, progress is hindered by the lack of a generally accepted conceptual disease model. In complex biological processes where different structures, tissues, and processes are involved, it is not possible to conduct 1 "experimentum crucis" to determine "the cause" of POP. Rather, the results of many experiments must be reviewed

From the *American Urogynecologic Society, Silver Spring, MD; †Duke University; ‡Oregon Health & Science University, Portland, OR; §Johns Hopkins University, Baltimore, MD; ‖University of Michigan, Ann Arbor, MI; ¶University of Alabama at Birmingham, Birmingham, AL; **Magee-Women's Hospital, University of Pittsburgh, Pittsburgh, PA; ††University of North Carolina; ‡‡University of California San Diego, San Diego, CA; §§University of Miami, Miami, FL; ‖‖Duke University and Durham Veterans Affairs Medical Centers, Durham, NC; and ¶¶University of Iowa, Iowa City, IA.

Reprints: Nazema Y. Siddiqui, MD, MHSc, Duke University Medical Center. E-mail: nazema.siddiqui@duke.edu.

This document was developed by the American Urogynecologic Society Scientific Committee with the assistance of Drs Nazema Y. Siddiqui, W. Thomas Gregory, Victoria L. Handa, John O. L. DeLancey, Holly E. Richter, Pamela Moalli, Matthew Barber, Samantha Pulliam, Anthony G. Visco, Marianna Alperin, Carlos Medina, Matthew O. Fraser, and Catherine S. Bradley.

The authors have declared they have no conflicts of interest.

Copyright © 2018 American Urogynecologic Society. All rights reserved.

DOI: 10.1097/SPV.0000000000000533

Copyright © 2018 Wolters Kluwer Health | Lippincott Williams & Wilkins. Unauthorized reproduction of this article is prohibited.

and reconciled to develop a comprehensive disease model. For POP, there is a need to describe interdependence of load-bearing structures such as levator ani muscles, connective tissue, and nerves because these structures relate to the bony anatomy and to the proposed components of pelvic support. Furthermore, there is a need to understand how expulsive forces are applied and distributed. This gap in our fundamental understanding of the condition will not be overcome without interdisciplinary teamwork, the introduction of new scientific perspectives, and the assimilation of evidence from a variety of fields. A meeting of multidisciplinary researchers with the goal of creating a draft disease model would facilitate overcoming this barrier. Longer-term strategies to facilitate mechanistic research might include convening a group to periodically review emerging data on POP pathophysiology and to iteratively revise the conceptual disease model, similar to systematic review groups, followed by periodic state of the science meetings.

A second issue that hinders progress is a shortage of investigators (such as fellows and postdoctoral trainees) who are fully trained in relevant research tools that are needed to study a complex condition such as POP. Although there has been some gradual improvement, developing mechanisms for attracting, supporting, and educating new investigators who can design, acquire funding for, and conduct needed experiments is of utmost importance.

Third, research into pelvic floor disorders requires an accurate understanding of in vivo pelvic floor anatomy. At present, opportunities or tools to gain a comprehensive understanding of the correct 3-dimensional living human anatomy are limited. Because of this, inaccurate anatomical principles are often used in research and carried forward. Creating opportunities for researchers to gain correct structural information could greatly enhance progress. Long-term solutions could include establishing which teaching tools optimize learning (eg, cadaver, 3-dimensional anatomy programs, serial section review).

Finally, there is a great need to integrate the growing body of basic science knowledge with clinical findings, as new mechanistic insights might lead to clinical trials and novel strategies for treatment of POP. Moreover, insights into why a treatment succeeds in one woman and fails in another could be gained by combining clinical and mechanistic research. Long-term strategies to facilitate such interactions might advance both types of research and improve patient outcomes.

Novel Prostheses or Implants That Address Pathophysiology and Provide Mechanical Support

Aside from pessaries, surgical repair constitutes the main therapeutic approach for POP. Consequent to high failure rates and frequent reoperations associated with native tissue repairs, pelvic surgeons have turned to mesh and graft-augmented procedures in many instances. To date, the most commonly used material for the treatment of POP is synthetic polypropylene mesh. This material was established as a standard for sacrocolpopexy and midurethral sling procedures. Then, despite limited data regarding their safety and efficacy, transvaginal mesh-augmented procedures became rapidly and widely adopted after 2005. This was mainly driven by the need to improve clinical outcomes associated with native tissue surgeries, and a desire to provide less invasive surgical options than mesh sacrocolpopexy via laparotomy. The resultant higher than expected complication rates associated with transvaginal mesh placement subsequently prompted the US Food and Drug Administration[3] to issue public health notifications in 2008 and 2011 and to upgrade these implants from class II to class III medical devices.[4] Despite the uncertainty regarding long-term outcomes of transvaginal mesh procedures, ongoing questions about the complications of this approach, and public perceptions of adverse outcomes, transvaginal mesh for POP remains part of the surgical armamentarium of up to 61% of AUGS members as of 2012.[5] Thus, there is a pressing need to develop safe, durable, and minimally invasive surgical treatment alternatives for women with POP. Novel graft and/or mesh materials that provide mechanical support, while maintaining compatibility with native vaginal tissue, have a high potential to address the aforementioned unmet need.

A major barrier hindering progress is our incomplete understanding of the host tissue mechanical properties that surgeons are trying to replace with mesh and/or grafts. The physiological loading conditions imposed on the pelvic support structures and variability across different phases of life (eg, adolescence, pregnancy, after menopause) are still poorly understood. Thus, the alterations in loading on the pelvic floor that lead to POP remain largely unknown and cannot be extrapolated from orthopedic or general surgery literature. Consequently, when mesh or grafts are developed to provide vaginal support, we are unable to identify the best locations for attachment and to determine how well various anchoring points replicate the physiological load distribution on the pelvic supportive structures. Therefore, an important initial step is to clarify the main mechanical goals of graft-augmented pelvic surgeries. This would allow for more effective collaborations with engineers and basic scientists from other disciplines.

An incomplete understanding of the key features of in vivo host responses to mesh and/or graft materials and how these correlate with clinical outcomes blocks progress. As we move forward with the development of novel materials, we must simultaneously create tools that enable identification of the subset of patients that have an innate ability to regenerate a high-quality supportive connective tissue or muscle. We need clarity on patient-level factors that provide an optimal environment for functional mesh or graft "integration" and which factors differentiate patients who develop mesh or graft-related complications. In addition, we must understand how the host response to mesh or graft materials evolves over time and how it differs from the default response to surgery and implantation of a foreign body. To achieve the above, an infrastructure for the collection of preoperative and postoperative biospecimens from patients undergoing native tissue and mesh and/or graft-augmented POP repairs should be built, along with the appropriate quality control measures and staff to maintain specimens.

Large-Scale Community-Based Research

Over the past 20 years, epidemiologic research has revealed that POP is highly prevalent: more than one-third of adult women demonstrate stage 2 to 4 pelvic organ support, and 13% undergo surgery for POP by age 80 years.[6,7] Longitudinal studies suggest that mild POP does not inevitably progress and may actually regress over time.[8,9] Epidemiologic research has also uncovered some important risk factors for the development of POP, such as age, obesity, and familial predisposition,[10] and has demonstrated the critical influence of vaginal childbirth.[11] However, important questions remain unanswered.

Prevention research is currently limited by our imperfect understanding of who is at greatest risk of developing POP. Further large-scale research is needed to identify genetic and phenotypic risk factors, as well as to understand the contribution of lifestyle, nutrition, obstetrical experiences, comorbid medical conditions, and other environmental influences. Longitudinal studies are required to investigate how various biological and environmental factors affect the course and progression of POP across a woman's life span. After discussion, 3 priority areas were identified that would facilitate large-scale community-based research.

© 2018 American Urogynecologic Society.

Copyright © 2018 Wolters Kluwer Health | Lippincott Williams & Wilkins. Unauthorized reproduction of this article is prohibited.

The first is the development of robust and inexpensive research tools for use in large-scale studies. This requires a standard set of "best outcome measures" that are reproducible and able to be incorporated into large-scale studies. Furthermore, there is value in developing patient self-assessment tools and/or simple assessments that could be incorporated into primary care settings. Modifications of current diagnosis and procedural codes to better distinguish clinically meaningful POP subtypes would facilitate more relevant administrative and health services research. Finally, the field would be advanced by the creation of instruments for assessment of lifestyle and behavioral factors that impact POP.

A second priority is to promote research to better understand biologic risk factors for POP development, progression, or recurrence. This includes scientific partnerships to investigate biological factors and their association with clinical phenotypes. Specimen repositories that link with clinical and research databases would be helpful.

Finally, a particularly important priority is the development of prevention strategies for POP. This requires the development of a rigorously tested conceptual framework to address prevention across a woman's life span. Researchers should promote the development of mathematical prediction models to identify women at greatest risk of POP and of POP recurrence. These prediction models should include research on modifiable risk factors that could minimize POP progression or recurrence and could also include mechanistic measurements (such as muscle strength or other biomarkers).

In summary, epidemiologic research in POP plays a vital role in improving our understanding of POP and may facilitate POP prevention and treatment. This scale of research will require the creation of partnerships across societies, industry, government, academic institutions, and the private sector (community practice).

Clinical Trials to Optimize Outcomes After POP Surgery

Well-designed randomized clinical trials provide the highest level of evidence on treatment safety and efficacy, and surgical trials have played a critical role in advancing our understanding of the treatment of POP. Certainly, rigorous multicenter trials have provided important knowledge about long-term outcomes after mesh sacrocolpopexy and comparative outcomes after different types of vaginal vault suspension.[2,12] However, despite significant advances in the last 20 years, 3 fundamental research issues remain unanswered: (1) what are the most effective surgical approaches for prolapse that also minimize complications, (2) which situations call for biologic graft or synthetic mesh augmentation versus native tissue repair, and (3) whether to remove the uterus (if present) at the time of POP surgery. Importantly, these issues may be influenced by patient characteristics such as age, comorbidities, sexual function, physical activity, and tissue quality. Moreover, a variety of physician factors may also influence the route and choice of surgical approach, such as physician training, experience, and bias/preference.

Generally, successful POP trials have had simple and clear inclusion and exclusion criteria that balance specificity and generalizability. Use of valid, reliable, outcome measures in multiple domains (ie, objective anatomic outcomes as well as patient-reported and quality-of-life outcomes) is necessary to capture the full impact of POP treatments. Masking patient assessments, in particular physical examinations, is important to minimize bias. Challenges that remain include physician bias, patient reluctance to accept randomization, the inefficiency of clinical trials to evaluate new technologies in a rapidly changing field, and the medicolegal environment. In addition, few POP trials follow patients for more than 1 to 2 years. Given the high risk of recurrence, there is a critical need for long-term follow-up studies (5–10 years or more). There is also a need for large pragmatic trials to provide patient-centered effectiveness information. Finally, there is a need to understand the risks and benefits of POP treatments for specific patient subgroups so treatments can be tailored and individualized to optimize outcomes. Promoting the development of standardized measurable outcomes, research to identify predictive biologic and/or clinical phenotypes, and innovative approaches while balancing safety will be important steps to facilitate POP surgical and clinical trials of the future.

Development of Evidence-Based Quality Measures for Prolapse Outcomes

In an era of quality-focused health care, it will be important to develop meaningful measures of quality for the care of women with POP. Several types of quality measures (eg, outcome measures, process measures, patient-centered outcomes [PCOs], and cost/resource use) can be used to assess care. The scientific acceptability of a proposed measure depends on supporting data, guidelines for implementation of the measure, data confirming the validity and reliability of the measure, and evidence suggesting that there are opportunities for practice improvement in the relevant area.

Currently, 3 outcome measures exist that apply specifically for POP procedures, and all pertain to the reporting of complications after POP repair surgery, specifically bladder, ureteral, and bowel injury (PQRS #432, 433, 434). Creation of a more robust collection of quality measures that focus on long-term outcomes is limited by the lack of globally accepted outcome measurement criteria. The Pelvic Organ Quantification System examination, an objective assessment of POP anatomy, has not been universally adopted, and anatomic definitions of success or failure are not universal. For subjective evaluation of outcomes, there are many validated questionnaires used to assess POP, but there is no consensus about their use or about scoring that could be used to define failure or success. Thus, an accepted set of "best outcome measures" would be very helpful toward the development of rigorous quality outcome measures for the treatment of POP. Furthermore, scientifically rigorous data about surgical outcomes would provide the ability to benchmark surgeon performance. Patient-reported outcomes for POP have not been well studied or defined, and there are currently no validated patient-reported outcome tools for use in patients with POP. These barriers are likely to be overcome by collaborating with clinical trialists and epidemiologists to create the data that can be incorporated into quality measures in the future.

In addition to outcome measures, there are 9 process measures in use or development for reporting to the Centers for Medicare & Medicaid Services: (1) cystoscopy at the time of hysterectomy (NQF #2063, PQRS #422), (2) apical suspension (ie, suspension of the most proximal or superior portion of the vagina) at the time of hysterectomy for POP, (3) assessment of POP prior to surgical repair (Merit-Based Incentive Payment System [MIPS]), (4) offering a pessary (MIPS), (5) use of a pessary (MIPS), (6) preoperative assessment of stress urinary incontinence prior to POP surgery (NQF #2677, PQRS #428), (7) assessment of sexual function prior to POP repair (MIPS), (8) exclusion of uterine malignancy prior to obliterative procedures (ie, procedures that close the vaginal cavity and may in theory prevent access to internal organs for diagnosis or treatment) (PQRS #429), and (9) rectal examination during posterior compartment POP repair (MIPS). Similar to outcome measures, process measures are also hampered by limited agreement regarding outcomes, as creation of these measures depends on actionable direction from systematic reviews and guidelines. Clear and actionable items are infrequently offered because of the

© 2018 American Urogynecologic Society.

Copyright © 2018 Wolters Kluwer Health | Lippincott Williams & Wilkins. Unauthorized reproduction of this article is prohibited.

challenges involved in linking processes to weakly defined outcomes. In addition, data regarding risk stratification and disparities in care within female pelvic medicine and reconstructive surgery are lacking.

There are critical initiatives that would facilitate the creation of new evidence-based quality measures for POP treatment. The development of a generally accepted measure of success (or failure) of surgery for POP could facilitate the successful measurement of surgical outcomes, as well as the creation of process measures that can be tied to outcomes. This effort is best led by a national professional organization that can promote the use of such a measure for research and clinical care purposes. Characterization of patient expectations and satisfaction regarding preoperative evaluation, the perioperative experience, and postoperative recovery expectations and limitations is a critical element to developing successful PCO tools. Examples of such tools used to assess surgical outcomes in other fields include the "Breast-Q,"[13] which evaluates PCOs for patients undergoing breast reconstructive surgery. Similar tools may be useful in women undergoing POP surgery. Finally, research using large data sets to describe the events and health care costs associated with typical patterns of care for a patient with POP can be used to develop measures of efficiency and cost-effective care.

DISCUSSION

The AUGS 2016 Prolapse Consensus Conference brought together researchers, clinicians, industry representatives, and patient advocates to review the current state of POP research and identify priority areas for future research where progress is most likely to impact clinical care and patient outcomes. We anticipate that the results summarized in this report will promote increased collaboration among researchers with diverse expertise, will serve to support the importance of POP research overall, potentially focus efforts in key areas that may rapidly improve care of POP patients, and may spur an interest in POP research among students and trainees in our urogynecology community.

The conference presentations and discussions centered around 5 critical topics, which arose from surveys of health care professionals and AUGS members. The priority areas identified for future research and summarized in this report include a wide spectrum of research types and disciplines, but common threads that would advance POP research were noted across the 5 topic areas. One such common thread is the pressing need for a standardized group of outcomes for POP or the set of "best outcome measures" that could be utilized in large trials, community-based research, and quality measures. We also saw many groups focus on the need for personalization of treatments and identification of factors that would allow for more successful individualized care. The ability to personalize treatments often depends on a combination of rigorous bioinformatics, biological data, and knowledge of outcomes over a clinically relevant period. Thus, several workgroups identified the need for specimen biorepositories that can integrate with clinical data and the capacity for this type of information to substantially advance research in POP. Finally, the ability to integrate different types of data for a complex condition such as POP requires collaborative, multidisciplinary research groups. These groups currently exist in specific institutions, but attracting more trainees with higher-quality research training may expand this type of collaborative research to allow our scientific community to tackle more challenging and complex questions.

One unique aspect and strength of the 2016 Prolapse Consensus Conference was that multiple stakeholders with diverse perspectives were included as presenters and attendees. An effort was also made to include patient advocates, trainees, and junior researchers in the workgroup discussions; these stakeholders contributed valuable insights across all topic areas. The Consensus Conference attendees were surveyed about the conference, and the overall response showed enthusiastic support for the format. Suggestions for improvements were also collected and generally focused on the need for enhanced advance communication to ensure adequate and broad participation from multiple perspectives.

In summary, the 2016 Prolapse Consensus Conference provided a venue to identify areas of POP research priority and an opportunity to collaboratively brainstorm about ways to improve the science of POP research. Suggestions from this conference will be considered carefully by the AUGS Scientific Committee and Board of Directors as they consider how AUGS might support POP researchers and existing research efforts in these critical areas.

REFERENCES

1. Jones J, Hunter D. Consensus methods for medical and health services research. *BMJ* 1995;311(7001):376–380.
2. Nygaard I, Brubaker L, Zyczynski HM, et al. Long-term outcomes following abdominal sacrocolpopexy for pelvic organ prolapse. *JAMA* 2013;309(19):2016–2024.
3. FDA Center for Devices and Radiological Health. *Urogynecologic Surgical Mesh: Update on the Safety and Effectiveness of Transvaginal Placement for Pelvic Organ Prolapse*. 2011. Available at: https://www.fda.gov/downloads/medicaldevices/safety/alertsandnotices/ucm262760.pdf. Accessed November 13, 2017.
4. Kux L. Department of Health and Human Services. Obstetrical and Gynecological Devices: Reclassification of Surgical Mesh for Transvaginal Pelvic Organ Prolapse Repair. *Federal Register* 2016;81(2):354–361. Available at: https://www.federalregister.gov/documents/2016/01/05/2015-33165/obstetrical-and-gynecological-devices-reclassification-of-surgical-mesh-for-transvaginal-pelvic. Accessed November 13, 2017.
5. Clemons JL, Weinstein M, Guess MK, et al. Impact of the 2011 FDA transvaginal mesh safety update on AUGS members' use of synthetic mesh and biologic grafts in pelvic reconstructive surgery. *Female Pelvic Med Reconstr Surg* 2013;19(4):191–198.
6. Swift S, Woodman P, O'Boyle A, et al. Pelvic Organ Support Study (POSST): the distribution, clinical definition, and epidemiologic condition of pelvic organ support defects. *Am J Obstet Gynecol* 2005;192(3):795–806.
7. Wu JM, Matthews CA, Conover MM, et al. Lifetime risk of stress urinary incontinence or pelvic organ prolapse surgery. *Obstet Gynecol* 2014;123(6):1201–1206.
8. Handa VL, Garrett E, Hendrix S, et al. Progression and remission of pelvic organ prolapse: a longitudinal study of menopausal women. *Am J Obstet Gynecol* 2004;190(1):27–32.
9. Bradley CS, Zimmerman MB, Qi Y, et al. Natural history of pelvic organ prolapse in postmenopausal women. *Obstet Gynecol* 2007;109(4):848–854.
10. Buchsbaum GM, Duecy EE, Kerr LA, et al. Pelvic organ prolapse in nulliparous women and their parous sisters. *Obstet Gynecol* 2006;108(6):1388–1393.
11. Handa VL, Blomquist JL, Knoepp LR, et al. Pelvic floor disorders 5–10 years after vaginal or cesarean childbirth. *Obstet Gynecol* 2011;118(4):777–784.
12. Barber MD, Brubaker L, Burgio KL, et al. Comparison of 2 transvaginal surgical approaches and perioperative behavioral therapy for apical vaginal prolapse: the OPTIMAL randomized trial. *JAMA* 2014;311(10):1023–1034.
13. Memorial Sloan Kettering Cancer Center. Breast-Q. 2012. Available at: http://qportfolio.org/breastq/. Accessed November 13, 2017.

© 2018 American Urogynecologic Society.

Copyright © 2018 Wolters Kluwer Health | Lippincott Williams & Wilkins. Unauthorized reproduction of this article is prohibited.

Manuscript prepared for publication in International Urogynecology Journal

EDITORIAL

Reinforcement of pelvic ligaments by tapes may be the answer to POP and the mesh problem

Peter EP Petros, DSc, PhD, MD
31/93 Elizabeth Bay Rd
Elizabeth Bay NSW 2011 AUSTRALIA
Reconstructive Pelvic Floor Surgeon and Certified Urogynaecologist
Professor, University of NSW Professorial Dept of Surgery, St Vincent's Hospital Sydney
Adjunct Professor, University of Western Australia School of Mechanical and Chemical Engineering, Perth WA
Tel +61 2 9361 3853 Cell phone (AUST) +61 411 181 731
Email: pp@kvinno.com
Website: www.integraltheory.org

27th December 2017

In 2011, the FDA issued a warning on mesh implantation for pelvic organ prolapse 'POP' [1]. This was the start of a major controversy with seismic manifestations: constant media stories about sufferers, government inquiries, massive legal suits, closure of mesh companies. On examination of the data, expert committees from learned bodies world-wide have endorsed the midurethral sling (MUS) but have expressed caution about mesh implantation for POP. No anatomical reasons were advanced by these expert committees for this difference in advice. Yet anatomical answers are required for the two questions below if a solution is to be found.

1. What is it about MUS that makes it work reasonable well, with mostly minor, manageable complications?

2. What is it about mesh sheets which can cause severe QOL complications which may not be easily manageable?

On weighing up 2, the question is not legal (a more comprehensive consent form). Nor is it a matter of "benefits outweighing risks". The question is ethical. Should surgeons be performing an operation which can have such catastrophic effects on QOL, albeit in a minority of patients? This is the thrust of the questions by the media campaign. Going back to native tissue repair is clearly not the answer. The Lancet PROSPECT TRIAL [2] conclusively proved the futility of any surgical intervention to vagina. At 6 months review, native tissue repair or mesh sheets applied behind vagina (level 2) had a >80% failure rate.

The answers to questions 1&2, the failed Lancet trial, the mesh fiasco, and the alternative ligament-based tape surgery described below can be found in one paragraph of the 1990 publication of the Integral Theory, summarized in fig1. It states clearly that ligament integrity is essential for structure and vaginal elasticity for function:

"*Essential to the understanding of this theory is the appreciation that the vagina has two distinct anatomical segments, which are pulled in opposite directions against the pubourethral ligament (PUL) to close the urethra. PUL acts as a fulcrum, Fig. 1. In order to transmit (mediate) these movements, sufficient elasticity is needed in the zone of critical elasticity of the vagina* (3)*."* The same 1990 publication extensively described the experimental animal work on which the TVT was based, precise implanting of tapes in the position of PUL to reinforce it, and to restore function, fig1, by creation of an artificial collagenous neoligament [4].

This quote begs a 3rd question, a concern that the elastic function of vagina, and the purpose of the tapes, [3, 4] was seemingly unknown by the developers of the mesh kits and indeed, those who planned the Lancet PROSPECT TRIAL. Neither apparently were aware of the fibrotic effect of implanted mesh on an elastic vagina, even though the experimental animal work, the basis of the TVT which most pelvic surgeons was practicing, had been described in the most detailed way in 1990. These facts touched a 4th question constantly raised by the mesh lawyers, where was the prior experimental work for the mesh? It was there all the time. The

experimental animal studies in 1987-8 [4] and the clinical experiments following the prototype midurethral sling [3], demonstrated that the use of alloplastic material was essential for longlasting strengthening of damaged ligaments. *Ligaments, not vagina.* The same ligament repair method as in MUS [4] was successfully applied to uterosacral ligaments (USL) for POP repair in 1997 [5]. Again, ligaments, not vagina. Major improvements in tape technology have revolutionized ligament repair surgery for POP. Using thin strips of 3rd generation non-stretch macropore tape, Sekiguchi et al (6) (n=60), Wagenlehner et al [7] (n=1420), Shkarupa et al [8] (n=148), all reported cure rates >90% at 12 months in patients with 3rd and 4th degree POP by minimally invasive repair of CL and USL. There was minimal post-operative pain and zero tape erosions for [6]&[8]. So this surgical methodology is well tested. Furthermore, this method [4] has been successfully applied to repair other key suspensory ligaments ATFP [6] and perineal body (PB) [9]. The ligament repairs [5-8] were combined with conventional site-specific repair of pubocervical, rectovaginal fascia and extraurethral ligament as required, *without vaginal excision*.

Figure 1 summarizes the synergistic but separate roles of ligament and vagina to function. Organ support is by ligaments, not vagina. The breaking strain for ligaments is approximately 300 mg/mm^2, for vagina 60 mg. The MUS tape restores function by creating a collagenous pubourethral (PUL) neoligament [3, 4], Figure 1. This technique has no effect on vaginal elasticity. In contrast, mesh sheets placed behind vagina only act as a barrier. They do not restore damaged anatomy. This is evident on transperineal ultrasound. The bulge is till there. Mesh sheets fibrose the vagina and reduce its elasticity. Many of the complications related to pelvic meshes can be explained by loss of vaginal elasticity. Pelvic tissues are innervated by visceral nerves that are sensitive to stretching. Mesh fibrosis may compress a nerve to cause visceral pain, which can be severe. Any fibrotic scarring, whether from excessive vaginal excision from 'native tissue repair' or vaginal mesh sheets, removes the elasticity required for independent closure action by vector forces, fig1. The more powerful backward vectors may overcome the weaker forward vectors to cause massive uncontrolled urine loss on getting off a chair or out of bed in the morning (the key diagnostic symptom). This was described in 1990 as the 'Tethered Vagina Syndrome" [3, 10]. Cure requires dissection of scar tissue and application of a skin graft to the bladder neck area of vagina. Vaginal mesh sheets are a time bomb. Even in successful mesh cases, the collagen formed by the mesh will stiffen with age and the patient may develop this problem 20-30 years later as an old woman. Clearly objective assessment of vaginal elasticity will be a very helpful tool.

Conclusion

All operations have complications. Where the complications can be very severe, it is not sufficient to simply judge risks *vs* benefits. The public outcry against vaginal mesh may well be the defining impetus for wider adoption of an already well-proven surgical approach for POP, ligament repair as per MUS. Lightweight mesh sheets are not the answer. Any mesh sheet will create neocollagen, fibrose vagina and limit its movement. The data emerging using 3rd generation tapes to repair major POP by ligament repair only, with no tape rejections [6, 8] is impressive and is undoubtedly the future. These methods do not significantly affect vaginal elasticity as they attach the organs directly to the skeleton. A whole new direction for pelvic floor science beckons as these ligament repair methods also achieve high rates of cure for symptoms such as chronic pain, bladder & bowel dysfunction [5-9]. Assessing ligament competence and vaginal elasticity will most likely become an important objective test to assist reconstructive surgery, certainly in patients with previous surgery and vaginal scarring. Patients with existing mesh complications fall into this category. Already, exciting new technology which can assess the biomechanical characteristics of pelvic structures (Advanced Tactile Imaging, Inc. NJ USA) [11] has been developed to objectively assess vaginal elasticity in such complex cases. It can potentially diagnose ligament looseness, vaginal fibrosis from mesh and any connective tissue cause of *de novo* symptoms after mesh sheet removal.

References

1. Urogynecologic Surgical Mesh: Update on the Safety and Effectiveness of Transvaginal Placement for Pelvic Organ Prolapse, July 2011.
2. Glazener CM, Breeman S, Elders A, Hemming C, Cooper KG, 83 Freeman RM, For the PROSPECT study group (2017) Mesh, graft, or standard repair for women having primary transvaginal anteri or or posterior compartment prolapse surgery: two parallel-group, multicentre, randomised, controlled trials (PROSPECT). *Lancet* 389:381–392.
3. Petros PE, Ulmsten U. An Integral Theory of female urinary incontinence. *Acta Obstet Gynecol Scand* 1990; 69:1–79.

4. Petros PE & Ulmsten U, Papadimitriou J, The Autogenic Neoligament procedure: A technique for planned formation of an artificial neo-ligament. *Acta Obstetricia et Gynecologica Scandinavica*, Supplement 153, Vol 69, (1990), 43-51

5. Petros PE New ambulatory surgical methods using an anatomical classification of urinary dysfunction improve stress, urge, and abnormal emptying. *Int J Urogynecology* (1997) vol 8, 5: 270-278.

6. Sekiguchi Y, Kinjo M, Maeda Y, Kubota Y. Reinforcement of suspensory ligaments under local anesthesia cures pelvic organ prolapse: 12-month results. Int Urogynecol J 2014; 25: 783–789.

7. Wagenlehner F, Perletti G, Sekiguchi Y, Inoue H, Goeschen K, Abendstein B, Sivaslioglu A, Haverfield M, Muller-Funogea I-A, [1]Richardson P., Vaginal apical prolapse repair using two different sling techniques improves chronic pelvic pain, urgency and nocturia – a multicentre study of 1420 patients. *Pelviperineology* 2016; 35: 99-104.

8. Shkarupa D Kubin N Pisarev A Anastasiya Zaytseva A Shapovalova E The hybrid technique of pelvic organ prolapse treatment: apical sling and subfascial colporrhaphy. *Int Urogynecol J* DOI 10.1007/s00192-017-3286-7.

9. Wagenlehner FM, Del Amo E, Santoro G, Petros P: Perineal body repair in patients with 3rd degree rectocele. A critical analysis of the tissue fixation system. Colorectal Dis 15:e760-e765;2013; 15, Issue 12, pages e760–e765.

10.Petros PE & Ulmsten U. *The free graft procedure for cure of the tethered vagina syndrome.* Scandinavian Journal of Urology and Nephrology,1993; - Supp. No 153 : 85-87.

11. Lucente V, van Raalte H, Murphy M, Egorov V. Biomechanical paradigm and interpretation of female pelvic floor conditions before a treatment. *International Journal of Women's Health* 2017; 9: 521-550.

FIGURE

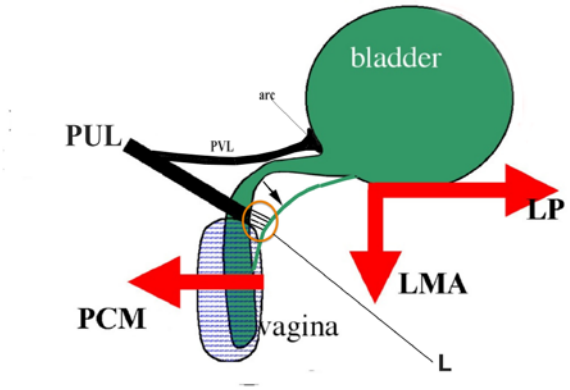

Figure 1. How a lax pubourethral ligament 'PUL' causes urinary stress incontinence. *The urethra has two separate closure mechanisms activated by oppositely acting muscle forces (arrows). Adequate elasticity in the bladder neck area of vagina is required for these to function separately (3). Distal closure: pubococcygeus muscle 'PCM' (arrow) contracts against competent pubourethral ligaments (PUL). This stretches suburethral vagina forward to close distal urethra (3). Bladder neck closure: levator plate 'LP' contracts backwards against PUL. Conjoint longitudinal muscle of the anus 'LMA' (arrow) rotates bladder base around the arc of Gilvernert to close urethra at bladder neck. Extension of PUL to 'L' indicates PUL loosening; PCM weakens; LP/LMA pull open posterior urethral wall (small diagonal arrow). Intraurethral resistance exponentially decreases. Patient loses urine on effort. PVL = pubovesical ligament. Surgical restoration of PUL with a tape restores vector muscle strength and continence (3).*

Book: **Biomechanics of the Female Pelvic Floor**, Editors L. Hoyte and M.S. Damaser, Elsevier, Jan-Feb 2016.

Chapter 17

Biomechanical characterization of the pelvic floor using tactile imaging

Vladimir Egorov[1], PhD, Heather van Raalte[2], MD, Vincent Lucente[3], MD, Armen Sarvazyan[1], PhD, DSc

[1] Artann Laboratories, 1459 Lower Ferry Rd, Trenton, NJ 08618, USA
[2] Princeton Urogynecology, 10 Forrestal Road South, Suite 205, Princeton, NJ 08540, USA
[3] The Institute for Female Pelvic Medicine & Reconstructive Surgery, 3050 Hamilton Blvd, PA 18104, USA

Used Abbreviations

E Young's modulus

FTI Functional Tactile Imaging

MRI Magnetic resonance imaging

P Pressure

POP Pelvic organ prolapse

SUI Stress urinary incontinence

TI Tactile imaging

VTI Vaginal tactile imager

1. Tactile imaging

1.1. Introduction

Over the centuries, soft tissue palpation has been the most prevalent and successful medical diagnostic technique [1]. Human sense of touch can distinguish structural mechanical changes in soft tissues that correlate with different disease conditions [2]. However, one of the problems with manual palpation is that it lacks quantification, objectivity and reproducibility across diverse examiners.

By the end of the last century, a new technology named Elastography, or Elasticity Imaging, for measuring and visualizing soft tissue viscoelastic characteristics emerged and the ancient art of palpation gained new life [3]. A review of the literature suggests the birth of a new chapter of Biomechanics evidenced by the substantial growth of Elastography related publications from 1 article in 1992 to 1,019 in 2014 (PubMed – search criteria "Elastography").

Elasticity imaging involves the application of a stress to soft tissue, and the measurement of the resulting tissue mechanical response. There are multiple methods for applying the stress to the tissue and measuring the response. The stress can be generated in at least four different ways: from an external source such as a compression probe, an external vibrator, acoustic radiation force and physiological sources of motion (e.g. cardiac motion, fluid flow) [3]. The most common types of measurement methods of tissue response include ultrasound, magnetic resonance imaging (MRI) and tactile imaging. Table 1

shows the different methods, their basic characteristics, equipment cost assessment and clinical applications.

Table 1. *Elasticity imaging methods and their basic characteristics.*

Method	Stress generation	Measurements	Imaging and resolution	Imaging depth	Equipment cost	Current Clinical applications
MRI Elastography	*Application of stress to the tissue surface, tissue vibration*	*3-D displacement patterns of induced waves*	*3-D 0.5-5 mm*	*200 mm*	*$$$*	*Breast, liver, brain, heart, lung, muscles, prostate, thyroid [3]*
Ultrasound Elastography	*Application of stress to the tissue surface, physiological motion*	*2-D/3-D tissue displacement/ strain*	*2-D/3-D 1-3 mm*	*60 mm*	*$$*	*Breast, thyroid, lymph nodes, arterial wall, heart liver, prostate [3]*
Share Wave Ultrasound Elastography	*Tissue vibration, radiation force*	*1-D/2-D share wave speed*	*1-D/2-D 1-2 mm*	*60 mm*	*$$*	*Breast, liver, muscle, prostate, thyroid [3]*
Tactile Imaging	*Application of stress to the tissue surface*	*2-D pressure pattern on the tissue surface, sensor location*	*2-D/3-D 1-2 mm*	*40 mm*	*$*	*Breast, prostate, muscle, vagina [4]*

The female pelvic organs are accessible to manual palpation, and may have varying viscoelastic characteristics across physiological states [5, 6], healthy and diseased conditions [7, 8]. This makes the pelvic floor tissues especially amenable to evaluation by elasticity imaging techniques [9]. It can potentially be applied to map the elasticity of pelvic floor tissues, and this opens up new possibilities for quantitative and reproducible biomechanical assessment and monitoring of pelvic floor conditions.

1.2. Definition

Tactile Imaging (**TI**), also called “Mechanical Imaging”, is a medical imaging modality that translates the sense of touch into a digital image. The tactile image is a function of ***P(x,y,z)***, where ***P*** is the pressure on soft tissue surface under applied deformation and ***x,y,z*** are coordinates where pressure ***P*** was measured [9-13]. The tactile image is a pressure map on which the direction of tissue deformation must be specified [13]. Tactile imaging closely mimics manual palpation, since the probe of the device with a pressure sensor array mounted on its face acts similarly to human fingers during clinical examination, deforming soft tissue by the probe and detecting resulting changes in the pressure pattern. The sensor head is moved over the surface of the tissue to be studied, and the pressure response is evaluated at multiple locations along the tissue under study. The results are used to generate 2-D or 3-D images showing the pressure distribution over the area of tissue under study.

Examples of TI can be seen at:

http://link.springer.com/content/esm/art:10.1007/s00192-014-2549-9/file/MediaObjects/192_2014_2549_MOESM1_ESM.mp4

Functional Tactile Imaging (**FTI**) is a variation of TI that translates muscle activity into a dynamic pressure pattern ***P(x,y,t)*** for an area of interest, where ***t*** is time *and* ***x,y*** are coordinates where pressure ***P*** was measured. Muscle activity to be studied may include a voluntary contraction (e.g., a pelvic floor squeeze), an involuntary reflex contraction (e.g., due to a cough), an involuntary relaxation, or a Valsalva (veering down) maneuver.

Examples of FTI can be seen at: *will be linked to video presentation at 2015 AUGS or vimeo server*

1.3. Interpretation

To fully characterize tissue as a mechanical system a great number of parameters are needed. These include the shear and Young's moduli bulk compressional modulus, nonlinearity, Poisson's ratio, viscosity, poroelastic parameters, anisotropy and heterogeneity indices [14-16]. However, in most practical cases, even just one elasticity parameter, such as Young's modulus (*E*), may be sufficient to address diagnostic tasks [17-20]. Detection of a mechanical heterogeneity by manual palpation is based exclusively on sensing the variations of the Young's modulus of tissue (or shear elasticity modulus, μ, which is approximately equal to E/3 for soft tissues) [3, 21-24]. Soft tissues are called "incompressible" because their bulk compressional modulus (*K*) is generally several orders of magnitude larger than the shear modulus. As a result, a short external stress applied to soft tissues causes mainly a change in the shape of the stressed tissue, while the volume remains constant with a high degree of precision. If a soft tissue is deformed, the relationship between the stress and strain patterns is completely defined by the Young's modulus only, regardless of the *K* value for the tissue. Bulk compressibility and shear elasticity are dependent on different features of tissue. Bulk compressibility modulus depends on short range molecular interactions and is defined mainly by tissue molecular composition while shear elasticity is defined by structural peculiarities of tissue, its cellular and higher level of architecture [23]. The bulk modulus for all the soft tissues is close to that of water and varies within only about 10% [23]. In contrast to that, the range of variability of structural features of tissues, such as geometrical parameters of cells in different tissues and the degrees of heterogeneity and anisotropy, is much greater. The shear elasticity for different soft tissues varies over four orders of magnitude and, even within one tissue, may change by hundreds of percent during such process as development of a tumor or an ordinary muscle contraction [25].

Generally, an inverse problem solution for the 3-D tactile image *P(x,y,z),* would allow reconstruction of the tissue elasticity distribution as function of the coordinates *x,y,z.* Unfortunately, the inverse problem solution is hardly possible for most real objects because it is non-linear and ill posed problem. Tactile Imaging reveals tissue or organ anatomy and elasticity distribution because it keeps the stress-strain relationship for deformed tissue [26, 27]. It appears that the 3-D tactile image can be transformed into an elasticity image with the use a linear transformation for a region of interest. That means, in general, the spatial gradients $\partial P(x,y,z)/\partial x$, $\partial P(x,y,z)/\partial y$ and $\partial P(x,y,z)/\partial z$ can be used in practice for quantitative assessment of tissue elasticity because they have a validated background [9-13, 26-31] allowing quantitative comparison and analysis for different tissues with anatomical variations.

1.4. History

Review of the literature reveals that the first description of a technical implementation related to tactile imaging was given in 1979 by Frei *et al.* [32, 33], who proposed an instrument for breast examination. That device used a plurality of spaced piezoelectric force sensors. The sensors were pressed against the breast by a pressure member, to apply a periodic or steady stress to the soft tissue. A different principle for evaluating the pattern of pressure distribution over a compressed breast was proposed by Gentle (1988) [34]. The pressure distribution was monitored optically by using the principle of frustrated total internal reflection to generate a brightness distribution. Using this technique, simulated lumps in breast prostheses were detected down to a diameter of 6 mm. But the author was unable to obtain any quantitative data on lumps in a real breast. The failure was explained by the insufficient sensitivity of the registration system, and that "the load that the volunteers could comfortably tolerate, was less than that used in the simulation." Then, Dario *et al.* (1988) and Sabatini *et al.* (1990) designed a robotic system capable of carrying out complex sensory-motor sequences intended for collecting information on some body functions through palpation with an articulated finger incorporating joint force and position sensors as well as piezoelectric polymer skin-like sensors aimed at detecting hardened regions embedded in soft biological tissues [35, 36]. Another attempt to use a robotic system to detect the presence of a lump in the breast described by Koganezawa et al. (1991) [37].

Sarvazyan in 1992 proposed a method, Mechanical Imaging, that can be used for both screening

purposes and documentation purposes. That method utilizes distributed pressure measurements at the surface of the tissue to estimate the properties of breast lesions and prostate nodules [7]. Mechanical imaging, as a modality of medical diagnostics and the imaging device with mechanical sensors, was introduced in 1997 [10, 38]. The PhD theses "Tactile Imaging" by Wellman (1999) and "Mapping Tactile Imaging Information" by Galea (2004) described a system for documentation of the properties of palpable breast lumps to improve the objectivity of clinical breast examination [40, 41]. Despite the first FDA approval for a tactile breast imaging device based on the Tekscan pressure array in 2003 [42], that device, proved unreliable, due to low sensitivity and poor reproducibility of electrical resistive sensors for that specific application. Many physical principles have been explored for the realization of tactile sensors: resistive, inductive, capacitive, optical optoelectric, magnetic, piezoelectric and electroacoustic principles, in a variety of configurations [43, 44]. Oie *et al.* (2009) designed a tactile mapping system, (scanning haptic microscope) with a spatial resolution of 5 μm (the tactile tip had a 5 μm diameter and used a lead zirconate titanate based sensor). Its applicability for elasticity assessment was demonstrated in a porcine artery model [45].

During last decade, several devices based on tactile imaging technology have been developed and clinically validated for soft tissue imaging and elasticity assessment for prostate [26], breast [27], myofascial trigger points [30] and vagina [9]. The capacitive pressure sensor arrays were used in all these applications. Each pressure sensor has sensing area of about 2 mm by 2 mm, the sensitivity of 20-70 Pa in the operational range up to 60 kPa. Probe design, number of sensors in the array (up to 256 sensors) and data processing algorithms were adapted to specific needs.

A directional vaginal probe with 4 force sensors has been developed Constantinou and Omata (2007) to evaluate the force and displacement produced during isotonic pelvic floor contractions [46]. The ManoScan 360 probe with 256 tactile-sensitive micro-transducers developed for anorectal application was tested for vaginal imaging [47].

1.5. Applications

Breast

The lifetime probability of developing breast cancer is evaluated as 13% [48]. A critical key to a continued reduction in mortality is early detection and accurate diagnosis made in a cost-effective manner. The tactile breast probe has a 2-D pressure sensor array (12 x 16 sensors) to acquire tactile imaging responses from the breast, with the aim of detecting worrisome lesions [27]. The probe head is lubricated and slid over the breast surface. No motion tracking or orientation system was used because tissue heterogeneity itself can be used as reference coordinates. When a suspicious site is detected, the manipulation of the probe is switched to a local scan accomplished by two procedure variations: probe pressings against the breast over the detected abnormality and circular motion of the probe. The examiner observes in real time accumulated cross-sectional images of a mass/lesion in orthogonal projections. The 3-D image composition and features calculations for the breast tissue are accomplished in real time [27]. A multisite clinical study on 179 subjects demonstrated that the breast mechanical imager provides a reliable image formation of breast tissue abnormalities and calculation of lesion features. Malignant breast lesions (histologically confirmed) demonstrated increased hardness and strain hardening as well as decreased mobility and longer boundary length in comparison with benign lesions. Statistical analysis of differentiation capability for 147 benign and 32 malignant lesions revealed sensitivity of 91.4% and specificity of 86.8% [28].

Prostate

We design the transrectal probe with 2-D pressure sensor array (8 x 16 sensors) to acquire pressure patterns from the prostate. It has additional 2-D pressure sensor array (3 x 16 sensors) to measure probe position relative sphincter and 3-D orientation sensor composed of accelerometers, magnetometers and gyroscopes. The probe provides a real time 3-D tactile image of the prostate by capturing its geometrical and elastic characteristics, and reveals the tissue abnormalities within the gland [26]. The correlation between the device and manual palpation (DRE) in detection of palpable nodularity was 81%, as indicated by the area under the receiver operating characteristic curve [29].

Myofascial trigger points

Presence of exquisitely tender nodules in a taut band of skeletal muscle and an associated symptom cluster may cause myofascial pain syndrome, which is prevalent and clinically significant [49]. We designed the muscle tactile imaging probe adapted for tender muscles with 192 durable tactile sensors. The clinical study on 50 subjects (27 healthy controls and 23 with symptomatic chronic neck pain) demonstrated that symptomatic muscle tissue in subjects with neck pain is mechanically more heterogeneous and stiffer compared to normal muscle in control subjects (p<0.05) [50]. At the same time, difficulties ware noted in 3-D tactile image composition and reliable trigger point discrimination by tactile imaging.

Female pelvic floor

Pelvic floor disorders affect the majority of women in their lifetime [51-53]. There is an 11% lifetime risk of undergoing surgery for prolapse or incontinence [54, 55]. Market data collected by FDA from manufacturers indicate that in 2010 approximately 300,000 women underwent surgical procedures in the US to repair POP and approximately 260,000 underwent surgical procedures to repair SUI [56]. The risk re-operation is high [57, 58]. Pelvic floor biomechanical changes occur in the course of applied nonsurgical therapy, in pregnancy and after giving a birth, with age, and under a heavy load in sporting and military activities. Sections below describe the tactile imaging approach to assess biomechanical properties and results of clinical research in this field.

1.6. Limitations

The first limitation of the TI method is the dependence of acquired tactile image or function *P(x,y,z)* on the probe size, tissue or organ anatomy and boundary conditions. Using lubrication, probes with contact area of 15 μm^2 [45] and 20 cm^2 [27] demonstrate different absolute values of *P(x,y,z)* acquired for the same tissue. But, comparison of the two image datasets reveals a lot of similarity and common features. Both probes show close relative distribution within *P(x,y,z)* and enable tissue characterization.

In general, an examination with a tactile imaging probe is highly operator dependent, similar to colonoscopy [59]. Operator training is required to quantify and standardize operator skills [60]. Minimization of the operator dependence is also possible by intentional probe design, data processing algorithms and real time feedback to the operator. For example, for the breast tactile imaging probe, the probe curvature was optimized to reduce the influence of applied tissue deformation on tactile imaging performance. In addition, probe skewness was calculated and subtracted as an image background at the software level [27]. The prostate probe was optimized for reproducible contact conditions with the prostate. To define and visualize probe location relative to the prostate in real time, we placed an additional tactile array for imaging of the urethral sphincter as a reference structure [26]. The vaginal probe, shown in Figure 1 (probe 3), was intentionally designed to eliminate dependence on operator skills as much as possible.

Tactile imaging reproducibility is an important consideration for imaging of soft tissue, which may exhibit nonlinear and viscoelastic properties with possible hysteresis. The technical reproducibility of pressure sensors, incorporated within the tactile imaging probe, is easy to establish in repeat calibrations using an air-pumped chamber with a highly precision reference air pressure sensor. Re-imaging of silicone models allows reproducibility assessment for elastic media. Clinical reproducibility evaluation requires completion of specific clinical protocols in controlled conditions. Establishing new diagnostic thresholds or imaging markers, sensitive to specific diseased conditions, does not require knowledge about clinical reproducibility, as long as the marker demonstrates statistically significant sensitivity/specificity or diagnostic accuracy or dependence on the diseased conditions.

Tactile imaging depth, detection capability and spatial resolution may contribute added limitations. These parameters depend on the probe/sensor geometry and targeted application. For the breast tactile imaging probe we observed superior sensitivity of the tactile imaging *versus* a human finger; the depth of nodules detected by tactile imaging has reached 40 mm, which is more than double the depth achieved with manual palpation [27]. A human finger can distinguish stiffness in pairs of elastic samples in the range from 0.13 to 0.46 [61-63] of the Weber fraction (defined as the relative increase above a baseline value

that can be reliably detected). That means the human finger cannot reliably discriminate the difference difference in tissue stiffness up to 46% of the time, using manual palpation cues [64]. These numbers do not take into account that the human mind remembers the perceived information for less than 2 seconds after a haptic exploration [65]. The stiffness discrimination of the pressure sensors, used in the vaginal tactile imaging probe [12], ranges from 2% to 10% for the entire elasticity range of tissues within the female pelvic floor.. Tactile imaging software can support resolutions of 1.0 millimeters, but current pressure sensors are 2.0 mm or larger. It has been demonstrated that, using dynamic and spatial motion components over the tissue in mechanical imaging, significant increases (10 times and more) in spatial resolution relative to the sensor size may be achieved [10].

Vaginal tactile imaging can clearly report $P(x,y,z)$ as a function of the deformation applied to vaginal tissue. However, the probe heads presented cannot "see" all the layers of anatomic structures or the full context underneath the tissues under study. Therefore, the probe is essentially reading the response of the tissue composite underneath the probe head (In the case of the distal posterior wall - vaginal mucosa, muscularis, serosa, rectovaginal septum, rectal serosa, muscularis, mucosa, lumen, stool if present, mucosa, muscularis, serosa, levator plate, anococcygeal raphe, depending on how hard you press). However, vaginal tactile imaging allows quantitative observations of all composite structures detectable by intravaginal manual palpation. Furthermore, the tactile imaging probe allows data acquisition from two opposite sides along the entire vagina in one visual frame with higher resolution than a human finger can provide (see Figures 14-17). The vaginal walls look "transparent" for the tactile probe, they are easily deformable allowing visualization of the pelvic floor support structures [13]. As demonstrated earlier, application of a 5-10 mm deformation to tissue models, allows the tactile probe to "see" 20-35 mm in depth [4, 27].

2. Bench testing

2.1. Probe design

Over 10 different tactile imaging probes have been designed and clinically tested over the past decade for prostate [26], breast [27], muscle [50], vaginal and pelvic floor assessments [9]. Four vaginal probes are shown in Figure 1. Probes 1 and 2, intended for 3-D imaging, were designed and tested subsequently. Probe 2 has an additional sensor array designed for contact with the cervix. Probe 3 was designed to reduce operator dependence and to image opposite sides of vagina along the entire length, including muscle function. Probe 4 is designed for 3-D perineal imaging under large deformations before delivery (prototype). As an example, probe 3 has capacitive pressure sensors with sensitivity, defined as an average noise level, of about 0.1 mmHg, accuracy ±3 mmHg, spatial resolution 1-2 mm, dynamic response 40 ms, with a measuring range up to 500 mmHg.

[Figure 1]

Tactile imaging probes need to be used with a lubricating gel to provide reproducible boundary/contact conditions with the deformed tissue; these conditions are classified as slip boundary conditions. The tactile probe measures an applied pressure, but not force. Force is a vector and by definition has amplitude and direction. The pressure sensors designed for tactile probes are not sensitive to the tangential component of a force which may arise during probe motion. The sensors measure pressure, defined as the orthogonal component of force divided by area. The probe may be used not only for tissue compression in the orthogonal direction to the tissue surface, but it can be used for sliding over the tissue and/or probe elevation. These probe maneuvers allow accumulation of multiple pressure patterns from the tissue surface to compose an integrated tactile image for the investigated area or organ [11, 26, 27].

2.2. Accuracy and reproducibility

The vaginal models, shown in Figure 2B, were built from two-component silicones (SEMICOSIL by Wacker Chemical Corporation (Adrian, MI) and RTV6166, 6186 by GE Silicones (Albany, New York))[66]. The range of Young's moduli of the parts manufactured from these components was varied from 2 kPa to 100 kPa and controlled by the tissue elastometer [67]. Soft tissue specimens were compressed

between the object plate of an electronic balance and a linearly actuated indenter with a small rounded tip. The elastometer was designed such that a deformation model for semi-infinite media is applicable for calculating the Young's modulus of test specimens from their collected force-displacement data (see page 367 in [14]). The used silicones can be considered as elastic, homogeneous and isotropic materials. The tested models were designed to approximate the pressure patterns collected under clinical conditions for normal and diseased pelvic floor conditions by the same tactile imaging probe. A non-linear model for transformation of spatial pressure gradients with the tactile images into Young's modulus was developed and validated on multiple silicone models.

Algorithms for 2-D image filtering were applied, along with 3-D coordinate translation to transform motion tracking data into the 3-D coordinate of each pressure sensor, in order to create the 3-D tactile image with a resolution of 1.0 mm [27]. Image rendering on the display is presented as in MRI by 3 orthogonal cross-sections.

Figure 2 demonstrates the imaging capability of probe 1 (Figure 1) with a pelvic floor model (Figure 2A), which is modified from a commercially available setup in which the internal rubber parts are replaced with silicone ones with realistic mechanical characteristics [11]. This model was used for imaging verification of anatomical features. A set of vaginal models, shown in Figure 2B, was used for imaging accuracy and reproducibility assessment.

[Figure 2]

The following numerical procedures were applied for processing the 2-D/3-D tactile images:

a) best fit as a mutual position of two images [27],
b) average image from multiple images acquired from the same tissue model or subject [26], and
c) image deviation for the analyzed image (I_{an}) relative to a reference image (I_{ref}).

The tactile image deviation (TID) is calculated as:

$$TID(x,y,z) = \frac{\sum_{x,y,z} (I_{an}(x,y,z\ ) - I_{ref}(x,y,z))^2}{\sum_{x,y,z} I_{ref}(x,y,z)^2} * 100\% \qquad (1)$$

The best fit procedure (a, above) was used before averaging of two images according to procedure (b, defined above). Averaging of multiple images is accompanied by recurrent application of procedures (a) and (b). The procedure (c) is used for imaging reproducibility assessment relative to an average image (I_{ref}).

Accuracy

The examination procedure included multiple compressions of the internal walls of a vaginal model, similar in design with the model shown in Figure 2B, until a circumferential 3-D tactile image was acquired. The operator observed in real time the probe location within the vaginal model and three cross-sections from the 3-D tactile image on display. Imaging accuracy was evaluated using a visual subjective score ranging from 1 to 5 (No image, Poor, Fair, Good, Excellent) to characterize relative comparison of 3-D tactile image with an actual map of the vaginal model. The average imaging score 3.9 was calculated for 35 examinations with tactile imaging probe 1 (Figure 2).

Calculation of TID for I_{an} (see equation 1) relative to the real elasticity map (I_{em}) for each vaginal model with two correction factors (constant and linear members), demonstrated deviations in the range of 30-40% which can be considered as a good result taking into account that we compare the 3-D pressure map (tactile image) with the 3-D elasticity distribution. Looking at the sagittal planes of the elasticity map and the tactile image in Figure 2B one may see a detectable correspondence. However, it is more appropriate to compare images of elasticity distribution, created as the result of the inverse mechanical problem solution for tactile image I_{an}, with the I_{ref}, or to compare a tactile image, created in the result of a direct mechanical problem solution for I_{an}, with an acquired tactile image I_{an}. Based on experiments with

vaginal tissue models of known composition we found that VTI allows differentiation of tissue elasticity within 2-10% and measurement accuracy of 10-15%, which is sufficient for quantitative elasticity assessment given that elasticity deviations related to diseased conditions are known to vary by up to 10,000% [4, 31, 67].

By incorporating softer parts into vaginal tissue models to mimic prolapse conditions, we estimated tactile imaging accuracy in size measurements to be ±2-5 mm; for stiffer parts we found VTI accuracy in size measurement as ±2-3 mm.

Reproducibility

Imaging reproducibility was calculated as a standard deviation (SD) for TID defined in equation (1) where an average image composed form multiple examinations of the same vaginal models are used as the reference. We found that the SD ranged from 4.2% to 5.8% depending on the model design and elasticity of included components. The reproducibility in measuring anatomical dimensions is within 1-3 mm; reproducibility in pressure measurements is 2 mmHg, reproducibility in Young's modulus measurement for the range from 2 kPa to 20 kPa is 0.3 - 1.8 kPa.

3. Clinical application

Following clinical evaluation of the feasibility of the VTI method, efforts focused on exploring findings in different stages of pelvic support, evaluating the possibility of identifying conditions which might predict the development of pelvic organ prolapse, and studying response of pelvic floor tissues across ranges of age and parity. Tactile imaging markers were identified for evaluating pelvic organ prolapse, and the response of the pelvic floor tissues to functional maneuvers was investigated.

3.1. Feasibility clinical study

Clinical feasibility of the VTI technique was evaluated in a clinical study with 13 subjects using probe 1 (Figure 1) equipped with a 2-D pressure sensor array and a tilt sensor. Examinations were performed with an empty bladder and rectum. The probe was held against the anterior or posterior vaginal wall (Figure 3), and the applied force *vs* the probe elevation angle was obtained and plotted. The elevation angle is proportional to the displacement of the probe head, which creates the applied stress. The results for two cases with normal and prolapse conditions are shown in Figures 4 and 5. A tissue elasticity index (E_s) was defined as the slope of the scanhead applied force *vs* elevation angle to characterize the tissue elasticity as stress to strain ratio [15]. These results show that the E_s for the anterior vaginal compartment in normal conditions was 7.2 (1.8 N/deg *vs* 0.25 N/deg) higher than in Stage 3 prolapse conditions ; The value of E_s for the posterior vaginal compartment in normal conditions is 3.1 (1.1 N/deg *vs* 0.35 N/deg) higher than in State 2 prolapse conditions. Such significant differences in tissue elasticity (720% and 310%) exceed the estimated measurement error of used approach [9].

[Figure 3]

[Figure 4]

[Figure 5]

The above mentioned tactile imaging probe was used to observe the tissue elasticity contrast between the native tissue and implanted mesh sections of a vaginal wall repair [9]. One such case (Figure 6) shows pressure patterns (tactile images) of the anterior and posterior compartments for a 59 year old woman with a history of a mesh augmented anterior repair, and a native tissue posterior colporrhaphy using a linear vertical posterior wall incision. The color pattern represents a contact pressure distribution under the applied load to the tissue. The spatial X, Y-coordinates for the color images show the transverse (X) and longitudinal (Y) direction for a vaginal wall over which the elasticity is being characterized. These patterns allow visualization and quantitative evaluation of increased rigidity at the mesh graft. Tactile imaging also shows a small rigidity increase (yellow colored zone) at the posterior vaginal wall after the posterior colporrhaphy, correlating with the incisional "scar" tissue detected by manual palpation. Quantitative evaluation of the most rigid tissue is presented in a graph where the horizontal axis is proportional to the total applied force to the scanhead, while the vertical axis is the peak pressure related to the maximum measured value inside the observed zone (see right panels in Figure 6).

The slope of these load curves characterizes the elasticity deviation of an embedded structure inside the soft tissue [26, 27].

[Figure 6]

This study shows that vaginal tactile imaging a) has the potential to contribute to quantitative biomechanical characterization of the tissues, b) has the potential for differentiating normal tissue from tissues involved in prolapse, and c) allows the characterization of implanted structures *in vivo* following reconstructive surgery.

3.2. Quantifying prolapse conditions

The basic purpose of the next study was to assess the clinical suitability of 3-D tactile imaging of the vagina and tissue elasticity quantification under normal and prolapse conditions. An improved tactile imaging design was used in this clinical study of 31 subjects [11].

The updated system includes a transvaginal probe, a motion tracking system, a data acquisition electronic unit, and a computer with touch screen monitor. The 2-D pressure sensor array was installed on the probe head surface contacting with the vaginal wall during the examination procedure. The probe head measures 45 mm in length, 20 mm in diameter. The pressure sensor array is comprised of 128 capacitive pressure sensors (probe 1, Figure 2). On average, each pressure sensor has a sensitivity of 0.15 mmHg; reproducibility is about 2.2 mmHg and an operational range of 225 mmHg. The six-degree-of-freedom motion tracking system provided probe positioning accuracy better that 1 mm and angular accuracy of about 0.25 degrees. The electronic unit provided data acquisition from the pressure sensors, synchronizes data from motion tracking sensor and communicates with the computer through a USB port. The data acquisition rate was about 25 pressure patterns per second.

The VTI examination was performed on patients in a standard position for a routine gynecologic exam. Examinations were performed with an empty bladder. During examination, the VTI probe is covered by a disposable plastic sheath with a lubricant. The full VTI examination required 3-5 minutes for completion. Three orthogonal projections of the 3-D vaginal pressure map with VTI probe location are observed by the operator in real time. The VTI clinical operators were trained on pelvic floor models prior to VTI clinical application to standardize imaging techniques. The examination procedure includes multiple compressions of the vaginal walls and allows composing a circumferential 3-D tactile image or pressure map of the vagina and storing the acquired data in digital format.

Thirty-one women were enrolled in this study. Of these, 23 were considered normal, with an average age of 58 years. Of the 8 women with prolapse, two each had stage I and stage II support, and four had stage III support. The average age of the 8 women was 70 years. Differences in the anatomy and tissue elasticity were found between the normal patients and those with prolapse. Figure 7 presents examples of examination results for normal and prolapse conditions. Specifically, Figure 7A shows transverse and sagittal cross-sections of the 3-D vaginal tactile image for a 63 year old patient with normal pelvic floor anatomy on manual palpation during physical examination. Young's modulus (E) was calculated for areas specified by the rectangles in the figure, and was found to be 7 kPa at the apical anterior location and 13 kPa at apical posterior location. On the right apical vagina, E was 10 kPa (transverse plane in Figure 7A). The anterior/posterior spacing at the apical vagina was measured as 14 mm (sagittal plane in Figure 7A). Figure 7B shows transverse and sagittal planes of 3-D vaginal tactile image received with VTI for a 77 year old patient with Stage III prolapse in the anterior and upper half of the posterior compartment that recurred less than a year from a vaginal hysterectomy and anterior repair. For this case that E was 1.8 kPa at the apical anterior wall and 1.5 kPa at the apical posterior wall. The left apical vaginal wall had E of 2.8 kPa (transverse plane in Figure 7B). The anterior/posterior spacing at the apical vagina was measured as 37 mm (sagittal plane in Figure 7B).

[Figure 7]

A notched boxplot shows the confidence interval for the median value (central horizontal line), 25% and 75% quartiles (Figures 8 and 9). The spacings between the different parts of the box help to compare a variance. The boxplot also identifies skewness (asymmetry) and outliers (small circles). The intersection or divergence of confidence intervals for two patient samples is a visual analog of the paired t-test. Figure 8 presents the vaginal tissue elasticity distribution for the apical and mid anterior aspects of the vagina

across varying POP conditions; among these were 19 normals (average age 55 years), 1 Stage I, 4 Stage II, and 7 Stage III (average age 70 years) cases. The data demonstrate the respective elasticity modulus decrease of 3.2 times for the apical anterior walls and up to 3.4 times for the mid anterior walls with Stage III prolapse relative to normal. From the apical to the mid anterior vaginal walls, the average elasticity modulus is increased by 80%. Figure 9 presents the vaginal tissue elasticity distribution for the apical and mid posterior vaginal walls across varying POP conditions; among them (23 normal (average age 58 y.o.), 2 Stage I, 2 Stage II, and 4 Stage III (average age 70 y.o.) cases). The data demonstrate the respective elasticity modulus decrease of 3.1 times for the apical posterior and up to 2.2 times for the mid posterior with Stage III prolapse relative to the normal conditions. From the apical to the mid posterior vaginal walls, the average elasticity modulus is increased by 95%. The average values for tissue elasticity for the anterior and posterior compartments for normal conditions were 7.4±4.3 kPa and 6.2±3.1 kPa, respectively. For Stage III prolapse the average values for tissue elasticity for the anterior and posterior compartments were 1.8±0.7 kPa and 1.8±0.5 kPa, respectively.

[Figure 8]

[Figure 9]

Figures 8 and 9 demonstrate significant differences in anterior and posterior vaginal tissue elasticity with POP stage. This difference is statistically significant as demonstrated by both the visual comparison of the confidence intervals for the presented sample median values and ANOVA testing ($p<0.0001$). The most affected locations are the mid and apical aspects of the anterior vaginal walls, where elasticity is decreasing up to 3.4 times from normal to POP Stage III. The lesser affected is the mid posterior part, where elasticity is decreased up to 2.2 times, the apical side walls of the vagina, where elasticity is decreased by 50%, and the mid sides of the vagina, where no statistically significant tissue elasticity decrease were detected [11]. That means the horizontal (anterior, posterior) support structures weaken the most under POP conditions.

These studies suggest that VTI may serve as a means for 3-D imaging of the vagina and a quantitative assessment of vaginal tissue elasticity, providing important information for furthering our understanding of pelvic organ prolapse and surgical treatment.

3.3. Detection of Pre-prolapse Conditions

The objective of next study was to estimate the ranges of normality for tissue elasticity of the vagina and pelvic floor support structures, and to explore the possibilities of 3D tactile imaging in early prolapse detection [68].

One hundred and thirty-six women were enrolled and examined using VTI in a case-control study to evaluate the method. Study subjects included 36 women with normal pelvic support, 11 women with stage I, 43 women with stage II, and 46 women with stage III prolapse. The average age was 56±22 years, with a range of 21 to 90 years. The VTI used the transvaginal probe shown in Figure 2 (probe 2) and a 6 Degree Of Freedom (DOF) motion tracking system. The transvaginal probe is comprised of two pressure sensor arrays, a temperature sensor, a micro-heater, and a motion tracking sensor. The first array contains 104 pressure sensors and is installed on the probe surface to contact the vaginal wall. The second array contains 12 pressure sensors and is mounted in the probe tip to contact the uterus during the examination procedure. The VTI examination was performed on patients in the dorsal lithotomy position with an empty bladder and rectum. The full VTI examination required 3 to 5 minutes to complete. Three orthogonal projections of the 3-D vaginal pressure map with the VTI probe location were observed in real-time by the operator. The VTI clinical operators were trained on pelvic floor models prior to the VTI clinical application to standardize imaging techniques. The examination procedure includes multiple compressions of the vaginal walls and allows a circumferential 3-D tactile image or pressure map of the vagina to be composed. The tissue elasticity, Young's modulus (E), was calculated from the spatial gradients in the resulting 3-D tactile images. A non-linear tissue deformation model used after having been validated with silicone samples with a known elasticity distribution (see section 2.2).

All 136 enrolled women were successfully examined with the VTI. 3-D images of the vagina and the surrounding structures were recorded and stored. The elasticity distribution and its variation for normal pelvic floor conditions were established. Substantial differences were found in the anatomy and tissue elasticity between normal and prolapse conditions. Specifically, changes from 150% to 300% in the

vaginal tissue elasticity were observed for stage II and III prolapse compared to normal conditions. The range of normality (normal pelvic support) for the tissue elasticity (Young's modulus; kPa) of the apical anterior is [5.3; 27]; the apical posterior is [4.4; 23]; the mid anterior is [6.7; 32]; the mid posterior is [8.0; 39]; and the mid lateral vaginal walls is [7.5; 31]. The results show that stage I prolapse cases have about 50% overlap with the ranges of the tissue elasticity for the normal conditions (Figure 10). The average value of the tissue elasticity for the anterior and posterior walls under prolapse stages II and III was estimated to be 2.9 ± 1.8 kPa; these cases have only about 5% overlap with the normal conditions [68].

[Figure 10]

The VTI enables the quantification of the vaginal tissue elasticity and the strong differentiation between normal and stage II and III prolapse conditions. The overlap in tissue elasticity between normal and stage I prolapse conditions means that a) in some cases under Stage I prolapse the tissue elasticity is the same as in normal conditions, or b) the normal case, as defined by the POPQ system, with lower values of Young's modulus, is already in the range for Stage I prolapse. In other words, the lower level of the normality range with the decreased tissue elasticity in Figure 10 may enable the detection of pre-prolapse conditions that require attention to delay the development of anatomically not observable prolapse conditions.

The pressure pattern on the surface of the vaginal wall under applied load reveals not only the elasticity conditions of the vaginal wall itself, but basically the elasticity distribution of the underlying structures. The greater the applied load from the probe, the deeper the structures surrounding the vagina may be visualized. The softer the tissues, the deeper the structures may be visualized by tactile imaging because these softer tissues may be deformed more. The elasticity values calculated at the mid lateral vaginal walls may be related to the conditions of the underlying puborectalis, levator ani, and obturator internus muscles; the mid posterior elasticity to the rectovaginal fascia and perineal body; the apical posterior elasticity to the uterosacral ligaments; and the anterior elasticity to vesical and pubocervical fascia. The pressure patterns on the surface of the vaginal walls together with the tissue displacement under the applied deformations can be considered as a documentation of the current elasticity state of the vagina and the pelvic floor support structures that are elements of biomechanical system providing a critically important set of physiological processes.

This study concluded that the normality ranges for the tissue elasticity of the vagina and the pelvic floor support structures evaluated by the VTI may be used as markers for characterizing pelvic floor conditions. It seems possible, at least in 50% of the cases, to use VTI for the detection of early pre-prolapse conditions not observed by the POPQ approach.

3.4. Changes with Age and Parity

The clinical data set presented in section 2.3.2 was analyzed to assess vaginal tissue elasticity measured with VTI in women across age and parity. Figure 11 presents the vaginal tissue elasticity distribution for the mid posterior region of the vagina across a range of age and parity. The average values of Young's modulus are reduced with age from 13.1±7.8 kPa to 6.14± 3.0 kPa and with parity from 15.3±9.7 kPa to 7.0±4.4 kPa.

[Figure 11]

In the apical anterior and posterior compartments, larger tissue elasticity changes were found. The average value of Young's modulus for the apical anterior vaginal compartment was 13.2±3.1 kPa for a group aged 28-35 years old, and 3.0±1.5 kPa for a group aged 76-90 years. The average value of tissue elasticity for the apical posterior vaginal compartment for the same age groups in comparison was 8.8±2.6 kPa and 2.6± 1.0 kPa, respectively. The apical anterior and posterior vaginal compartments of nulliparous women showed values Young's modulus of 10.4±4.2 kPa and 7.0±3.4 kPa, respectively. For women having 5-6 pregnancies the average values for tissue elasticity for the apical anterior and posterior compartments were 3.6±2.5 kPa and 2.8±2.2 kPa, respectively. It is important to note that the analyzed data set has poor correlation (r=0.21) between the age and parity.

This study suggests that, in vaginal tissues, Young's modulus may be affected by 77% due to age and by 66% due to childbirth.

3.5.

3.6. Tactile Imaging Markers

In another clinical study, VTI was performed on on 22 subjects with probe 3 (Figure 1) [12, 13]. The examination consisted of four tests: 1) probe insertion, 2) elevation, 3) rotation, and 4) muscle contraction. These tests yielded the following information:

- Test 1: Tactile image for the vaginal anterior and posterior compartments along the entire vagina; pressure gradients (elasticity) and anatomical measures.
- Test 2: Tactile image for apical anterior and posterior compartments related to pelvic floor support structures; pressure gradients and anatomical measurements.
- Test 3: Tactile images for left and right sides of vagina (circumferential tactile image from vaginal walls); anatomical measurements.
- Test 4: Dynamic pressure response from pelvic floor muscle contractions recorded from the opposite sides along the entire vagina; static and dynamic components.

Review of the tactile images revealed several anatomic areas with consistently observed pressure peaks across the VTI scans. These areas were selected as marker sites for further analysis. There were 2 anterior marker sites (A1, A2), 2 posterior sites (P1, P2), and 1 lateral site (L1). Specifically, the following locations along the pelvic floor were used for marker analysis: A1 – anterior in the vicinity of the hymen with maximum pressure feedback; A2 – Anterior and proximal to A1; P1 – posterior in the vicinity of hymen; P2 – posterior and proximal to P1; L1 – vaginal sides with maximum pressure peaks in the vicinity of hymen. Figure 12 illustrates the listed locations. Unlike the static locations of POPQ points (e.g., Aa & Ba), the pressure peaks used for A1, A2, B1, B2, L1 are not in fixed locations, but varied among the patients.

[Figure 12]

Figure 13-16 summarize the study results in boxplot panels and provide examples of acquired images for four tests [13].

[Figure 13]

[Figure 14]

[Figure 15]

[Figure 16]

The data showed that, in patients with prolapse, pressure gradient measurements decreased 2-4 fold (200%-400%) at specific locations (see Figure 13 panels B and D) which can be interpreted as being 2-4 fold softer compared to patients with normal support. Pelvic floor muscle contractive capabilities (muscle strengths) decrease up to 5 times (500%) in prolapse subjects compared to normal subjects (see Figure 16). These results demonstrate that women with prolapse have significant mechanical differences within the vaginal and surrounding pelvic floor supportive systems. In addition to recording tactile feedback during the tissue deformation, the VTI obtains measurement of muscle strength and allows evaluation of the relative functional impact of muscle contraction on measured biomechanical properties. Of the five pressure peaks observed during pelvic floor muscle squeezing (see Figure 16 panel E), site A1 (see Figure 16 panel E), is potentially exaggerated or an artifact because of the pubic bone, but this peak does have a lateral component which contradict sole resistance from the static structure. These peaks have a complex, dynamic pattern and require further investigation.

The results of this study demonstrate that the vaginal tactile images can be acquired and coupled with functional pelvic muscle assessment in one VTI examination [13].

3.7. Functional imaging

Vaginal Tactile Imaging was used to investigate the behavior of the pelvic floor muscles during Valsalva maneuver, voluntary muscle contraction, involuntary relaxation and involuntary contraction, in a group of 77 women, using probe 3 (Figure 1). The subjects were classified as being normal, having POP and having SUI [70, 71].The data analysis reveals the following findings (*will be links to 2015 AUGS and ICS video presentations*):

1) During Valsalva nonuniform pressure patterns are observed along the anterior and posterior compartments which are substantially different than those observed during pelvic floor muscle contraction. The high pressure zones correspond to softer tissues with low support capability; these high pressure zones (30-50 mmHg) appear to have been created by penetration of surrounding load through an internal strain (easily flexed). That means that this test allows detection of biomechanically weak structures and their locations.

2) Significant amplitude difference (i.e., the ratio in voluntary muscle contractions) for anterior *vs* posterior and left *vs* right side, which may allow recognizing of muscle avulsion and further characterization of their functional conditions. It seems possible to re-create their dynamics in 3-D.

3) During the involuntary muscle relaxation, the patient was asked to maintain a sustained pelvic muscle strain. By quantifying the pressure decline *vs* time (angle) at a region of interest or for specific muscle it seems possible to characterize functional conditions of multiple pelvic dynamic structures.

4) The pressure patterns during involuntary muscle contraction (cough) are substantially different from voluntary contractions as in amplitudes as well as in peak locations.

5) Patients with normal pelvic floor conditions demonstrate higher pressure applied amplitudes in both voluntary and involuntary muscle contractions than the patients with SUI.

6) The pressure patterns during involuntary muscle contraction (cough) with SUI conditions have distinctive structure from the patterns without SUI.

7) It seems possible to characterize functional conditions of multiple dynamic pelvic structures.

4. Summary

There is a complex relationship between the supportive ligaments, fascias and pelvic floor muscles to provide the resulting support and contribute into diseased conditions. Tactile imaging allows allocation and quantitative assessment of biomechanical defects such as changes in tissue elasticity at specified locations, possible muscle avulsion and weakness in muscle function within the pelvic floor.

VTI offers an opportunity to assess the vaginal support along the entire length of the anterior, posterior and lateral vaginal walls at rest, with manually applied deflection pressures and with voluntary and involuntary muscle contraction, involuntary relaxation and Valsalva maneuveres. This allows a large body of measurements to evaluate individual variations in support defects as well as identify specific potential markers to measure tissue properties as they correlate to pelvic floor support in patients with POP and/ or SUI. This technology gives the ability to measure pelvic floor muscle strength at specific locations along the vaginal wall and help correlate the relative contributions to measured tissue properties. These measurements provide insight into the pelvic floor function and conditions of the support structures, which in turn, will allow quantitative diagnostics of the affected or defective biomechanical components. There may be very important distinctions in muscle function between a patient with a large distention defect of the vaginal wall and a primary apical defect, symptomatic and asymptomatic prolapse or among patients with associated SUI or rectal complaints. For future studies, it would be important to evaluate symptom severity for pelvic floor disorders to determine whether there is a correlation between pelvic floor muscles function, resting tone and associated elasticity measurements of the underlying tissue. This may help further differentiate the types of pelvic floor conditions, their underlying severity and understand how to tailor treatments for the individual patient by the most effective manner.

To date, it has been challenging to combine functional anatomy with *in vivo* tissue properties. It would be extremely useful to correlate mechanical properties measured by the VTI with dynamic MRI and ultrasound measurements. The combination of these modalities, image fusions, anatomic and functional

valuation will provide the best assessment of pelvic floor conditions before making any decision about application of a cure.

5. Conclusions

- Tactile imaging VTI may serve as a means for 3-D imaging of the vagina and a quantitative assessment of vaginal tissue
- Tactile imaging provides biomechanical insight into POP development by evaluating pelvic floor conditions and functions
- Tactile Imaging may allow assessment of pelvic muscle conditions/defects which contribute into SUI by quantitative, anatomically sensitive and specific manner

Acknowledgements

The authors would like to thank Robin Haff, RN, BSN, and Alison Cooke, RN, for study coordination; Lioudmila Lipetskaia, MD, Miles Murphy, MD, Cristina Saiz, MD, Vladimir Kalis, MD, Zdenek Rusavy, MD, and Andrea Barker, PA, for participation in clinical studies; Randee Wood, MS, RDMS, for clinical research documentation and data management; Milind Patel, MS, for technical assistance with the device; Victor Kurtenok, BS, for electronics and firmware/software development, Noune Sarvazyan, PhD, MBA, for text editing assistance and project management.

The work was supported by the National Institute on Aging, USA, grant AG034714 “Vaginal Tactile Imager for Pelvic Floor Biomechanical Assessment”.

17 Emerging Imaging Technologies and Techniques

Kang Kim, Vladimir Egorov, and S. Abbas Shobeiri

Learning Objective

1. To learn the conceptual framework for shear wave elastography
2. To learn the conceptual framework for photoacoustic imaging
3. To understand the emerging field of vaginal tactile imaging

Ultrasound Elasticity Imaging

Since it was introduced in the early 1990s as a noninvasive tool to assess the tissue mechanical properties [1–3], ultrasound elasticity imaging, also known as ultrasound elastography or sono-elastography, has been widely used in pre-clinical and clinical settings [4–14]. In clinics, elastography is intended to yield additional visual and clinically valuable information of compliance overlaid on gray-scale B-mode morphological images.

Ultrasound elasticity imaging technologies have been applied on female reproductive systems.

Freehand ultrasound real-time elastography (RTE) was used in a pilot study in 12 healthy pregnant women who underwent transvaginal ultrasound. RTE was performed by applying light repetitive compression with the hand-held vaginal transducer over the area of interest. During this palpation procedure, real-time elastogram overlaid on B-mode image and full B-mode image were displayed side by side on the screen (Fig. 17.1), resulting in easy correlation between elasticity by color distribution and the anatomical structures. A general trend of overall increased elasticity of the cervix was found in this study with a limited number of subjects [15].

In the study conducted by Swiatkowska-Freund et al., 29 women who underwent term labor induction were evaluated by elastography. The cervix was scanned while being mildly compressed with the ultrasound probe. They reported a significant difference in mean elastography index of the internal os between the patients with successful induction and those with failed induction. On the other hand, tissues near the external os and the middle of the canal did not show similar trends. The authors observed that

K. Kim
Medicine and Heart and Vascular Institute, University of Pittsburgh Medical Center, Pittsburgh, PA, USA

University of Pittsburgh School of Medicine, Pittsburgh, PA, USA

V. Egorov
Technology Development, ARTANN Laboratories, Inc, West Trenton, NJ, USA

S. Abbas Shobeiri (✉)
Department of Obstetrics and Gynecology, Gynecologic Subspecialties, INOVA Women's Hospital, Virginia Commonwealth University, 3300 Gallows Road, Second Floor South Tower, Falls Church, VA 22042-3307, USA

Department of Bioengineering, George Mason University, Fairfax, VA 22030, USA
e-mail: Abbas.shobeiri@inova.org

© Springer International Publishing AG 2017

S. Abbas Shobeiri (ed.), *Practical Pelvic Floor Ultrasonography*, DOI 10.1007/978-3-319-52929-5_17

vegorov@artannlabs.com

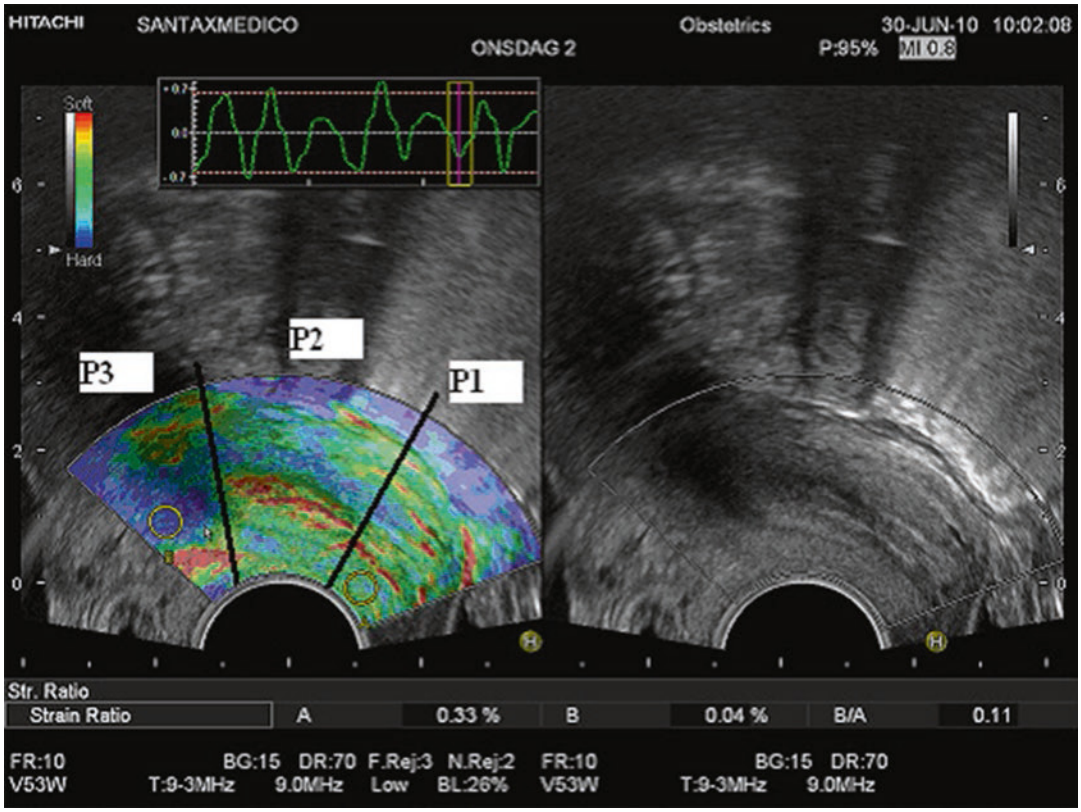

Fig. 17.1 The B-mode image (*right panel*) and the elastogram (*color*) overlaid on B-mode image (*left panel*) were displayed side by side. Lower part P1, middle part P2, upper part P3 (about one-third each) and the cervical channel. The strain ratio (*left*) in P1 is higher than the strain rate (*right*) in P3, which corresponds to the color distribution. (From Khalil et al. [15], with permission)

elastography "may guide decisions about need for cervical ripening before labor induction," noting that "the technology is limited without standardization between subjects" [16, 17]. In a cross-sectional study of 112 pregnant women at all points in gestation, no statistically significant difference between cervices was found. From the noticeable strain readings in the area where the compression was directly received, the authors addressed concerns that "measurements of rate-of-change in tissue displacement" may be "a mere reflection of the force being applied by the transducer" and might not "reflect histological changes that could provide a measure of cervical ripening." A serious step has to be taken for standardizing compression procedures that can vary between scans and subjects before elastography can be a reliable clinical tool [17, 18]. It also should be noted that the underlying structures of women's reproductive systems are complex, making it more challenging to apply pressure in a standardized way.

Acoustic Radiation Force Impulse and Shear Wave Elasticity Imaging (ARFI and SWEI) of the Cervix and Uterus

An operator-independent method that does not require standardization would be ideal. Instead of applying compression using an ultrasound probe, acoustic radiation force due to focused ultrasound can be used for remote and controlled palpation: (1) monitoring the tissue response in displacement within the radiation force region of excitation (ROE) and generating images of relative differences in tissue stiffness (acoustic radiation

vegorov@artannlabs.com

force impulse [ARFI] imaging); and (2) monitoring the speed of shear wave propagation away from the ROE to quantify tissue stiffness (shear wave elasticity imaging [SWEI]). In response to electronically controlled acoustic radiation force, the resulting tissue displacement and the shear wave propagation speed directly reflect stiffness of the underlying tissue [19]. The ability of SWEI to classify ripened versus unripened tissue samples was assessed by Carson et al. using excised human hysterectomy samples. The authors stated that "if the location is accounted for, comparisons between patients can distinguish between ripened versus unripened subjects" [20].

In their human subject study, Su et al. applied ARFI and SWEI ultrasound imaging of the uterine cervix on 58 patients with pathologically confirmed cervical cancer prior to surgery. They found a statistically significant difference between the malignant lesions (stiff) and normal cervical tissues (soft). With relatively high sensitivity and specificity in the evaluation of cervical cancer, the authors stated that ARFI or SWEI can be an objective method for stiffness assessment and "may have good diagnostic value in clinical applications" [21]. In a case study of two subjects with strongly suspected leiomyosarcoma and leiomyoma, Furukawa et al. reported that SWEI can be a useful method for diagnosing uterine smooth muscle tumors (Fig. 17.2) [22].

Gennisson et al. applied SWEI on the cervix and uterus of women during pregnancy, which enabled the quantification of cervix elasticity, the follow-up of uterine elasticity during contraction, and the investigation of uterine anisotropy. In their study, cervix elasticity was quantified in 20 gravid women using a 7 MHz endocavitary probe. Uterus elasticity was quantified externally on 5 patients, through the abdomen, using an 8 MHz linear probe. Changes of elasticity were monitored in real time during uterus contraction (Fig. 17.3). SWEI was performed with the same probe by assessing shear wave speed variations with respect to probe angle, which allowed the investigation of uterine anisotropy at different depths. Elasticity values during contraction were correlated to a gold standard of uterine pressure measure [23].

In the study conducted by Tanaka et al., to investigate whether baseline stiffness of the uterine corpus and cervix changed after placental delivery, SWEI was applied on 11 patients with normal vaginal delivery before, immediately after, and 1 and 2 h after placental delivery. It was found that "the stiffness of the uterine corpus significantly changed over time, although that of the uterine cervix was not significantly altered." The authors also reported that (1) "The stiffness of the uterine corpus was significantly higher immediately after and 1 and 2 h after placental delivery as compared with that before placental delivery," and (2) "The uterine corpus had a significantly higher stiffness than the uterine cervix at each of the four time points examined" [24]. While some effects due to acoustic attenuation at depth are

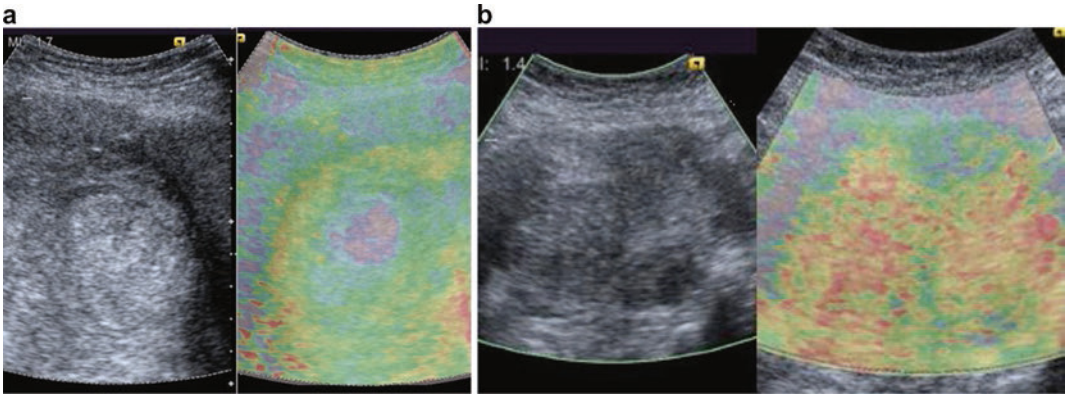

Fig. 17.2 Ultrasound images of uterine leiomyosarcoma (**a**) and leiomyoma (**b**). *Left:* Ultrasound B-mode image. *Right*: Acoustic radiation force impulse (ARFI) image. Irregular distribution of *blue*, *yellow*, *green,* and *red* was seen in the ARFI image, suggesting a heterogeneous inner structure. Notable *blue* was present in high echoic spots shown on *gray-scale* imaging. (From Furukawa et al. [22], with permission)

vegorov@artannlabs.com

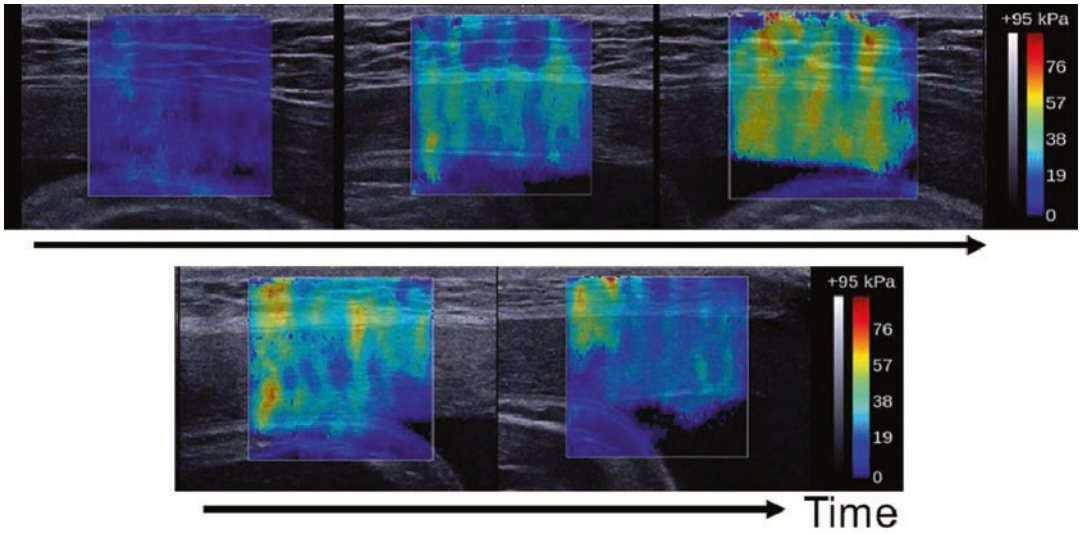

Fig. 17.3 Snapshot of the quantified elasticity map of the uterus during contraction. (From Gennisson et al. [23], with permission)

naturally expected, Hernandez-Andrade et al. demonstrated that depth from the ultrasound probe to different regions in the cervix did not significantly affect the shear wave speed estimations in the cervix of 154 pregnant women at 11–36 weeks of gestation [25].

Using tissue motion tracking methods, some important information associated with dynamic responses of the pelvic floor muscles (PFM) to potentially incontinence-producing stress, which cannot be readily captured and assimilated by the observer during the scanning process, was assessed by Peng et al. In their study, perineal ultrasonography was performed on 22 asymptomatic females and nine stress urinary incontinent (SUI) patients with a broad age distribution and parity. The ventral dorsal and cephaladcaudal movements of the anorectal angle were resolved, and kinematic parameters, in terms of displacement, trajectory, velocity, and acceleration were analyzed. The results revealed the possible mechanisms of PFM responses to prevent the urine from incontinence in fast and stress events. The statistical analyses showed the PFM responses of the healthy subjects and the SUI patients are significantly different in both the supine and standing experiments [26].

Photoacoustic Imaging of Ovarian Tissue and the Cervical Canal

Photoacoustic (PA) technology is the promising state-of-the-art medical imaging modality to provide a non-invasive quantitative optical contrast, at depth, and in real-time by using energy conversion from absorbed light energy to acoustic wave in tissue [27–29]. Salehi et al. used a hand-held transvaginal probe they designed for co-registered photoacoustic and ultrasound imaging to image ex vivo benign and malignant human ovaries (Fig. 17.4). They were able to produce co-registered images that displayed different vasculature distributions on the surface of the benign cyst and the malignant ovary [30, 31].

Using their 1.75-D array transducer, Aguirre et al. imaged normal porcine ovarian tissue as compared to histological images (see Fig. 17.4). The authors stated that their results showed excellent co-registration of ultrasound and photoacoustic images. They described strong optical absorption from vasculature, especially highly vascularized corpus luteum and low absorption from follicles [32].

vegorov@artannlabs.com

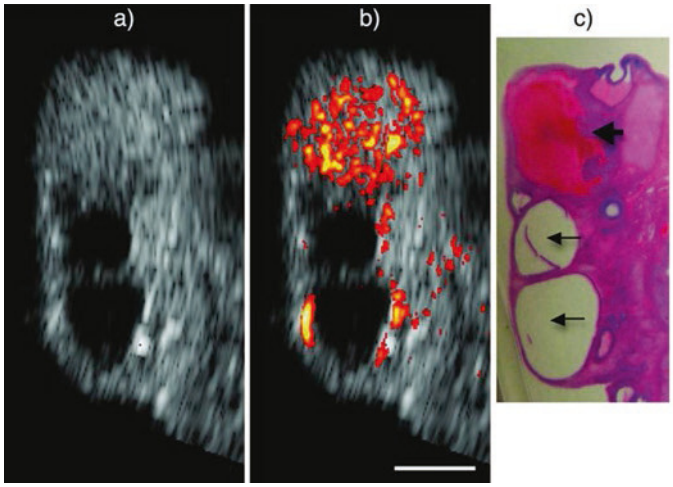

Fig. 17.4 Co-registered image of ovary 3. (**a**) Ultrasound-only image. **(b)** Photoacoustic image on top of the ultrasound image. (**c**) Hematoxylin and eosin (H&E) stained histological slide. The *white bar* represents 5 mm. (From Aguirre et al. [32], with permission)

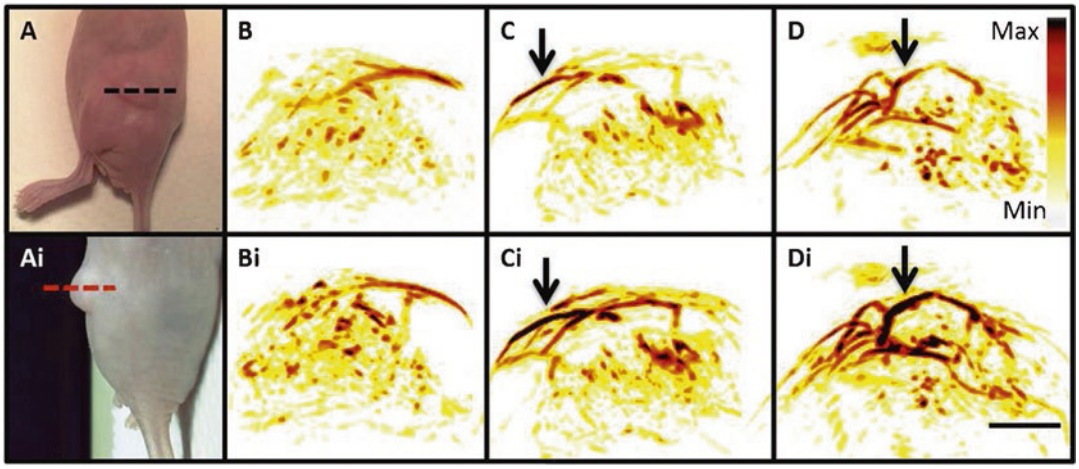

Fig. 17.5 Photoacoustic imaging of mouse tumor. *Panels A* and *Ai* are two different views of the imaging plane used to create the renderings in panels *B–D* (*dashed lines*). The top images are before injection of carbon-based nanopipettes (CNPs) and lower panels denoted by "*i*" are post-injection. *B,* no injection; *C,* 1.2 mg/mL; and *D,* 2.4 mg/mL. *Intensity bar* in *D* applies to all images, as does the *scale bar* in *Di*, which represents 3 mm. *Arrows* highlight regions with particularly increased photoacoustic contrast in post-injection images. (From Jokerst et al. [34], with permission)

Photoacoustic imaging (PAI) is sensitive to the abnormal angiogenesis deep in biological tissue, and may be capable of intact scanning both around the external orifice and in cervical canal. With this hypothesis, Peng et al. applied PAI on 30 human tissue sample harvested from the cervical canal by biopsy during a cervical colposcopical screening. They reported stronger absorption from the cervical lesions compared to normal tissue. The estimated mean optical absorption from PAI between normal tissue and cervical lesion exhibited statistically significant difference [33].

Using cellulose-based nanoparticles with a peak photoacoustic signal of 700 nm, photoacoustic imaging was applied on a mouse model of human ovarian cancer (Fig. 17.5). An obvious increase of photoacoustic signal intensity in the tumor was observed when the pre-injection images (*Panels B-D*) were compared to the post-injection (*Panels Bi-Di*). Of note, the cellulose-based nanoparticles were shown to biodegrade in the presence of cellulose, a naturally occurring enzyme, indicating important advantages for clinical translation [34].

vegorov@artannlabs.com

Tactile Imaging of the Female Pelvic Floor

At the end of the last century, a technology named elastography, or elasticity imaging (EI), for measuring and visualizing soft tissue viscoelastic characteristics, emerged and the ancient art of palpation gained new life [35]. The areas of applications of EI in medical diagnostics and treatment monitoring are steadily expanding. It has been shown that the elasticity of soft tissue is highly sensitive to its structure and conditions. The range of variation of the Young's modulus of soft tissues is over three orders of magnitude, from a fraction of kPa to hundreds of kPa and appears to be one of the most sensitive physical characteristics of soft tissue, yielding valuable diagnostic information [5, 36]. Many pelvic floor disorders, including prolapse, SUI, sexual dysfunction, congenital anomalies, and others, are clearly manifested in the mechanical properties of pelvic structures. Therefore, the ability of EI to map elasticity of pelvic floor opens new possibilities in the biomechanical assessment and monitoring of pelvic floor conditions [37, 38]. EI technique based on tactile imaging additionally allows measuring muscle contraction capability.

Tactile imaging (TI), also called "mechanical imaging," is a medical imaging modality that translates the sense of touch into a digital image. The tactile image is a function of $P(x,y,z)$, where P is the pressure on soft tissue surface under applied deformation, and x,y,z are coordinates where pressure P was measured [39, 40]. The tactile image is a pressure map on which the direction of tissue deformation must be specified [40].

Functional Tactile Imaging

Functional tactile imaging (FTI) is a variation of TI that translates muscle activity into a dynamic pressure pattern $P(x,y,t)$ for an area of interest, where t is time and x,y are coordinates where pressure P was measured. Muscle activity to be studied may include a voluntary contraction (e.g., a pelvic floor squeeze), an involuntary reflex contraction (e.g., due to a cough), an involuntary relaxation, or a Valsalva (veering down) maneuver [41, 42].

A vaginal tactile imaging (VTI) probe, as shown in Fig. 17.6**,** is equipped with 96 pressure (tactile) sensors laid out at every 2.5 mm along the both sides of the probe, an orientation sensor (accelerometer), and temperature sensors with micro-heaters [43]. During the clinical procedure, the probe is used to acquire pressure responses from the vaginal walls. The VTI examination procedure includes data collection from all segments of the vagina. During an examination, data are sampled from the probe sensors and displayed on the VTI monitor in real time. The resulting pressure maps (tactile images) of the vagina integrate all of the acquired pressure and positioning data for each of the pressure-sensing elements. In addition, the VTI records the dynamic contraction for pelvic floor muscles.

The Vaginal Tactile Imager, model 2S (Advanced Tactile Imaging, Artann Laboratories, West Trenton, NJ, USA), includes data analysis tools and reporting functions. It visualizes the anatomy of the vagina, incorporating spatial measurements, pressure levels, calculated pressure gradients within the pressure maps, and assesses pelvic floor muscle contraction capability (muscle strength) (Fig. 17.7). The examination procedure allows eight clinical tests (Table 17.1).

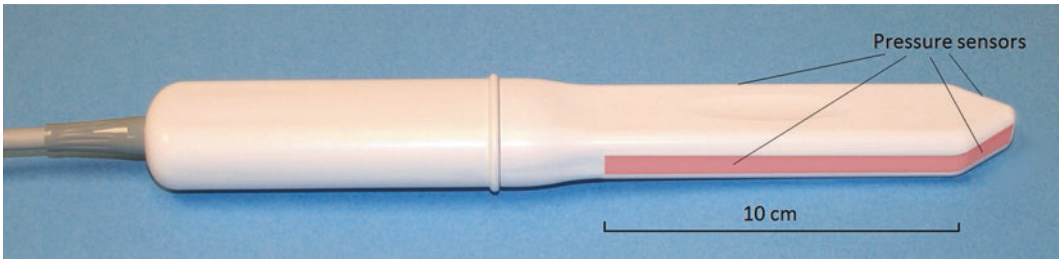

Fig. 17.6 The Vaginal Tactile Imager, model 2S (Advanced Tactile Imaging, Artann Laboratories, West Trenton, NJ, USA). Pressure sensors are aligned on the outer surface of the probe (*highlighted*)

vegorov@artannlabs.com

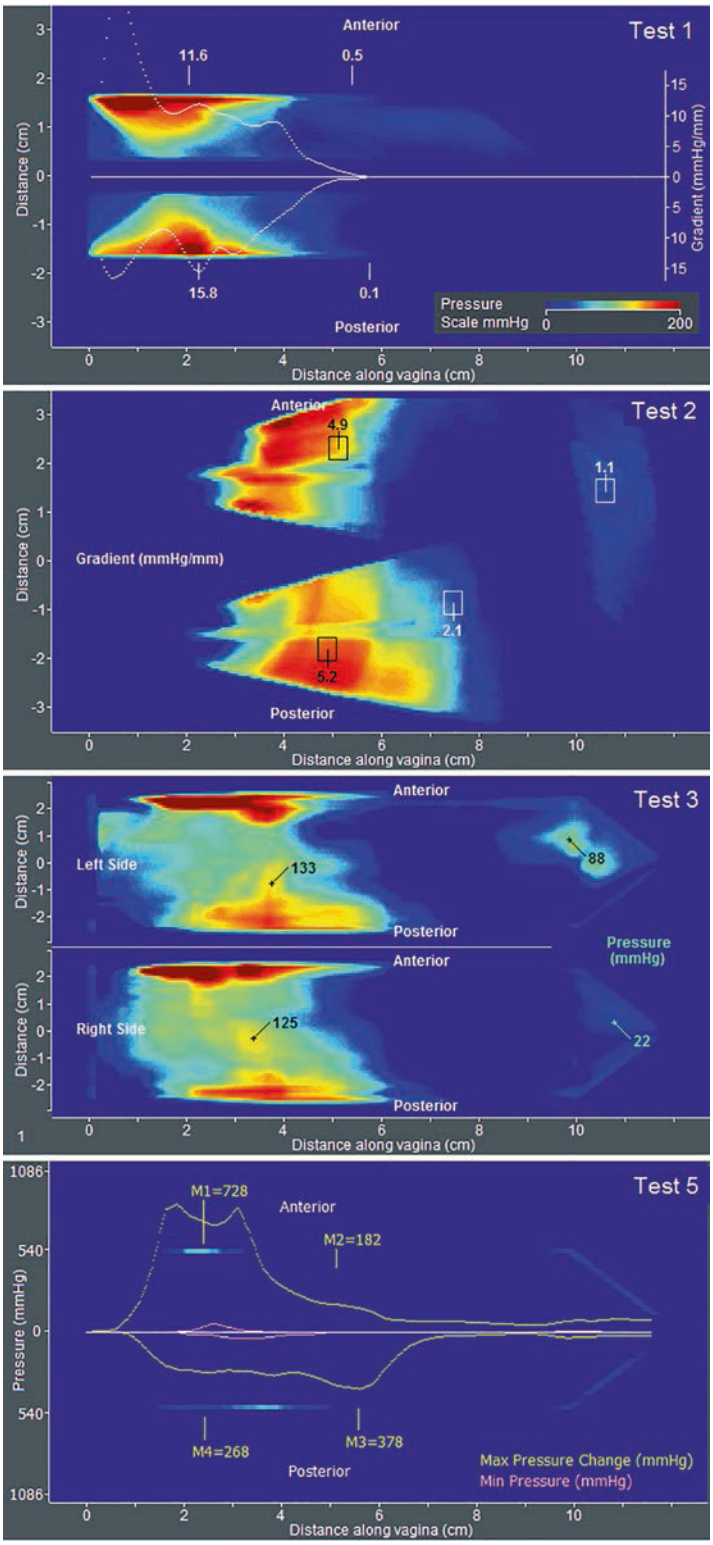

Fig. 17.7 Clinical imaging results acquired with the Vaginal Tactile Imager (Advanced Tactile Imaging, Artann Laboratories, West Trenton, NJ, USA) for 26-year-old subject with normal pelvic floor support, Test 1: Probe insertion; Test 2: Probe elevation; Test 3: Probe rotation; and Test 5: Voluntary pelvic floor muscle contraction

vegorov@artannlabs.com

Table 17.1 Examination procedure and test description of the Vaginal Tactile Imager, model 2S (Advanced Tactile Imaging, Artann Laboratories, West Trenton, NJ, USA)

Test	Description
Test 1: Probe insertion	Tactile image for vaginal anterior and posterior compartments along the entire vagina; pressure gradients and anatomical sizes can be calculated
Test 2: Probe elevation	Tactile image for apical anterior and posterior compartments, relating to pelvic floor support structures; pressure gradients and anatomical sizes can be calculated
Test 3: Probe rotation	Tactile images for left and right sides of vagina (circumferential tactile image from vaginal walls); anatomical sizes can be calculated
Test 4: Valsalva maneuver	Dynamic pressure response from pelvic floor muscle contractions during Valsalva maneuver is recorded from anterior and posterior for along the entire vagina
Test 5: Voluntary muscle contraction (anterior vs. posterior)	Dynamic pressure response during voluntary pelvic floor muscle contractions is recorded from anterior and posterior along the entire vagina
Test 6: Voluntary muscle contraction (left vs. right side)	Dynamic pressure response during voluntary pelvic floor muscle contractions is recorded from left and right sides along the entire vagina
Test 7: Involuntary muscle relaxation	Dynamic pressure response during involuntary muscle relaxations is recorded from anterior and posterior along the entire vagina
Test 8: Involuntary muscle contraction	Dynamic pressure response during a cough is recorded from anterior and posterior along the entire vagina

The tactile imaging markers, sensitive to the pelvic organ prolapse (POP) conditions, were analyzed for VTI tests 1-4 (as listed in Table 17.1) in a pilot clinical study with 22 subjects [40, 43]. Nine markers were found sensitive to POP conditions ($P < 0.05$ for one-way ANOVA [analysis of variance] and/or $P < 0.05$ for t-test with correlation factor r from −0.73 to −0.56) [44, 45]. Multiple pressure peaks are observed during the pelvic floor muscle contractions. The list of markers (parameters) includes pressure, pressure gradient, and dynamic pressure response during muscle contraction at identified locations. These parameters may be used for biomechanical characterization of female pelvic floor conditions to support an effective management of pelvic floor prolapse.

The data analysis completed for VTI tests 4-8 in another clinical study with 26 subjects allowed the conclusion that pressure mapping during Valsalva maneuver, pelvic floor muscle contractions, and involuntary relaxation also may be used for quantitative characterization of POP [41]. Functional imaging of the pelvic floor muscles may offer a needed insight into the biomechanics of the functional pelvic floor to help understand the relative contribution of pelvic floor muscles in POP development and its effective treatment. Significant amplitude deference was observed in voluntary muscle contractions for the anterior vs. posterior and left vs. right side, which may allow recognition of muscle avulsion and further characterization of their functional conditions; the pressure patterns during involuntary muscle contraction (e.g., cough) are substantially different from voluntary contractions in amplitudes as well as in peak locations; patients with normal pelvic floor conditions demonstrate higher pressure applied amplitudes in both voluntary and involuntary muscle contractions than the patients with SUI; the pressure patterns during involuntary muscle contraction (cough) with SUI conditions have distinctive structure from the patterns without SUI [42].

Summary

While ultrasonography visualizes the integrity of structures and dynamics of movement, elastography and vaginal tactile imaging aim to quantify the properties of visualized structures. The ideal pelvic floor imaging modality would ultimately combine the 3D ultrasound and elastography/VTI capabilities into one single modality.

vegorov@artannlabs.com

References

1. Lerner RM, Parker KJ, Holen J, Gramiak R, Waag RC. Sono-elasticity: medical elasticity images derived from ultrasound signals in mechanically vibrated targets. In: Kessler LW, editor. Acoustical imaging. Vol. 16. Proceedings of the Sixteenth International Symposium, June 10–12, 1987. New York/London:Plenum Press; 1988. p. 317–27.
2. Ophir J, Céspedes I, Ponnekanti H, Yazdi Y, Li X. Elastography: a quantitative method for imaging the elasticity of biological tissues. Ultrason Imaging. 1991;13(2):111–34.
3. Skovoroda AR, Emelianov SY, Lubinski MA, Sarvazyan AP, O'Donnell M. Theoretical analysis and verification of ultrasound displacement and strain imaging. IEEE Trans Ultrason Ferroelectr Freq Control. 1994;41(3):302–13.
4. Gao L, Parker KJ, Lerner RM, Levinson SF. Imaging of the elastic properties of tissue—a review. Ultrasound Med Biol. 1996;22(8):959–77.
5. Sarvazyan A, Hall TJ, Urban MW, Fatemi M, Aglyamov SR, Garra BS. An overview of elastography – an emerging branch of medical imaging. Curr Med Imaging Rev. 2011;7(4):255–82.
6. Zaleska-Dorobisz U, Kaczorowski K, Pawluś A, Puchalska A, Inglot M. Ultrasound elastography - review of techniques and its clinical applications. Adv Clin Exp Med. 2014;23(4):645–55.
7. Ribbers H, Lopata RG, Holewijn S, Pasterkamp G, Blankensteijn JD, de Korte CL. Noninvasive two-dimensional strain imaging of arteries: validation in phantoms and preliminary experience in carotid arteries in vivo. Ultrasound Med Biol. 2007;33(4):530–40.
8. Hall TJ, Zhu Y, Spalding CS. In vivo real-time freehand palpation imaging. Ultrasound Med Biol. 2003;29(3):427–35.
9. Kim K, Johnson LA, Jia C, Joyce JC, Rangwalla S, Higgins PDR, Rubin JM. Noninvasive ultrasound elasticity imaging (UEI) of Crohn's disease: animal model. Ultrasound Med Biol. 2008;34(6):902–12.
10. Burnside ES, Hall TJ, Sommer AM, Hesley GK, Sisney GA, Svensson WE, et al. Differentiating benign from malignant solid breast masses with US strain imaging. Radiology. 2007;245(2):401–10.
11. Luo J, Fujikura K, Homma S, Konofagou EE. Myocardial elastography at both high temporal and spatial resolution for the detection of infarcts. Ultrasound Med Biol. 2007;33(8):1206–23.
12. Rubin JM, Xie H, Kim K, Weitzel WF, Emelianov SY, Aglyamov SR, et al. Sonographic elasticity imaging of acute and chronic deep venous thrombosis in humans. J Ultrasound Med. 2006;25(9):1179–86.
13. Stidham RW, Xu J, Johnson LA, Kim K, Moons DS, McKenna BJ, et al. Ultrasound elasticity imaging for detecting intestinal fibrosis and inflammation in rats and humans with Crohn's disease. Gastroenterology. 2011;141(3):819–26.e1.
14. Weitzel WF, Kim K, Rubin JM, Wiggins RC, Xie H, Chen X, et al. Feasibility of applying ultrasound strain imaging to detect renal transplant chronic allograft nephropathy. Kidney Int. 2004;65(2):733–6.
15. Khalil MR, Thorsen P, Uldbjerg N. Cervical ultrasound elastography may hold potential to predict risk of preterm birth. Dan Med J. 2013;60(1):A4570.
16. Swiatkowska-Freund M, Preis K. Elastography of the uterine cervix: implications for success of induction of labor. Ultrasound Obstet Gynecol. 2011;38(1):52–6.
17. Feltovich H, Hall TJ, Berghella V. Beyond cervical length: emerging technologies for assessing the pregnant cervix. Am J Obstet Gynecol. 2012;207(5):345–54.
18. Molina FS, Gómez LF, Florido J, Padilla MC, Nicolaides KH. Quantification of cervical elastography: a reproducibility study. Ultrasound Obstet Gynecol. 2012;39(6):685–9.
19. Nightingale K. Acoustic radiation force impulse (ARFI) imaging: a review. Curr Med Imaging Rev. 2011;7(4):328–39.
20. Carlson LC, Feltovich H, Palmeri ML, del Rio AM, Hall TJ. Statistical analysis of shear wave speed in the uterine cervix. IEEE Trans Ultrason Ferroelectr Freq Control. 2014;61(10):1651–60.
21. Su Y, Du L, Wu Y, Zhang J, Zhang X, Jia X, et al. Evaluation of cervical cancer detection with acoustic radiation force impulse ultrasound imaging. Exp Ther Med. 2013;5(6):1715–9.
22. Furukawa S, Soeda S, Watanabe T, Nishiyama H, Fujimori K. The measurement of stiffness of uterine smooth muscle tumor by elastography. SpringerPlus 2014;3:294. doi:10.1186/2193-1801-3-294.
23. Gennisson JL, Muller M, Ami O, Kohl V, Gabor P, Musset D, Tanter M. Shear wave elastography in obstetrics: quantification of cervix elasticity and uterine contraction. In: 2011 IEEE International Ultrasonics Symposium, Orlando, FL. 2011. p. 2094–7. doi: 10.1109/ULTSYM.2011.0519. Accessed 21 Nov 2016.
24. Tanaka T, Makino S, Saito T, Yorifuji T, Koshiishi T, Tanaka S, et al. Attempt to quantify uterine involution using acoustic radiation force impulse before and after placental delivery. J Med Ultrason. 2010;38(1):21–5.
25. Hernandez-Andrade E, Aurioles-Garibay A, Garcia M, Korzeniewski SJ, Schwartz AG, Ahn H, et al. Effect of depth on shear-wave elastography estimated in the internal and external cervical os during pregnancy. J Perinat Med. 2014;42(5):549–57.
26. Peng Q, Jones R, Shishido K, Constantinou CE. Ultrasound evaluation of dynamic responses of female pelvic floor muscles. Ultrasound Med Biol. 2007;33(3):342–52.
27. Ntziachristos V. Going deeper than microscopy: the optical imaging frontier in biology. Nat Methods. 2010;7(8):603–14.

vegorov@artannlabs.com

28. Emelianov SY, Li PC, O'Donnell M. Photoacoustics for molecular imaging and therapy. Phys Today. 2009;62(8):34–9.
29. Wang LV, Hu S. Photoacoustic tomography: in vivo imaging from organelles to organs. Science. 2012;335(6075):1458–62.
30. Salehi HS, Kumavor PD, Li H, Alqasemi U, Wang T, Xu C, Zhu Q. Design of optimal light delivery system for co-registered transvaginal ultrasound and photoacoustic imaging of ovarian tissue. Photoacoustics. 2015;3(3):114–22.
31. Salehi HS, Wang T, Kumavor PD, Li H, Zhu Q. Design of miniaturized illumination for transvaginal co-registered photoacoustic and ultrasound imaging. Biomed Opt Express. 2014;5(9):3074–9.
32. Aguirre A, Guo P, Gamelin J, Yan S, Sanders MM, Brewer M, Zhu Q. Coregistered three-dimensional ultrasound and photoacoustic imaging system for ovarian tissue characterization. J Biomed Opt. 2009;14(5):054014. doi:10.1117/1.3233916.
33. Peng K, He L, Wang B, Xiao J. Detection of cervical cancer based on photoacoustic imaging—the in-vitro results. Biomed Opt Express. 2014;6(i):135–43.
34. Jokerst JV, Van de Sompel D, Bohndiek SE, Gambhir SS. Cellulose nanoparticles are a biodegradable photoacoustic contrast agent for use in living mice. Photoacoustics. 2014;2(3):119–27.
35. Sarvazyan AP. Elastic properties of soft tissues. In: Levy M, Bass HE, Stern RR, editors. Handbook of elastic properties of solids, liquids and gases, vol. 3. New York: Academic Pres; 2001. p. 107–27.
36. Sarvazyan A, Egorov V. Mechanical imaging - a technology for 3-D visualization and characterization of soft tissue abnormalities: a review. Curr Med Imaging Rev. 2012;8(1):64–73.
37. Egorov V, van Raalte H, Sarvazyan A. Vaginal tactile imaging. IEEE Trans Biomed Eng. 2010;57(7):1736–44.
38. Egorov V, van Raalte H, Lucente V. Quantifying vaginal tissue elasticity under normal and prolapse conditions by tactile imaging. Int Urogynecol J. 2012;23(4):459–66.
39. Sarvazyan A. Mechanical imaging: a new technology for medical diagnostics. Int J Med Inform. 1998;49(2):195–216.
40. van Raalte H, Egorov V. Characterizing female pelvic floor conditions by tactile imaging. Int Urogynecol J. 2015;26(4): 607–9 (with video supplement).
41. van Raalte H, Lucente V, Egorov V. High definition pressure mapping of the pelvic floor muscles during Valsalva manever, voluntary muscle contraction and involuntary relaxation (abstract). In: American Urogynecologic Society 36th Annual Meeting, Seattle, WA, 13–17 Oct 2015.
42. van Raalte H, Lucente V, Egorov V. Pressure mapping of voluntary and involuntary muscle contraction for assessment of SUI conditions (abstract). In: International Continence Society 45th Annual Meeting. Montreal, Canada, 6–9 Oct 2015.
43. van Raalte H, Egorov V. Tactile imaging markers to characterize female pelvic floor conditions. Open J Obstet Gynecol. 2015;5(9):505–15.
44. Egorov V, Sarvazyan AP. Mechanical imaging of the breast. IEEE Trans Med Imaging. 2008;27(9):1275–87.
45. Egorov V, Ayrapetyan S, Sarvazyan AP. Prostate mechanical imaging: 3-D image composition and feature calculations. IEEE Trans Med Imaging. 2006;25(10):1329–40.

vegorov@artannlabs.com

International Journal of Women's Health

Dovepress
open access to scientific and medical research

Open Access Full Text Article

ORIGINAL RESEARCH

Biomechanical paradigm and interpretation of female pelvic floor conditions before a treatment

Vincent Lucente[1]
Heather van Raalte[2]
Miles Murphy[1]
Vladimir Egorov[3]

[1]The Institute for Female Pelvic Medicine and Reconstructive Surgery, Allentown, PA, USA; [2]Princeton Urogynecology, Princeton, NJ, USA; [3]Artann Laboratories, Trenton, NJ, USA

Background: Further progress in restoring a woman's health may be possible if a patient with a damaged pelvic floor could undergo medical imaging and biomechanical diagnostic tests. The results of such tests could contribute to the analysis of multiple treatment options and suggest the optimal one for that patient.

Aim: To develop a new approach for the biomechanical characterization of vaginal conditions, muscles, and connective tissues in the female pelvic floor.

Methods: Vaginal tactile imaging (VTI) allows biomechanical assessment of the soft tissue along the entire length of the anterior, posterior, and lateral vaginal walls at rest, with manually applied deflection pressures and with muscle contraction, muscle relaxation, and Valsalva maneuver. VTI allows a large body of measurements to evaluate individual variations in tissue elasticity, support defects, as well as pelvic muscle function. Presuming that 1) the female pelvic floor organs are suspended by ligaments against which muscles contract to open or close the outlets and 2) damaged ligaments weaken the support and may reduce the force of muscle contraction, we made an attempt to characterize multiple pelvic floor structures from VTI data.

Results: All of the 138 women enrolled in the study were successfully examined with the VTI. The study subjects have had normal pelvic support or pelvic organ prolapse (stages I–IV). The average age of this group of subjects was 60±15 years. We transposed a set of 31 VTI parameters into a quantitative characterization of pelvic muscles and ligamentous structures. Interpretation of the acquired VTI data for normal pelvic floor support and prolapse conditions is proposed based on biomechanical assessment of the functional anatomy.

Conclusion: Vaginal tactile imaging allows biomechanical characterization of female pelvic floor structures and tissues in vivo, which may help to optimize treatment of the diseased conditions such as prolapse, incontinence, atrophy, and some forms of pelvic pain.

Keywords: female pelvic floor, biomechanics, diagnostic, treatment, tactile imaging, tissue elasticity, pelvic muscles

Introduction

The interaction between the anatomic structures of the female pelvic floor anatomy and their inter-related functions are among the most complex in the human body. Therefore, true understanding of how to best restore function that has been lost due to anatomic changes can be extremely problematic. The female pelvic floor comprises a bladder with urethra for storage and evacuation of urine, a uterus with cervix, a vagina for reproductive and sexual function, and a rectum with anus for storage and elimination of stool, along with a complicated and interdependent muscular web with its required neuronal innervation and variable connective tissues. Together, they are protected by and are structurally dependent on the surrounding pelvic bones. The multitasking

Correspondence: Vladimir Egorov
Artann Laboratories, 1459 Lower Ferry Rd, Trenton, NJ 08618, USA
Tel +1 609 883 0100
Email vegorov@artannlabs.com

submit your manuscript | www.dovepress.com
Dovepress
http://dx.doi.org/10.2147/IJWH.S136989

© 2017 Lucente et al. This work is published and licensed by Dove Medical Press Limited. The full terms of this license are available at https://www.dovepress.com/terms.php and incorporate the Creative Commons Attribution – Non Commercial (unported, v3.0) License (http://creativecommons.org/licenses/by-nc/3.0/). By accessing the work you hereby accept the Terms. Non-commercial uses of the work are permitted without any further permission from Dove Medical Press Limited, provided the work is properly attributed. For permission for commercial use of this work, please see paragraphs 4.2 and 5 of our Terms (https://www.dovepress.com/terms.php).

and codependence of these structures create the inherent nature whereby, more often than not, pelvic floor disease conditions are often interrelated. As a result of the various types of trauma and injury that can be sustained to the soft tissues of the human pelvic floor during a vaginal delivery, along the typical degree of mechanical stress and strain to the pelvic floor with extended life expectancy, many women have clinically relevant pelvic floor problems at some point in their lifetime.[1–6]

Female pelvic floor multitasking is realized at a macro level as a result of biomechanical actions (micturition, defecation, intercourse, pregnancy, childbirth). Active muscle structures play a role as the basic drivers required to release or apply pressure for specific task completion. Passive connective tissue attachments keep the pelvic organs in the proper three-dimensional (3D) spatial orientation, so that they may be optimally "acted on" by the pelvic floor musculature.[7–9] The complex biomechanical actions, such as urination or voluntary control of defecation, cannot be completed in a normal manner if muscular or connective tissues have altered mechanical properties (passive and/or active). As the pelvic floor muscle resting tone decreases and connective tissue (ligament) laxity ensues, a significant anatomic distortion can develop, which could lead to a decrease in contractive capabilities and physiologic malfunction. Even more damaging can be the avulsion of pelvic floor muscle and more severe connective tissue disruption, which are not readily reversible without a surgical intervention. The intent of this manuscript is to demonstrate how one can evaluate these changes in the mechanical properties of pelvic floor structures (muscular and connective tissues) using vaginal tactile imaging to gain a better understanding of an individual patient's pelvic floor dysfunction, and thereby ultimately improve guidance toward optimal selection from the various surgical and nonsurgical therapeutic choices available.

Perhaps the greatest frustration the surgeons specializing in female pelvic reconstructive procedures encounter during their career is that the restoration of pelvic floor anatomy does not necessarily lead to functional recovery. The reasons are not well understood, but no doubt include the following:

- suboptimal or absence of biomechanical assessment and a misdiagnosis or an underappreciation of the pelvic floor defects as a result;
- a pelvic reconstructive surgeon proposes/selects a pelvic floor treatment from a limited list she/he feels proficient with vs all the options and approaches that are available to choose from; and
- limitations in the overall success rates of applied treatments to address the full spectrum of symptoms a patient may present with.

As a result, a surgeon may routinely perform a midline plication of the fibromuscular wall of the vagina for a Stage IIB cystocele in patients who actually have an apical detachment of DeLancey Level I support, because he/she does not feel comfortable performing any of the apical suspension procedures and/or did not properly diagnose the true underlying biomechanical defect. This scenario and other contributing factors help explain why surgical failure rate of correction of anterior compartmental defects is often quite high.[10–12]

Further progress in restoring women's health may be possible if a patient with a problematic pelvic floor condition could undergo very detailed imaging and biomechanical diagnostic tests; the results of such tests could be fed into a structured patient-specific diagnostic workflow to consider multiple treatment options and to suggest the optimal one to treat that unique patient. Global biomechanical assessment of the pelvic floor and then tailoring treatment of its biomechanical dysfunction is the logical route to improve clinical success (Figure 1); this is the preferred process.

The ultimate goal of this research is to develop an improved patient-specific approach for diagnostic biomechanical characterization of basic support and functional components in the female pelvic floor. This approach is based on our current understanding of female pelvic floor

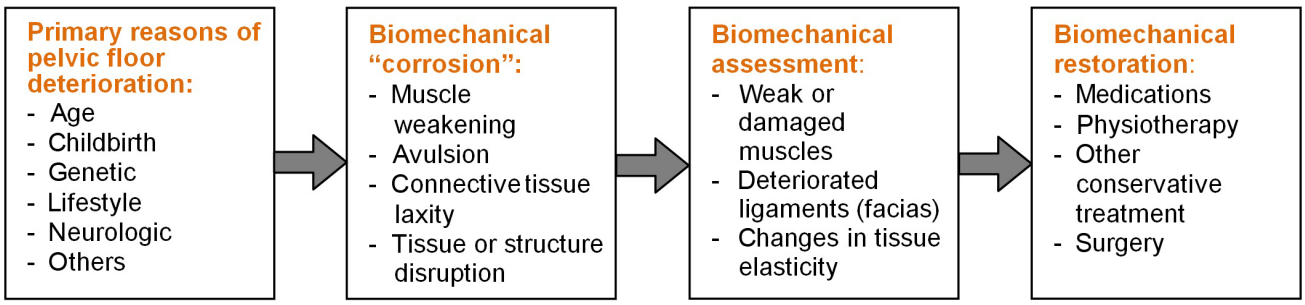

Figure 1 Preferred process in urogynecology.

functional anatomy and our interpretation of clinical results with Vaginal Tactile Imaging (VTI).[6–9] A VTI probe allows acquisition of the pressure patterns along the entire length of the vagina for the two opposite sides. This opens up new possibilities for the quantitative biomechanical assessment and monitoring of pelvic floor conditions.

Methods

Understanding of female pelvic floor functional anatomy

A consideration of any complex life system must include selection of key components playing a significant role in physiologic processes. In this consideration, we will pay attention to the structure, and related passive as well as active biomechanical aspects.[6–9,13]

Characterizing soft tissue elasticity

From classical mechanics, we know that to characterize an object as a mechanical system, a great number of parameters are needed. These include the shear and Young's moduli, bulk compressional modulus, nonlinearity, Poisson's ratio, viscosity, poroelastic parameters, hysteresis, anisotropy, and heterogeneity indices.[14–16] At the first glance, this requirement does not seem realistic to meet. However, over the centuries, soft tissue palpation has been the most prevalent and successful medical diagnostic technique.[17] Two critical factors explain this: 1) detection of a mechanical heterogeneity by manual palpation is based exclusively on sensing the variations of the Young's modulus (E) of the tissue (or shear elasticity modulus, which is approximately equal to E/3 for soft tissues) and 2) the elasticity modulus varies by hundreds of percent during development of pathologic or diseased conditions in the soft tissues.[18–20] The key terms related to soft tissue elasticity require additional explanation to understand the tactile imaging approach.

Pressure

Pressure is the force applied per unit area to an object or a portion of the object. Here, pressure refers to the cause of soft tissue deformation as a force (pressure) is applied to the tissue surface. The units of pressure include force (Newton) per unit area (square meter), that is, N/m^2 (called Pascals or Pa). Other units of pressure, such as cmH_2O and mmHg (millimeter of mercury), are also used; for example, 1 mmHg =0.0075 Pa. Pressure is a scalar described by a magnitude alone.

Stress

Stress is the force that neighboring particles of a continuous material exert on each other. Stress refers to the cause of the tissue deformation. The unit of stress here is force (Newton) per unit area (square meter), that is, N/m^2 or Pa. Stress is a vector described by both a magnitude and a direction.

Strain

Strain is the measure of the deformation of the material under applied load (pressure or stress). Strain may characterize deformation of a soft tissue surface or displacement of internal particles. Strain is expressed as the ratio of total deformation to the initial dimension of the object. Strain is dimensionless (m/m).

Elasticity

In mechanics, elasticity is the ability of a material to resist applied stress and to return to its original shape when the stress is removed. The elastic moduli characterize the ability to resist the applied stress as an intrinsic property of a specific material.[14–16] If the deformed tissue has returned by 98% to its initial size, is it elastic? Yes, it is elastic; it just may require additional characterization. A perfect (100%) elastic material is an illusory approximation from the real world. In the case of a one-dimensional deformation of a uniform object, the stress to strain ratio is the Young's modulus (stress/strain = $N/m^2/m/m$ = Pa; Hooke's law). Many materials, including human soft tissues, noticeably deviate from Hooke's law well before their elastic limits (tissue break) are reached. However, the stress to strain ratio directly characterizes the soft tissue elasticity.

Stiffness

Stiffness is the ability of an elastic object to resist an applied force. Stiffness is not only a function of the material, but is also influenced by the object shape. It is measured as a ratio of applied force (Newton) per object linear compression or elongation (meter), that is, N/m.

Pressure vs deformation

Pressure response patterns are measured with a pressure sensor array by applying a probe to the surface of a soft tissue object, to allow acquisition of the stress data. If we know the exact displacement coordinates (the strain) of every pressure sensor during the tissue deformation, we can map the pressure response data in this coordinate continuum to obtain stress–strain or tactile images. It seems that tactile image can be acquired not only for tissue compression by a probe with pressure/tactile sensors, but also for probe sliding over lubricated soft tissue or combination of compression and sliding. Such an approach makes it possible for the composition of a 3D tactile image that looks similar to the original structure

and allows its elasticity assessment. The tactile compound image integration is also possible if the object exceeds the probe size.[21–23]

Tactile imaging

Tactile imaging is a medical imaging modality translating the sense of touch into a digital image. The tactile image is a function of $P(x,y,z)$, where P is the pressure on the soft tissue surface under the applied deformation, and x, y, and z are the coordinates where pressure P is measured.[15] The tactile image is a pressure map on which the direction of tissue deformation must be specified. The probe has a pressure sensor array mounted on its face that acts similarly to human fingers during a clinical examination, deforming the soft tissue and detecting the resulting changes in the pressure pattern on the surface. The sensor head is moved over the surface of the tissue to be studied, and the pressure response is evaluated at multiple locations along the tissue. The results are used to generate two-dimensional or 3D images showing the pressure distribution over the area of the tissue under study.

Elasticity assessment

Generally, an inverse problem solution for the 3D tactile image $P(x,y,z)$ would allow reconstruction of the tissue elasticity distribution as a function of the coordinates x, y, and z. Unfortunately, the inverse problem solution is hardly possible for most real objects because it is a nonlinear and ill-posed problem. However, the tactile imaging reveals tissue or organ anatomy and elasticity distribution because it keeps the stress–strain relationship for the deformed tissue.[21,22] It appears that the 3D tactile image can be transformed into an elasticity image with the use of a linear transformation for a region of interest. That means, in general, the spatial gradients $\partial P(x,y,z)/\partial x$, $\partial P(x,y,z)/\partial y$, and $\partial P(x,y,z)/\partial z$ can be used in practice for a quantitative assessment of soft tissue elasticity, despite structural and anatomic variations.[23]

Functional tactile imaging

Functional tactile imaging is a variation of tactile imaging that translates the muscle activity into a dynamic pressure pattern $P(x,y,t)$ for an area of interest, where t is time and x, y are the coordinates where pressure P is measured. Muscle activity to be studied may include a voluntary contraction (eg, a pelvic floor squeeze), an involuntary reflex contraction (eg, due to a cough), an involuntary relaxation, or a Valsalva (veering down) maneuver.[23] The functional tactile imaging is similar to the high-definition manometry used for muscle contraction studies along the gastrointestinal tract. With this approach, muscle strength (MS) is calculated as the difference between the maximum pressure amplitude $P_2(x)$, as measured by the VTI probe at muscle contraction (voluntary or involuntary), and the pressure amplitude $P_1(x)$ in the same location x at muscle rest. This means $MS = P_2(x) - P_1(x)$.

Vaginal tactile imager

A VTI allows acquisition of pressures applied to the vaginal walls along with the probe location to visualize vaginal and pelvic floor support structures and to record pelvic floor muscle contractions. The VTI software provides visualization, analysis, information, and reporting tools. The acquired data and information from the subsequent analysis can then be used for quantitative assessment of the vaginal and pelvic floor conditions.

The VTI comprises the vaginal probe (Figure 2) and a movable computer display cart. The VTI probe is equipped with 96 pressure (tactile) sensors positioned every 2.5 mm along both sides of the probe, an orientation sensor, and temperature sensors with microheaters.

During the patient examination procedure, data are sampled from the probe sensors and displayed on the VTI computer display in real time. The probe surfaces that contact the vaginal walls are preheated to human body temperature. A lubricating jelly is used for patient comfort and to provide

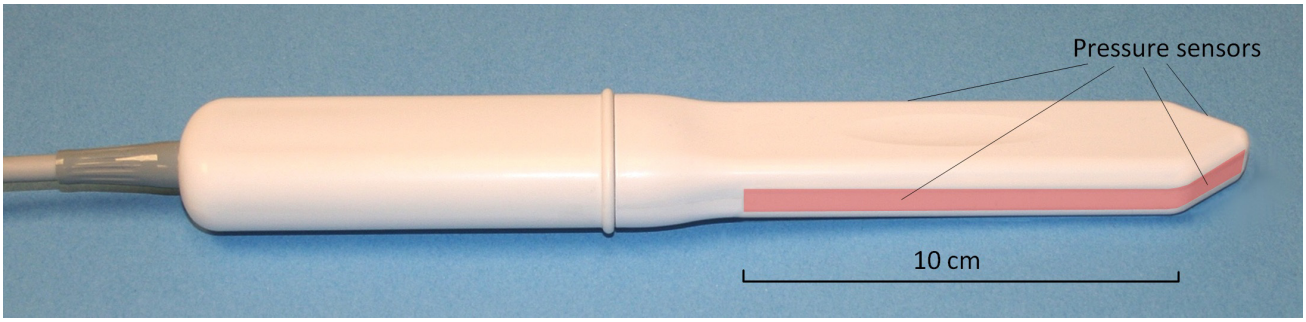

Figure 2 Vaginal tactile imaging probe.
Note: Pressure sensors are aligned on the opposite sides of the probe (highlighted on the image).

reproducible boundary/contact conditions with deformed vaginal tissue; these conditions are classified as slip boundary conditions.

The tactile probe measures an applied pressure, but not force. Force is a vector, and by definition has amplitude and direction. The pressure sensors designed for the VTI probe are not sensitive to the tangential component of a force that may arise during probe motion and measurements; pressure = force (orthogonal to probe surface)/area. This probe is used for tissue compression in an orthogonal direction to the tissue surface during the probe insertion (Test 1), tissue deformation during the probe elevation (Test 2), pressure pattern acquisition during the probe rotation (Test 3), Valsalva maneuver (Test 4), and pelvic muscle contractions and relaxation (Tests 5–8). The probe's maneuvers in Tests 1–3 allow accumulation of multiple pressure patterns from the tissue surface to compose an integrated tactile image corresponding to each test for the investigated area using the image composition algorithms.[22]

The VTI allows assessment of tissue elasticity, pelvic floor support, and function. The target population comprises adult women with pelvic organ prolapse (POP), urinary incontinence, tissue atrophy, and pelvic floor pain. The device is intended for use by physicians, surgeons, and medically trained personnel. The previous clinical results obtained with the VTI have been reported.[23–35]

Patient position and data acquisition

The VTI scan is performed on a patient in the dorsal lithotomy position with an empty bladder and rectum. The full VTI examination takes 3–5 minutes to complete. The VTI probe is calibrated being placed in a calibration chamber for about 20 seconds before every clinical application. Figure 3 shows the VTI probe placement into a patient's vagina during her examination (data acquisition).

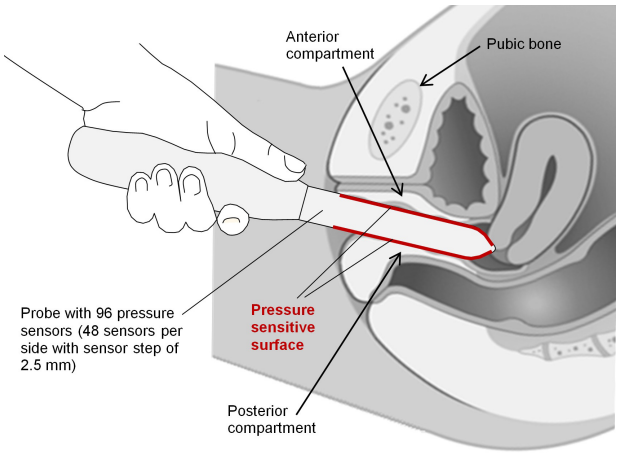

Figure 3 Vaginal tactile imaging probe during pelvic floor examination.

Population description

We enrolled 138 subjects into an observational case–control clinical study in 2014–2015 (clinical trials identifier NCT02294383 at https://ClinicalTrials.gov). Local institutional review board approvals were received from St Luke's University Health Network (Bethlehem, PA) and Princeton HealthCare System (Princeton, NJ). The study subjects have had normal pelvic support or POP (stages I–IV). The average age was 60±15, with subjects' individual ages ranging from 26 to 90 years. The clinical protocol was approved by the local institutional review board, and all the participating women gave written informed consent. The study was conducted in compliance with the Health Insurance Portability and Accountability Act. The VTI images were obtained and recorded at the time of scheduled routine gynecologic visits.

The study workflow comprised the following steps: 1) recruiting women who routinely undergo vaginal examination as a part of their diagnostic treatment of concerned areas; 2) acquisition of clinical diagnostic information related to the studied cases by standard clinical means; 3) performing a VTI examination; and 4) review of acquired VTI images and capture of illustrative VTI results. For prolapse staging, we used a Pelvic Organ Prolapse Quantification [POP-Q] system.[36] Additionally, the patients were asked to assess the comfort level of a VTI examination relative to manual palpation.

VTI examination procedure

The complete VTI study consists of eight independent tests:

- Test 1: probe insertion
- Test 2: probe elevation
- Test 3: probe rotation
- Test 4: Valsalva maneuver
- Tests 5 and 6: voluntary muscle contraction
- Test 7: involuntary muscle relaxation
- Test 8: involuntary muscle contraction (cough).

Results

Test 1: probe insertion

The vaginal probe is designed to deform the vaginal walls in an orthogonal direction from the vaginal channel during the probe insertion, as shown in Figure 4A. The linear motion of the probe is translated into vaginal tissue deformation in

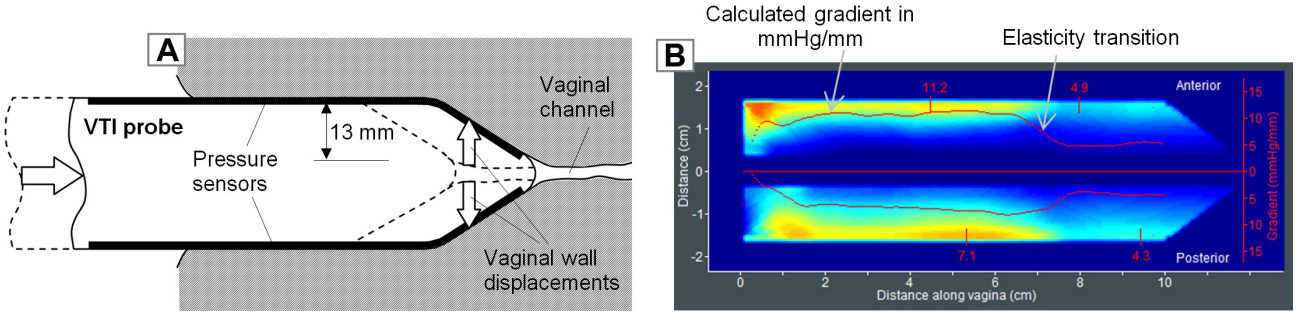

Figure 4 (**A**) VTI probe insertion to deform vaginal walls in a definitive manner and (**B**) a tactile image for VTI probe insertion into a silicone model with known elasticity distribution.
Abbreviation: VTI, vaginal tactile imaging.

a definitive manner, and the pressure sensors of the angled probe tip measure the tactile feedback from the vaginal walls – for a 13 mm deformation per side (Figure 4A). Figure 4B shows the tactile image recorded for a silicone model, which has a tissue elasticity transition from 10 to 5 kPa (Young's modulus). This transition is clearly manifested in the calculated pressure gradients (mmHg/mm, orthogonally to vaginal channel) for both sides from the center of the channel.

During the clinical examination, before the probe insertion, the anterior and posterior vaginal walls are almost in contact with each other when a patient is in a relaxed condition in the dorsal position. The internal pressure along the vaginal channel is close to zero. During the VTI probe insertion, the probe itself finds equilibrium from two opposite sides (anterior vs posterior) and an operator allows the probe to follow the insertion angle offering the least resistance along the vaginal channel. The probe insertion can be completed in <10 seconds and the operator observes an acquired tactile image in real time. If the composed image has some obvious distortions or is incomplete, the insertion test must be repeated to get a consistent pattern.

Figure 5 shows two clinical examples for strong tactile response (Figure 5A) and much softer vaginal tissue (Figure 5B). Locations of specific pelvic floor structures are marked on these images. The tactile image for this test characterizes the vaginal tissue elasticity behind the vaginal walls at a distance comparable with the value of the tissue deformation (2–10 mm). The vaginal wall itself seems significantly softer than the structures we observe deeper beneath the wall. Specifically, from left to right, in the anterior vaginal compartment, we see responses from the pubic bone, the urethra, the "zone of critical elasticity" (ZCE), and the cervix.[6–9] In the posterior compartment, from left to right, the responses are observed from a perineal body (PB); the levator ani muscles and levator plate (LP) are present (Figure 5A). Most likely, the puborectal muscle (PRM) is the dominant muscle observed in the levator ani muscle zone. White dotted lines in Figure 5A and B are spatial pressure gradients calculated from the center of the vaginal channel in the anterior and posterior directions.

The tactile image in Figure 5B demonstrates a relatively low pressure gradient (up to 5.2 mmHg/mm) for the posterior compartment vs 34.4 mmHg/mm for the left image shown in Figure 5A. These gradient values may be interpreted as vaginal tissue elasticity within 10–15 mm from the vaginal walls. Changes in the vaginal wall tissue, such as surgical scar tissue or vaginal atrophy, can be observed. An anatomic factor may also contribute to this image; for example, an enlarged vaginal hiatus size will show a low pressure gradient at the entrance (the first 2–3 cm). However, as the VTI probe moves deeper into the vagina, the probe pushes apart the anterior and posterior vaginal walls simultaneously and records the pressure response from their displacements. The pressure responses (see the pressure graphs along anterior and posterior compartments in Figure 5C and D) are proportional to the tissue resistance due to the deformation of the vaginal walls at probe insertion; they (pressure responses) also reveal the distribution of the vaginal tissue elasticity. A weak signal from the cervix, in the case in Figure 5B compared to the case in Figure 5A, may characterize weak (laxity) conditions of uterosacral ligament (USL)/cardinal ligaments (CLs).

Test 1 may allow assessment of the following:

- vaginal tissue elasticity distribution ($\partial P/\partial y$) along the anterior and posterior compartments. The elasticity values are captured from multiple layers composed of the vaginal wall and structures behind the vaginal wall at a depth of up to 2–10 mm;

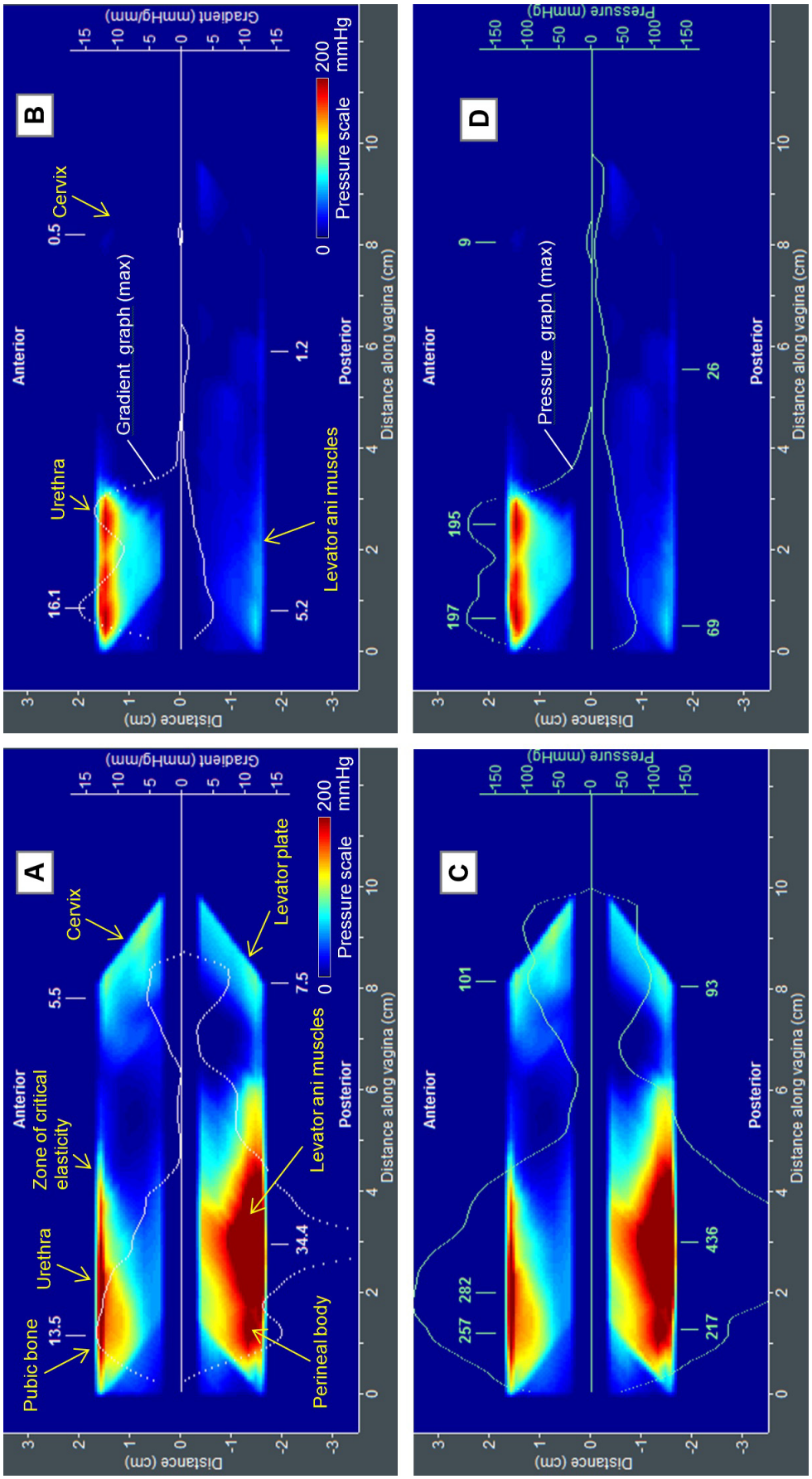

Figure 5 Test 1 (VTI probe insertion) results for two patients with (**A**) stiff and (**B**) much softer vaginal tissue.
Notes: White lines show spatial pressure gradients for anterior and posterior compartments. Panels (**C**) and (**D**) are the same data as in panel (**A**) and (**B**), but with maximum pressure graphs (green lines) along the anterior and posterior compartments.
Abbreviation: VTI, vaginal tactile imaging.

- strength (P) and, possibly, elasticity ($\partial P/\partial y$) of urethra (U) in distal anterior;
- strength (P) and elasticity ($\partial P/\partial y$) of the ZCE in mid-anterior;
- strength (P) and elasticity ($\partial P/\partial y$) of the USL/CL in apical anterior and posterior;
- strength (P) and elasticity ($\partial P/\partial y$) of PB in distal posterior;
- rest tone (P) and elasticity ($\partial P/\partial y$) of levator ani muscles and, possibly, PRM in mid-posterior;
- strength (P) of LP in apical posterior; and
- hiatus strength as combined distal anterior and posterior pressure (P).

Clinical value of Test 1:

- detection of defects in the vaginal wall and underlying structures, PB, PRM, LP and USL/CL;
- comparative analysis of vaginal elasticity changes after applied treatment (surgery,[25] physiotherapy, RF, or laser procedures[26]); and
- scar detection and characterization of ZCE for urinary incontinence diagnosis (tethered vagina syndrome).
- Characterization of postpartum pelvic floor remodeling.

Test 2: probe elevation

The vaginal probe elevation test is shown in Figure 6A. It allows acquisition of tactile feedback from the pelvic floor structure, at a 15–40 mm depth, under significant tissue deformation for the anterior and posterior vaginal compartments. The probe has an orientation sensor to measure an elevation angle, such that the pressure feedback may be mapped along the elevation angle as shown in Figure 6B. The up and down elevation of the probe is advised relative to the hymen.

Figure 7 presents two clinical cases, A and B. Locations of specific pelvic floor structures are marked on these images. The upper panel presents the tactile images, and the lower panel the gradient images calculated from these tactile images. The spatial pressure gradients (mmHg/mm) were calculated from the center horizontal vaginal line to the anterior (vertical) and from the center horizontal vaginal line to the posterior compartment. In the anterior compartment, from left to right, we noted tactile responses from the pelvic bone, the urethra, and the cervix (see upper panel in Figure 7A). In the posterior compartment, from left to right, we found tactile responses from puboperineal muscle (PPM), PRM, puboanal muscle (PAM), and pubovaginal muscle (PVM), which are parts of the pubovisceral (pubococcygeal) muscle, the iliococcygeal muscle (ICM), as well as the LP.[6–8]

The pressure feedback values at the selected locations in tactile images (upper panels in Figure 7) and the pressure gradients (bottom panels) are relatively smaller (P=60–81 mmHg and $\partial P/\partial y$ =0.7–3.7 mmHg/mm in the posterior compartment) than they are in case B (P=254–402 mmHg and $\partial P/\partial y$ =4.7–24.6 mmHg/mm in the posterior compartment). The gradient values for the posterior compartment may be interpreted as pelvic floor support conditions, because they characterize the capability of the pelvic floor support structures to resist applied deformation, which is higher (up to 40 mm) than that in Test 1. The softer the tissues, the deeper the structures visualized by the VTI probe, because these softer tissues may be deformed more with weaker response to reveal a support if available. Possibly, the PUL and the arcus tendineus fascia pelvic ligament also contribute to the tactile response at full posterior deformation, in addition to the muscles listed in the upper panel of Figure 7A.

These test results correlate with the pelvic floor conditions, demonstrating pressure as well as gradient decreases from normal to prolapse Stage III conditions.[27,33,34] The VTI enables quantification of the vaginal tissue elasticity and the strong differentiation between normal, Stage II,

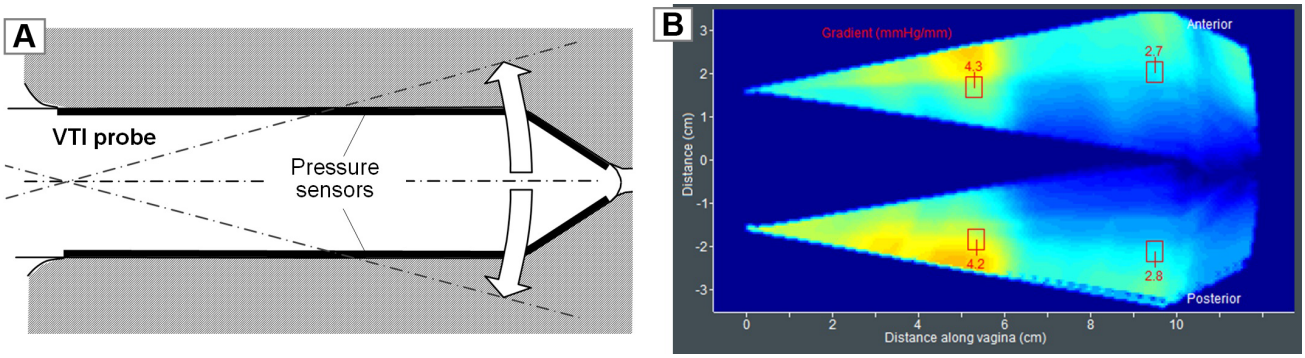

Figure 6 (**A**) VTI probe elevation to acquire tactile feedback from deep structures and (**B**) a tactile image for VTI probe elevation inside a silicone model with known elasticity distribution.
Abbreviation: VTI, vaginal tactile imaging.

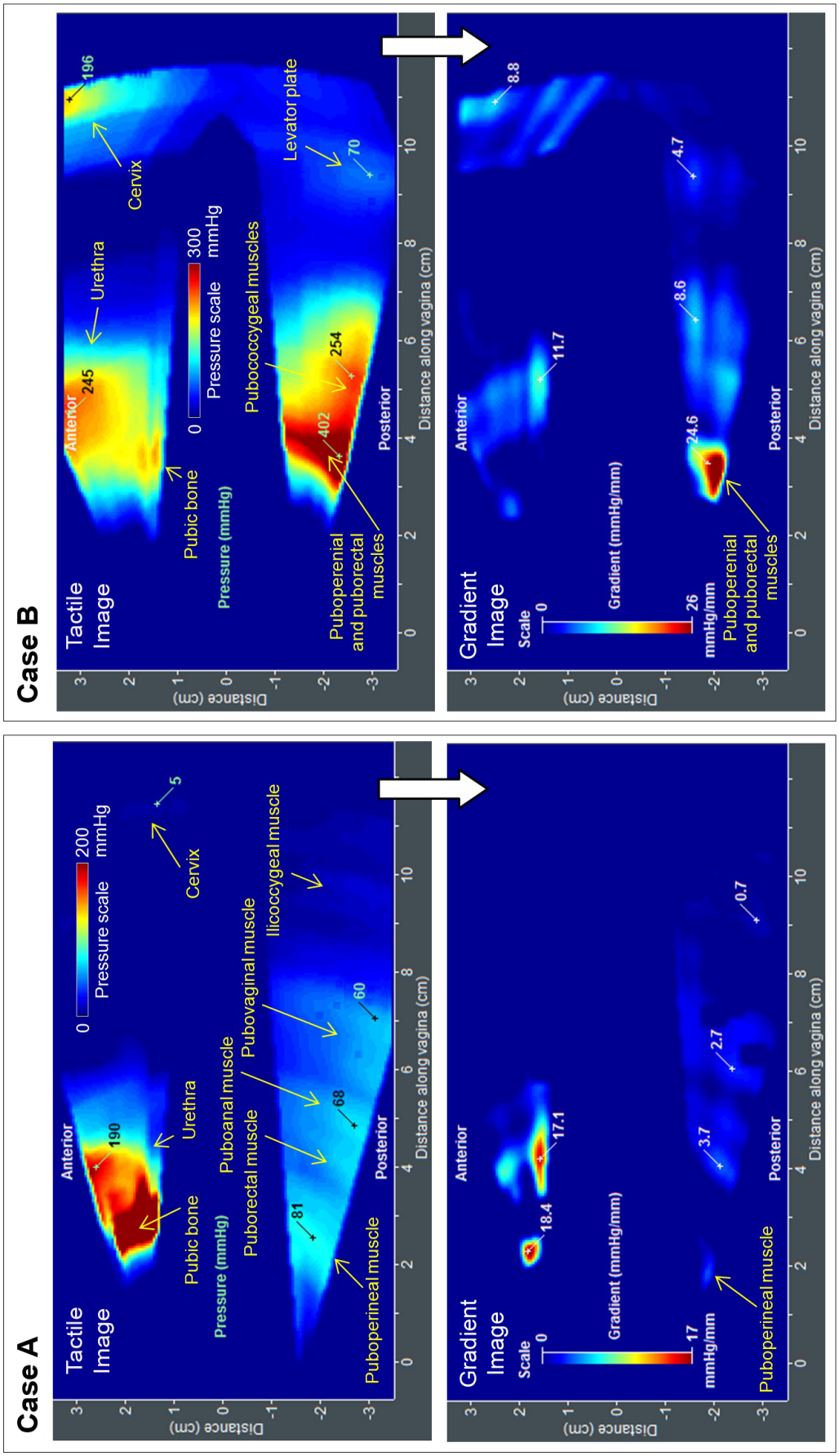

Figure 7 Test 2 (VTI probe elevation) results for two patients with (**A**; Case A) weak and (**B**; Case B) strong pelvic floor support.
Abbreviation: VTI, vaginal tactile imaging.

and Stage III prolapse conditions. The overlap in tissue elasticity and pelvic floor support between normal and Stage I prolapse conditions means that 1) some cases under Stage I prolapse show the same values as in normal conditions or 2) the normal case, as defined by the POP-Q system, with lower pressure feedbacks and gradients, is already in the range of Stage I prolapse. In other words, the lower level of the normality range with the decreased numbers may enable the detection of preprolapse conditions that require attention to delay the development of anatomically not observable prolapse conditions.[32] Pelvic floor reconstructive surgery also changes the tactile image as well as the gradient values at specific locations.[25]

Test 2 may allow assessment of the following:

- strength (P) of pelvic floor support structures along the posterior compartment;
- elasticity ($\partial P/\partial y$) of urethra (U) in the distal anterior;
- elasticity ($\partial P/\partial y$) of the USL/CL in apical anterior;
- elasticity ($\partial P/\partial y$) of the PRM, PAM, and PVM, and ICM; and
- elasticity ($\partial P/\partial y$) of the LP.

The clinical value of Test 2 lies in the following advantages:

- detection of defects in the pelvic floor support structures including PRM, PAM, PVM, ICM, and USL/CL;
- comparative analysis of pelvic floor support after applied treatment; and
- characterization of postpartum pelvic floor remodeling.

Test 3: probe rotation

The vaginal probe being rotated, as shown in Figure 8A, allows acquisition of circumferential tactile feedback from the vaginal walls. The probe has an orientation sensor to measure its rotational angle, such that the pressure feedback may be mapped along the rotation angle, as shown in Figure 8B, for both left and right sides. It is recommended that the VTI probe be rotated slowly for better control of the image quality on the VTI computer display. The vaginal walls are deformed up to 7 mm during the VTI probe rotation.

Figure 9 presents two clinical cases, both with normal pelvic floor support, one of them (A) with strong pressure feedback at the center of left and right sides at the distal part (P=133–168 mmHg) and the other (B) with relatively low values at the same locations (P=11–76 mmHg). Any local pressure peaks at the vaginal sides may be interpreted as stiff irregularities or lumps on the vaginal wall or behind it at a depth of 0–7 mm. The vaginal width definitely contributes to the tactile feedback at the center of both the sides when the probe is oriented horizontally, such that the right side is exactly imaged vs the left side. Asymmetry in pressure patterns on one side vs the other side conveys information about the asymmetry in pelvic floor structures behind the vaginal walls. Cumulative (integral) contact pressure inside the vagina characterizes a "vaginal strength".

We found the pressure maximum at both sides (P_{max}), as shown in Figure 9, correlated with the pelvic floor conditions, demonstrating P_{max} decrease from normal to prolapse conditions.[27] Pelvic floor reconstructive surgery may also change the tactile image of this test at the affected locations.

Test 3 will allow the assessment of the following:

- irregularities on the vaginal walls along the entire vagina as pressure peak value (P) and its size;
- asymmetry in pelvic floor structures behind the vaginal walls; and
- cumulative (integral) contact pressure inside the vagina ("vaginal strength").

The clinical value of Test 3 lies in the following:

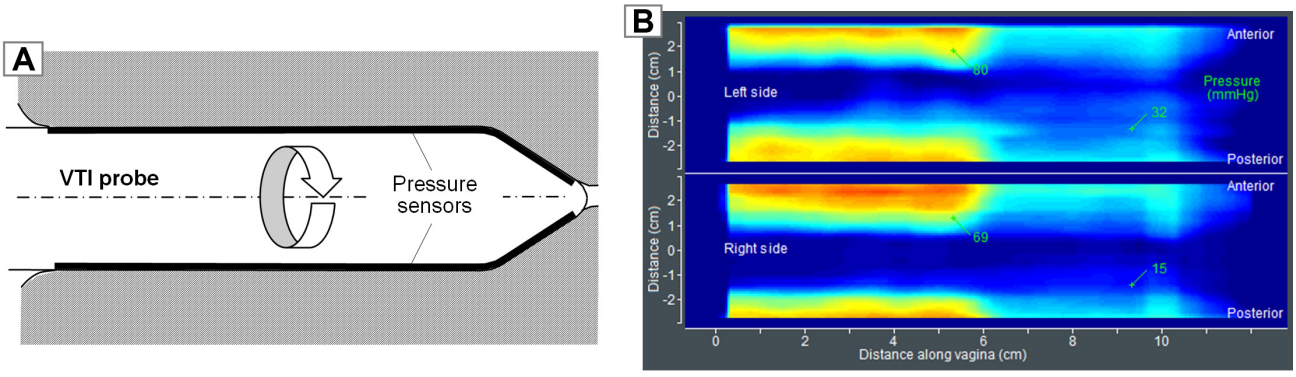

Figure 8 (**A**) VTI probe rotation to acquire circumferential tactile feedback from the vaginal walls and (**B**) tactile images acquired inside a silicone model with known elasticity distribution.
Abbreviation: VTI, vaginal tactile imaging.

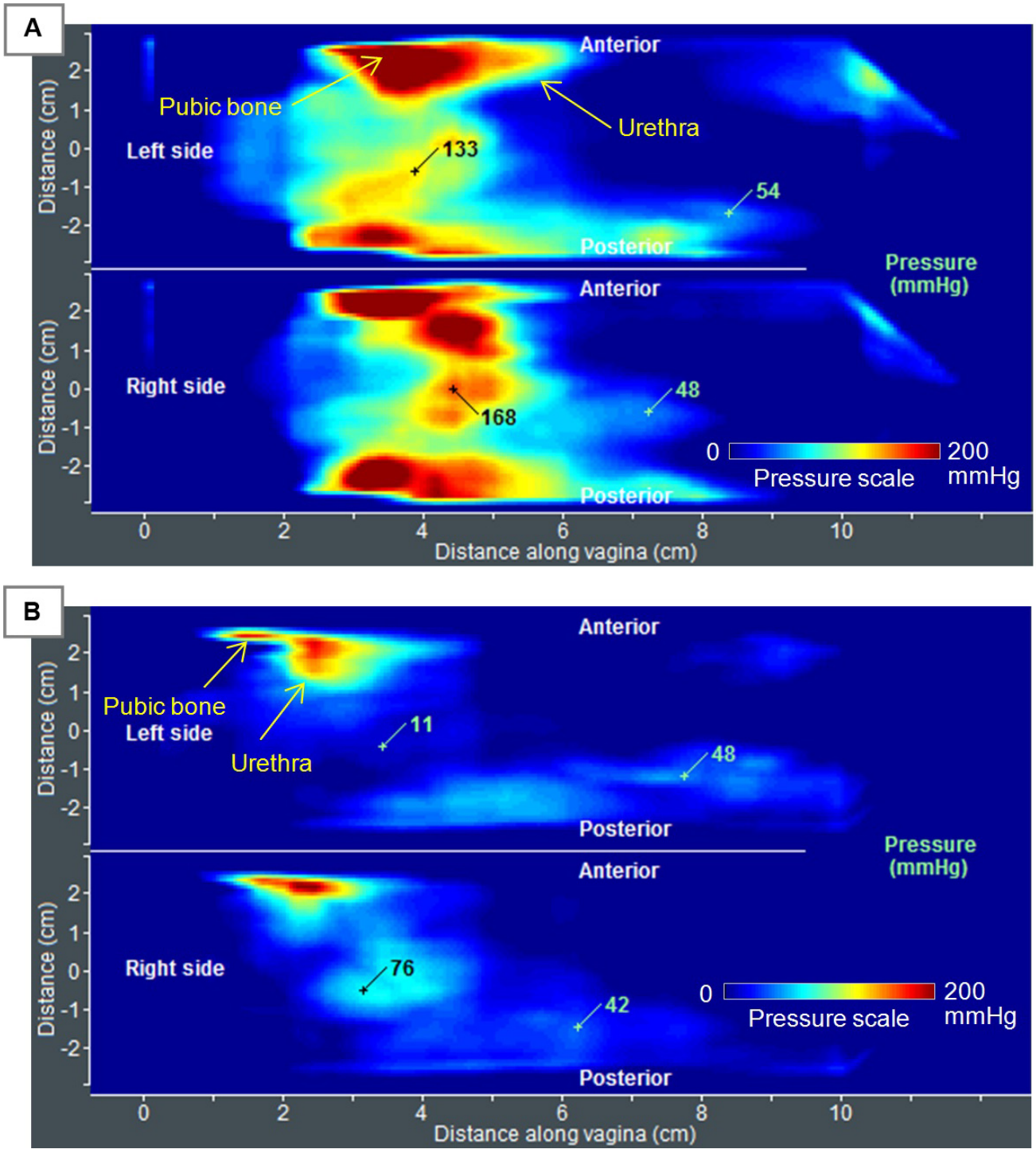

Figure 9 Test 3 (VTI probe rotation) results for two patients with normal pelvic floor support and (**A**) irregular strong and (**B**) weak vaginal wall response.
Abbreviation: VTI, vaginal tactile imaging.

- irregularities detection/characterization on vaginal walls;
- monitoring of vaginal wall changes after applied treatment; and
- postpartum vaginal wall changes.

Test 4: Valsalva maneuver

Figures 10–13 present the VTI data observed during Valsalva maneuver for a patient with normal pelvic floor support (Figures 10 and 11) and with a prolapse (Figures 12 and 13).

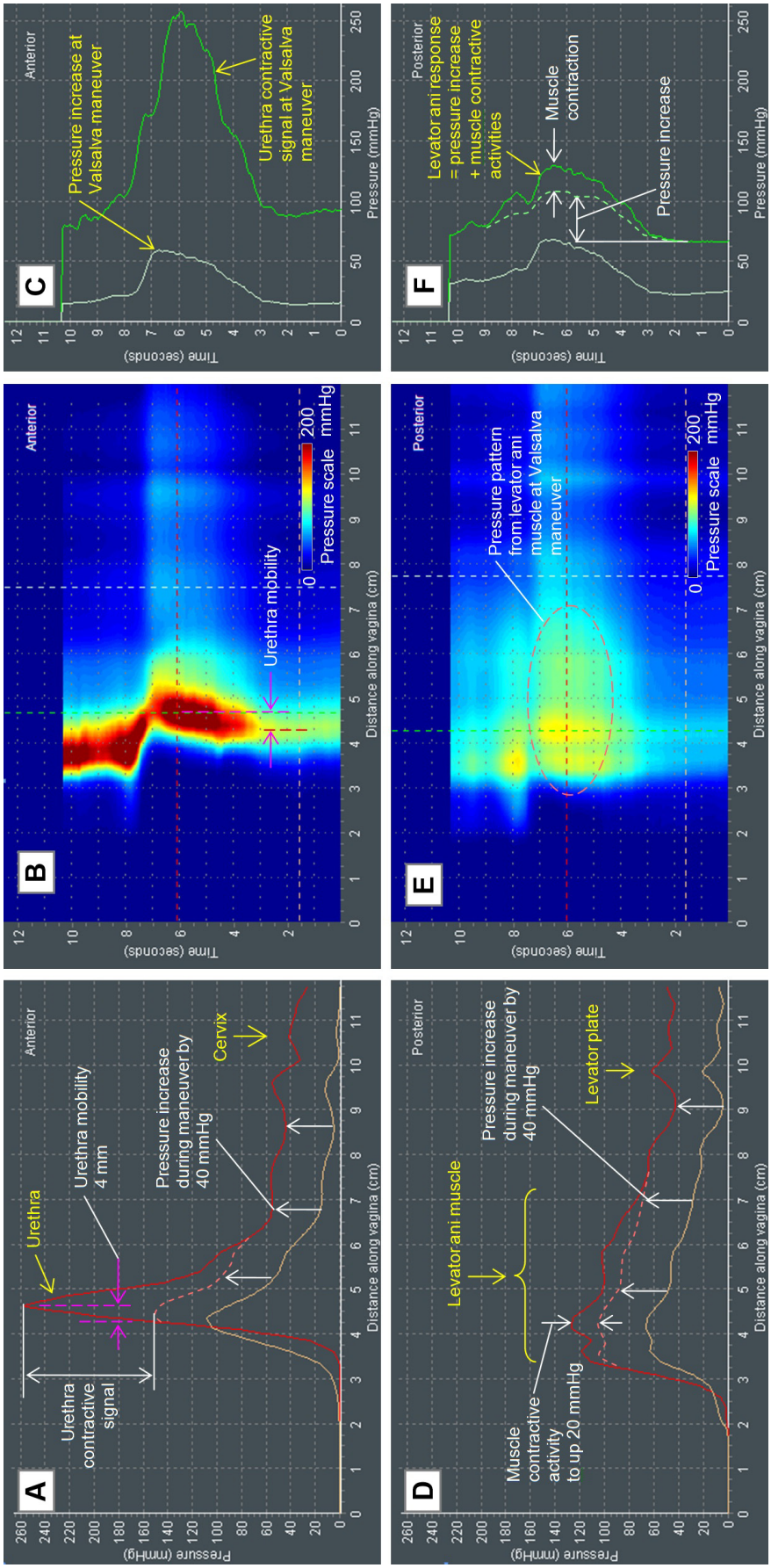

Figure 10 Test 4 (Valsalva maneuver) results for a 51-year-old patient with normal pelvic support.
Notes: (**A**, **D**) Anterior and posterior pressure patterns at Valsalva maneuver (red lines) and at rest (light brown lines); (**B**, **E**) anterior and posterior dynamic pressure pattern along the vagina; (**C**, **F**) pressure dynamic at specific locations (see dotted lines in **B**, **E**).

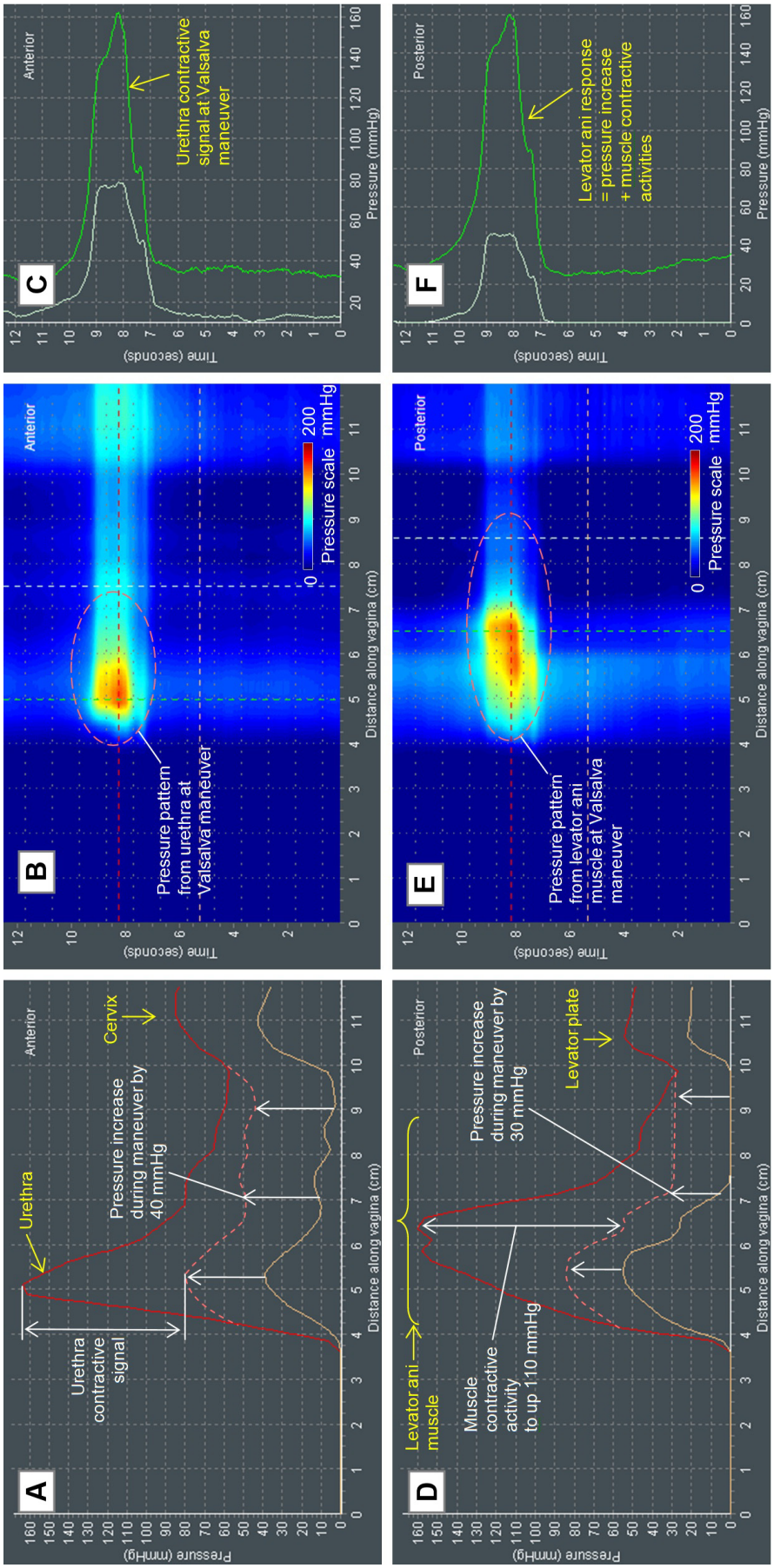

Figure 11 Test 4 (Valsalva maneuver) results for a 52-year-old patient with normal pelvic floor support.
Notes: (**A**, **D**) Anterior and posterior pressure patterns at Valsalva maneuver (red lines) and at rest (light brown lines); (**B**, **E**) anterior and posterior dynamic pressure pattern along the vagina; (**C**, **F**) pressure dynamic at specific locations (see dotted lines in **B**, **E**).

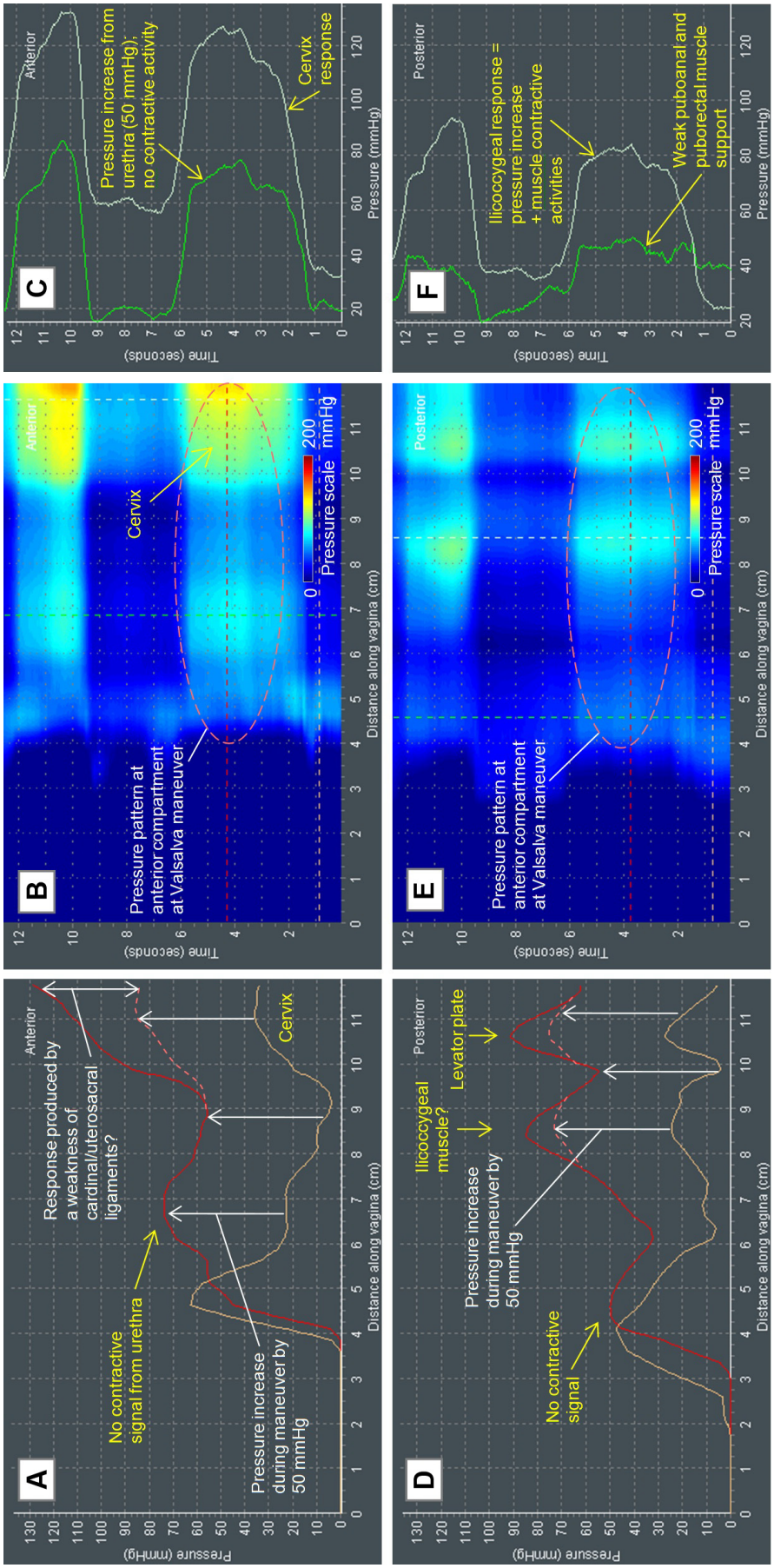

Figure 12 Test 4 (Valsalva maneuver) results for a 66-year-old patient with Stage IV prolapse.
Notes: (**A**, **D**) Anterior and posterior pressure patterns at Valsalva maneuver (red lines) and at rest (light brown lines); (**B**, **E**) anterior and posterior dynamic pressure pattern along the vagina; (**C**, **F**) pressure dynamic at specific locations (see dotted lines in **B**, **E**).

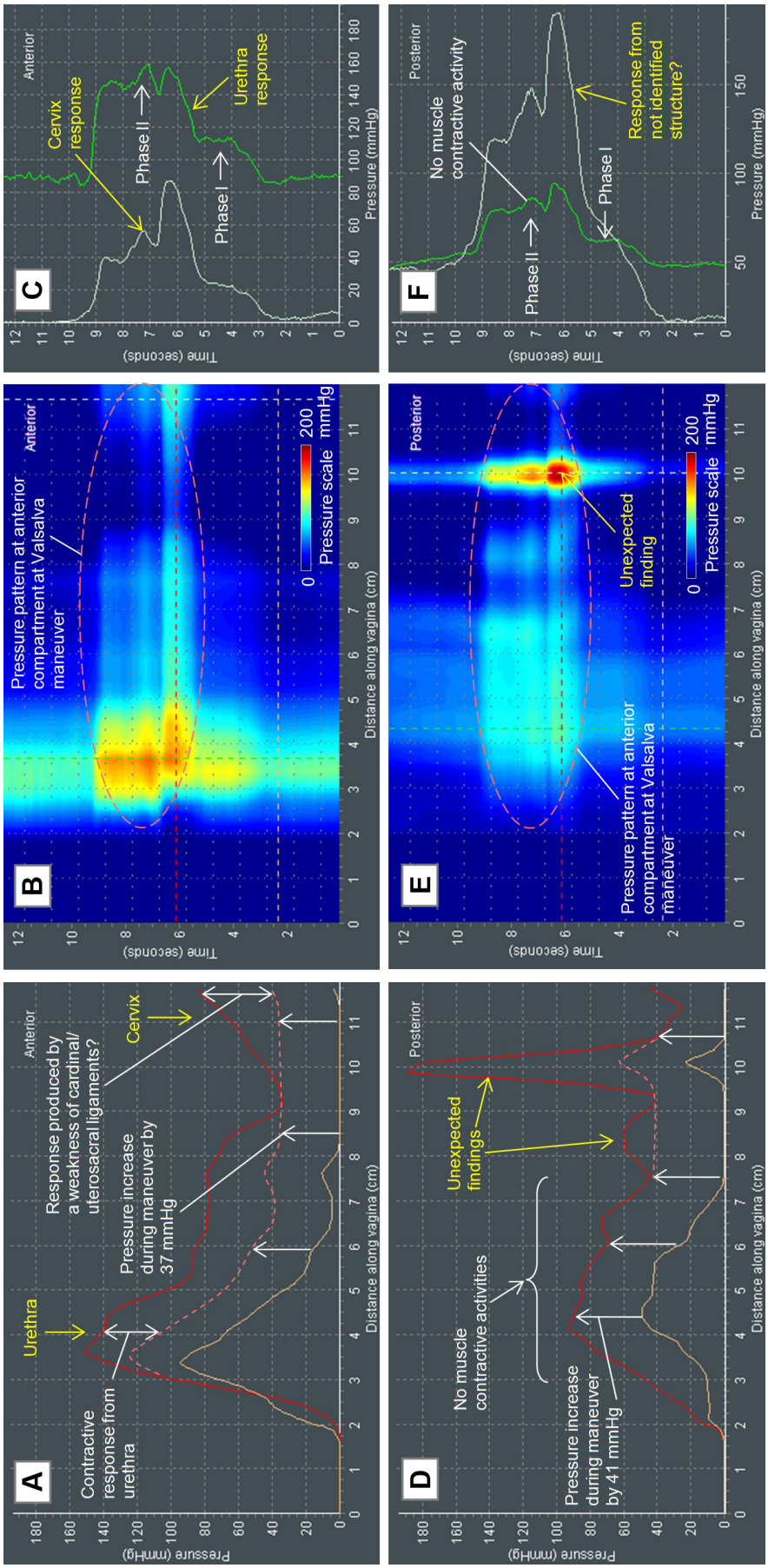

Figure 13 Test 4 (Valsalva maneuver) results for an 84-year-old patient with Stage III prolapse.
Notes: (A, D) Anterior and posterior pressure patterns at Valsalva maneuver (red lines) and at rest (light brown lines); **(B, E)** anterior and posterior dynamic pressure pattern along the vagina; **(C, F)** pressure dynamic at specific locations (see dotted lines in **B, E**).

Two cases with normal pelvic floor support allow measurement of contractive signals from the urethra (Figures 10A and C and 11A and C) and mobility of the urethra. The first case shows a 4 mm displacement (Figure 10A) and the second shows no displacement (Figure 11A and B). Further, we observe a relatively uniform pressure increase under the Valsalva maneuver along the entire vagina in the anterior and posterior compartments (Figures 10A and D and 11A and D). The cervix fixation by USL/CL is strong because no additional pressure signals except for the uniform pressure increase have been detected. Contractive signal amplitude and width of the levator ani muscle (Figures 10D and 11D) are also measurable. The pressure response dynamics has a single-phase response during the Valsalva maneuver in the posterior compartment (Figures 10F and 11F).

Two cases with pelvic floor prolapse conditions allow detection of contractive signals from the urethra: weak contractive signals at Stage III prolapse (Figure 13A and C) and no contractive signal at Stage IV prolapse (Figure 12A and C). These cases demonstrate weak mobility at Stage III prolapse (Figure 13A and B) and no urethral mobility at all at Stage IV prolapse (Figure 12A and B). While a uniform pressure increase (transference) under Valsalva maneuver is also observed along the entire vagina in the anterior and posterior compartments (Figures 12A and D and 13A and D), in patients with prolapse, there is a very different pattern. In patients with normal support, the majority of pressure increases are carried by the distal vaginal regions, consistent with the supportive pelvic floor muscles. In patients with prolapse, there is a widened pressure distribution observed in the mid-to-upper vagina, with these areas being subject to increased pressures than that in a patient with normal support.

From the presented data, we may conclude that the cervix has a weak fixation by USL/CL because of additional pressure signals above the uniform pressure increase (Figure 12B). Absence of contractive signals is found from the levator ani muscle (Figures 12D and 13D). A two-phase response at Valsalva maneuver is observed in the posterior compartment (Figures 12F and 13F). Finally, unexpected findings (pressure pikes) are detected as shown in Figures 12D and 13F, which require additional consideration and interpretation based on patient history.

Test 4 (Valsalva maneuver) will allow assessment of the following:

- contractive capability (*P*) of the urethra (U);
- mobility of the urethra (U);
- uniform pressure increase (*P*) under along the entire vagina in anterior and posterior compartments;
- cervix fixation by USL/CL;
- contractive strength and width of levator ani muscles;
- two- or single-phase response in the posterior compartment; and
- irregular structures by unexpected pressure pikes (*P*).

The clinical value of Test 4 lies in the following:

- detection of defects in urethra (U);
- conditions/strength of USL/CL;
- contractive phases, strength, and width of levator ani muscles; and
- detection of structure irregularities in the posterior compartment.

Tests 5 and 6: voluntary muscle contraction

Figures 14–17 show the VTI data for a patient with normal pelvic floor support (Figures 14 and 15) and with Stage II prolapse (Figures 16 and 17) during voluntary pelvic floor muscle contractions.

Data are presented for two vaginal probe orientations, anterior vs posterior (vertical probe orientation, Figures 14 and 16) and left vs right (horizontal probe orientation, Figures 15 and 17). The case with normal pelvic floor support reveals two posterior peaks (Figure 14D and E) at pelvic muscle contractions; it seems that these peaks are produced by PPM and PRM. Their MS is estimated as the pressure during the muscle contraction (Figure 14F). In the anterior compartment, the pressure response from urethra is detectable (Figure 14A and C). Figure 14F shows an example of PPM–PRM desynchronization in part (not full synchronization at contraction). Both left and right vaginal sides present two peaks identified as PPM and PRM contractions (Figure 15). The left side has stronger PRM and weaker PPM contractions relative to the right side (compare Figure 15A and D). It seems that we can also observe ICM contraction (Figure 15F).

The muscle contraction patterns in the second case with Stage II prolapse (Figures 16 and 17) are significantly different than for normal pelvic floor conditions. The muscle contraction amplitudes at the prolapse are about 40%–60% less than at normal conditions. We observe the posterior muscle mobility along the vagina (at mid-vagina), about 15 mm in the apical direction (Figure 16D and F). This case also revealed two posterior peaks (Figure 16D and E) at pelvic muscle contractions produced by the PPM and PRM. In the anterior compartment, the pressure response from the urethra is hardly detectable (Figure 16), but we see pressure response at muscle contraction from the posterior mid-vaginal tissue (Figure 16C). Figure 16F shows that the posterior muscle

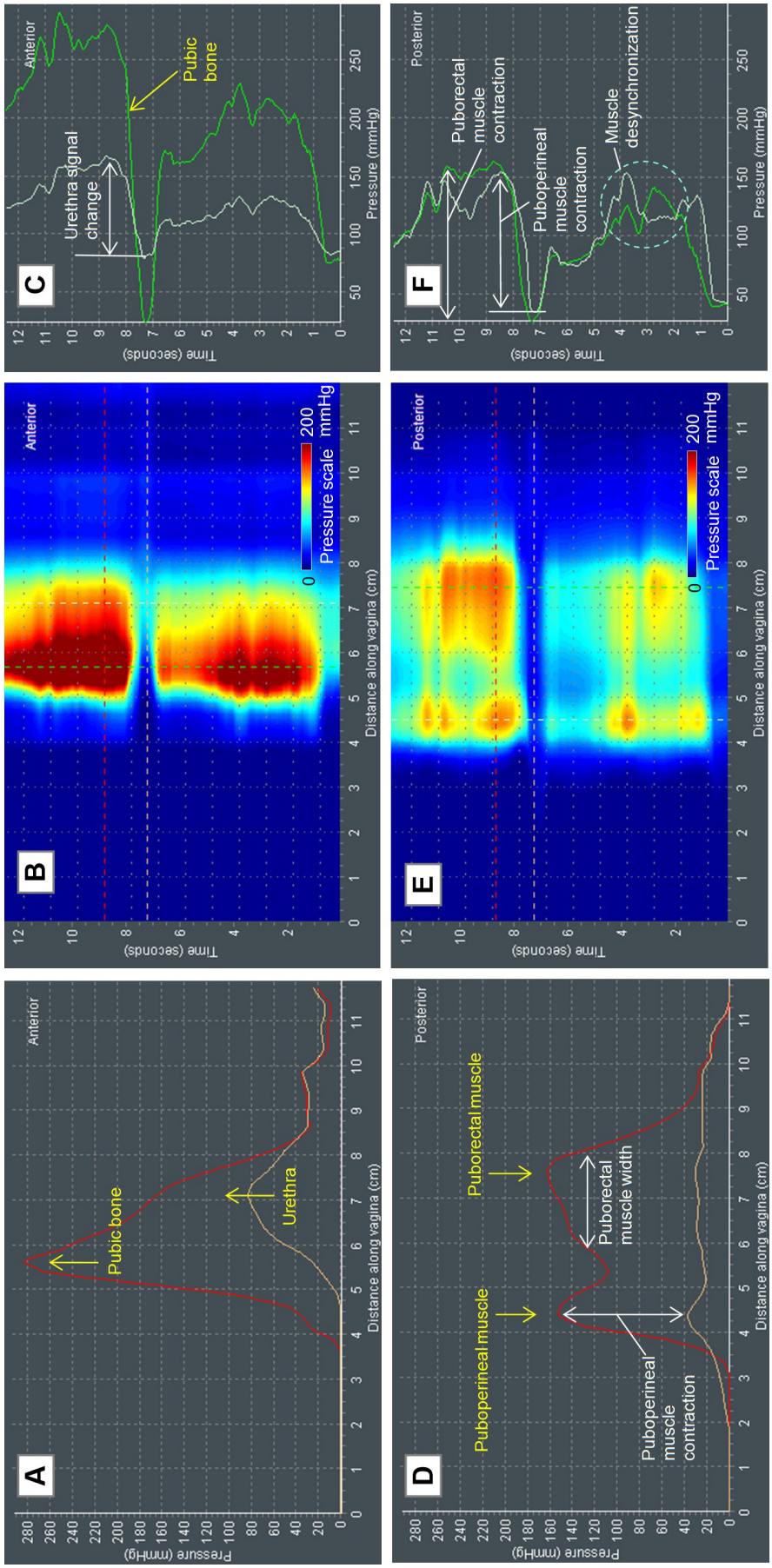

Figure 14 Test 5 (voluntary muscle contraction) results for a 35-year-old patient with normal pelvic floor support.
Notes: (**A**, **D**) Anterior and posterior pressure patterns at muscle contraction (red lines) and at rest (light brown lines); (**B**, **E**) dynamic pressure pattern along the vagina; (**C**, **F**) muscle contraction dynamic at specific locations (see dotted lines in **B**, **E**).

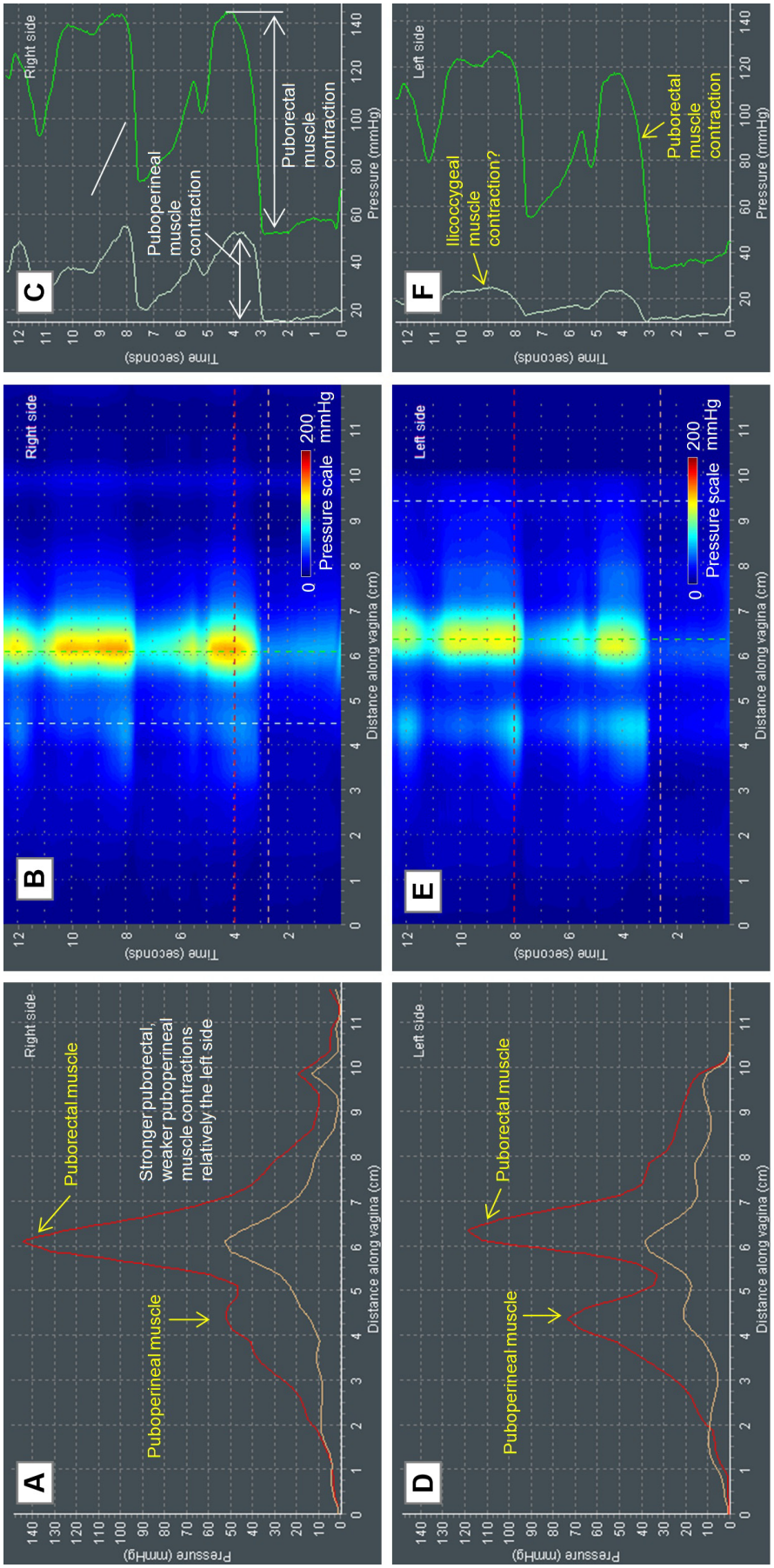

Figure 15 Test 6 (voluntary muscle contraction) results for a 35-year-old patient with normal pelvic floor support.
Notes: (**A**, **D**) Right and left side pressure patterns at muscle contraction (red lines) and at rest (light brown lines); (**B**, **E**) dynamic pressure pattern along the vagina; (**C**, **F**) muscle contraction dynamic at specific locations (see dotted lines in **B**, **E**).

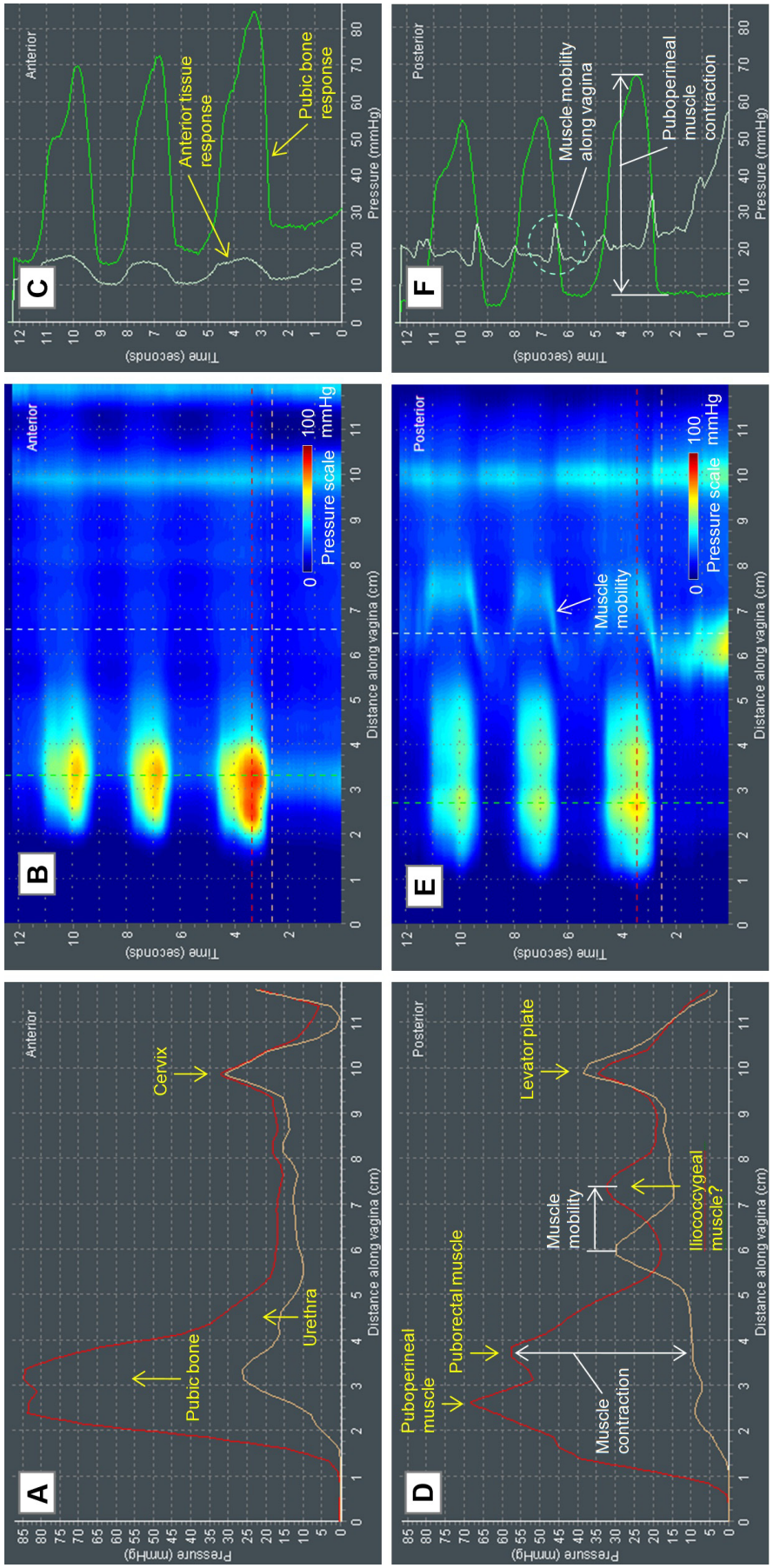

Figure 16 Test 5 (voluntary muscle contraction) results for an 80-year-old patient with Stage II prolapse.
Notes: (**A**, **D**) Anterior and posterior pressure patterns at muscle contraction (red lines) and at rest (light brown lines); (**B**, **E**) dynamic pressure pattern along the vagina; (**C**, **F**) muscle contraction dynamic at specific locations (see dotted lines in **B**, **E**).

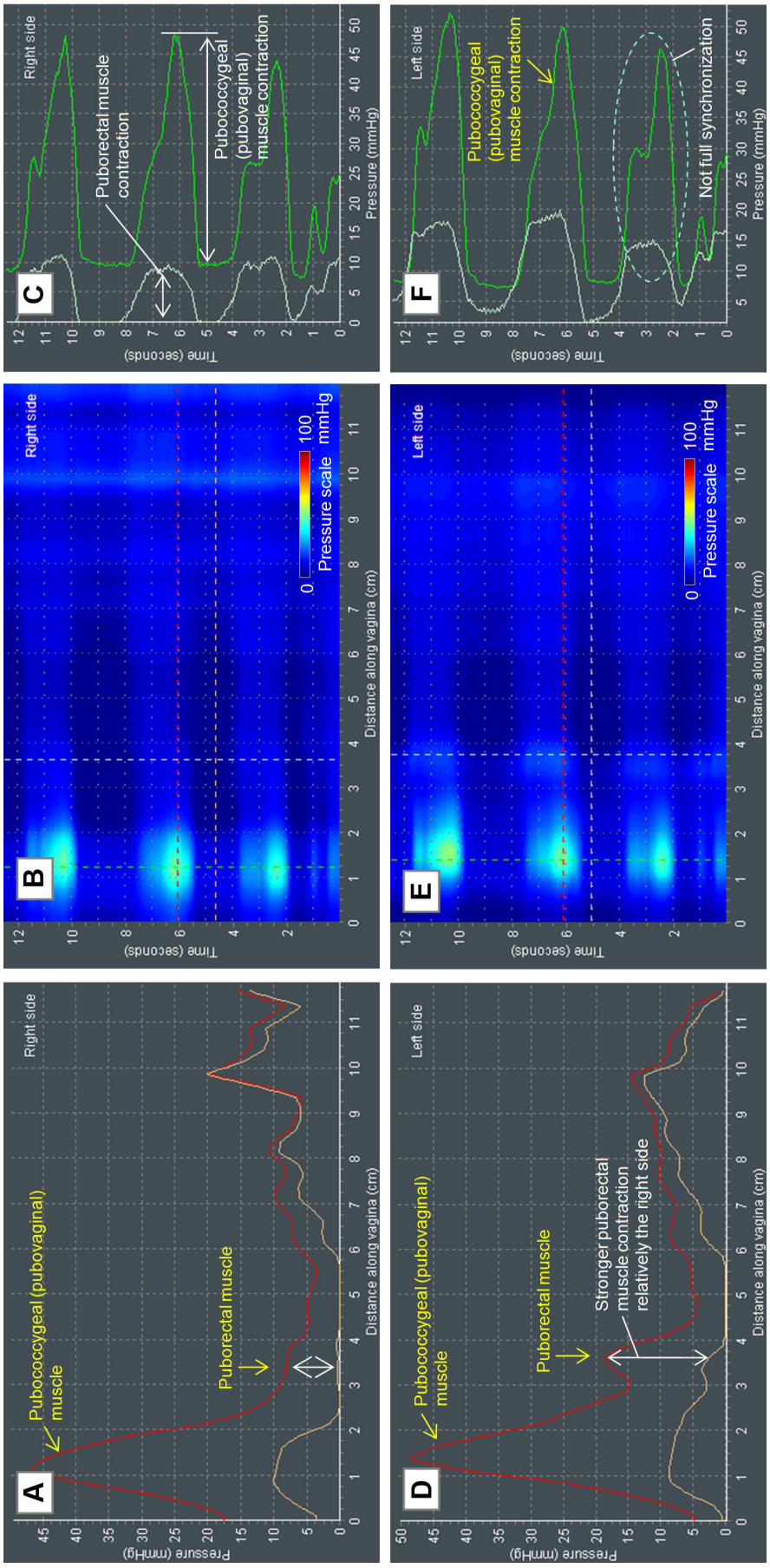

Figure 17 Test 6 (voluntary muscle contraction) results for an 80-year-old patient with Stage II prolapse.
Notes: (**A**, **D**) Right and left side pressure patterns at muscle contraction (red lines) and at rest (light brown lines); (**B**, **E**) dynamic pressure pattern along the vagina; (**C**, **F**) muscle contraction dynamic at specific locations (see dotted lines in **B**, **E**).

displacement begins at the initial stage of pelvic muscle contraction. Both left and right vaginal sides present one basic peak identified as the pubococcygeal (pubovaginal) muscle contraction (Figure 17). The left side also demonstrates some puborectal contractive activity (Figure 17D). For both the left and right sides, we observe that a full synchronization for PVM and PRM does not occur (Figure 17F); the pubovaginal contraction consists of two phases, primary peak and secondary at about 60% of amplitude; however, the pubovaginal contractive signal does not have such a significant decrease at the second contraction phase.

Tests 5 and 6 (voluntary muscle contraction) will allow assessment of the following:

- PPM, PRM, PVM, and ICM strength;
- contractive capability (*P*) of the urethra (U);
- contractive desynchronization or not full synchronization among levator ani muscles;
- muscle asymmetry (left vs right) in levator ani muscles (weakness or avulsion);
- muscle mobility along the vagina in the mid-posterior compartment;
- contractive width of levator ani muscles; and
- multiphase muscle contraction.

The clinical value of Tests 5 and 6 lies in their following characteristics:

- detection of defects in pelvic floor muscle PPM, PRM, PVM, ICM;
- contractive capability of the urethra (U);
- comparative analysis of pelvic floor MS after pelvic floor treatment;
- muscle characterization of postpartum pelvic floor remodeling;
- muscle changes with lifestyle: sport, military load influence, and so on; and
- muscle changes with age.

Test 7: involuntary muscle relaxation

Figures 18 and 19 show the VTI data during involuntary pelvic muscle relaxation for a patient with normal pelvic floor support (Figure 18) and with Stage II prolapse (Figure 19).

For this test, a patient is instructed to perform a pelvic floor muscle contraction or Kegel and urged to hold the contraction as long as possible.

The normal pelvic floor support case demonstrates 1) pelvic muscle relaxation rate (MRR) of 5 mmHg/s (Figure 18F), 2) one-stage muscle relaxation (Figure 19F), and 3) uniform relaxation for levator ani muscles by 33 mmHg (Figure 18D).

Under Stage II prolapse, we observe 1) pelvic MRR of 16 mmHg/s, 2) two-stage muscle relaxation (Figure 19F), and 3) nonuniform relaxation for levator ani muscles – PVM relaxed by 70 mmHg, but RPM relaxed by only 34 mmHg (Figure 19D). These two muscles (pubovaginal and puborectal) not only show a distinctive relaxation rate, but also have two separate peaks (Figure 19D and E).

Test 7 (involuntary muscle relaxation) may allow assessment of the following:

- PVM, PRM, and ICM to keep the load measured as the MRR (mmHg/s);
- uniformity/nonuniformity of muscle relaxation; and
- multistage muscle relaxation.

The clinical value of Test 7 lies in the following:

- detection of muscle relaxation defects in PVM, PRM, ICM;
- comparative analysis of pelvic floor MS after pelvic floor treatment;
- muscle characterization of postpartum pelvic floor remodeling;
- muscle changes with lifestyle: sport, military load influence, and so on; and
- muscle changes with age.

Test 8: involuntary muscle contraction (cough)

Figures 20 and 21 show the VTI data for a patient with normal pelvic floor support (Figure 20) and with Stage IV prolapse (Figure 21) during involuntary pelvic floor muscle contractions (cough).

The normal pelvic floor support case reveals a strong signal from the urethra in the anterior (Figure 20A–C) and distributed response from the levator ani contraction (Figure 20D–F) in the posterior compartment at cough. It seems that in both compartments, the VTI probe pressure signals at cough have two components: 1) the first one is produced by pressure increase by 43 mmHg around the vagina and 2) the second one is related to the muscle activities (Figure 20A and D). The pressure increase from urethra (Figure 20C) occurs with a urethra displacement of 9 mm, as observed in Figure 20A and B. The levator ani muscles contract synchronously as seen in Figure 20E, F. Possibly, the strongest contractive signal comes from the PAM (Figure 20F).

The pressure patterns at cough for a patient with Stage IV prolapse are much different from the normal pelvic floor conditions. We find no confirmation of any muscle activities at cough (Figure 21). Instead of localized muscle contraction signals, we observe a uniform and synchronized pressure

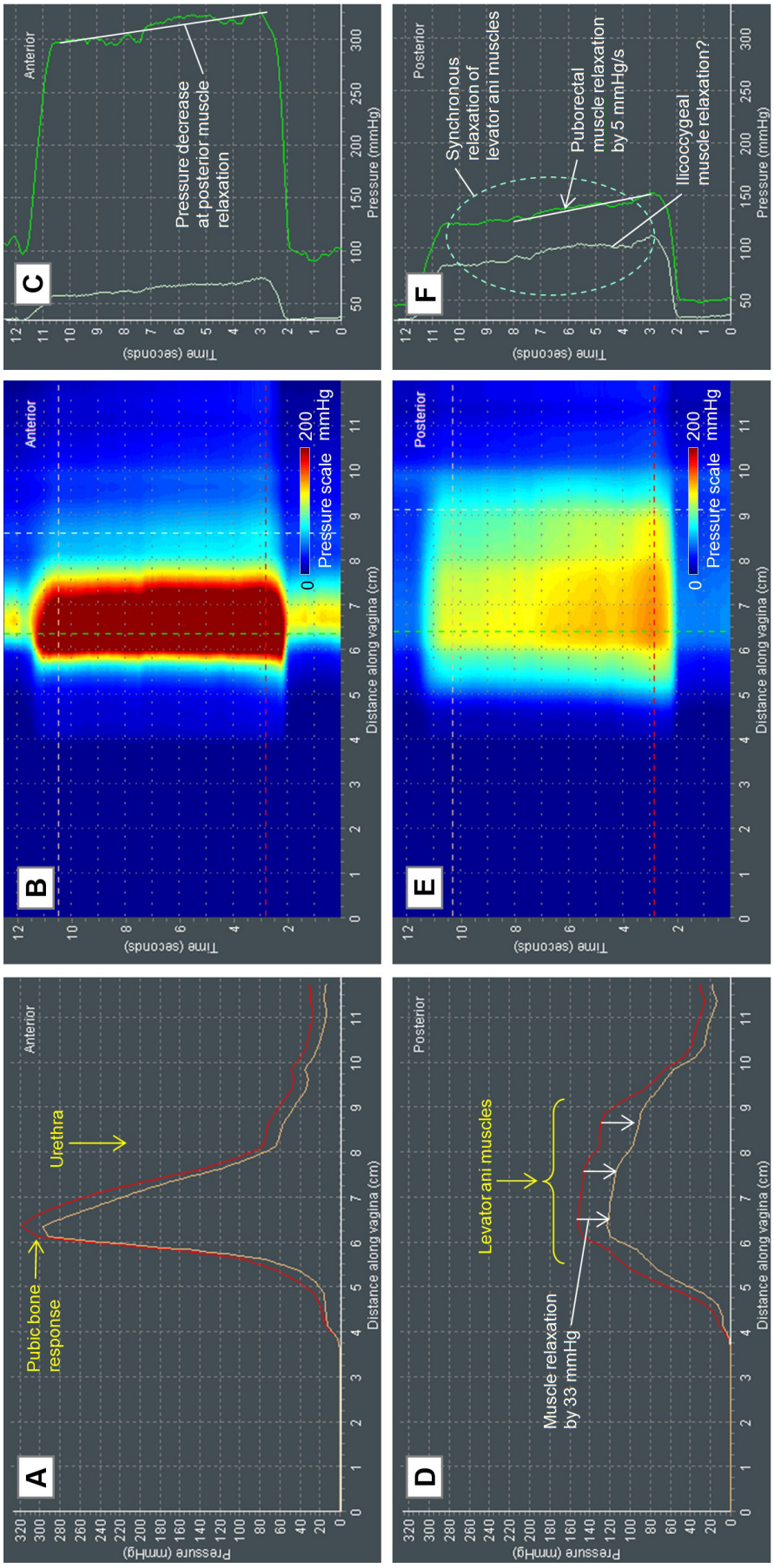

Figure 18 Test 7 (involuntary muscle relaxation) results for a 74-year-old patient with normal pelvic floor support.
Notes: (**A**, **D**) Anterior and posterior pressure patterns at muscle relaxation (from red to light brown lines); (**B**, **E**) dynamic pressure pattern along the vagina; (**C**, **F**) muscle relaxation dynamic at specific locations (see dotted lines in **B**, **E**).

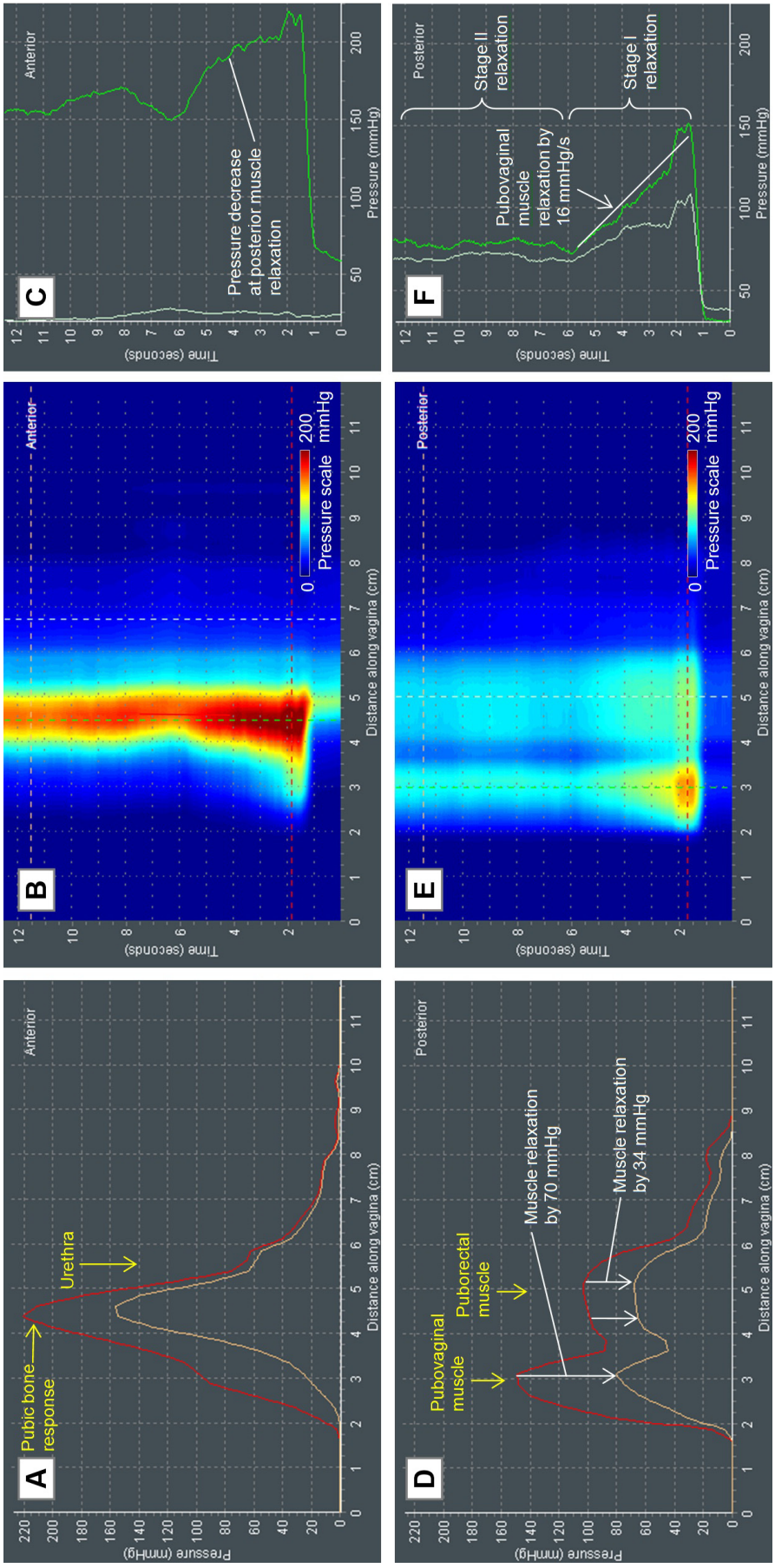

Figure 19 Test 8 (involuntary muscle relaxation) results for a 71-year-old patient with Stage II prolapse.
Notes: (**A**, **D**) Anterior and posterior pressure patterns at muscle relaxation (from red to light brown lines); (**B**, **E**) anterior and posterior dynamic pressure pattern along the vagina; (**C**, **F**) muscle relaxation dynamic at specific locations (see dotted lines in **B**, **E**).

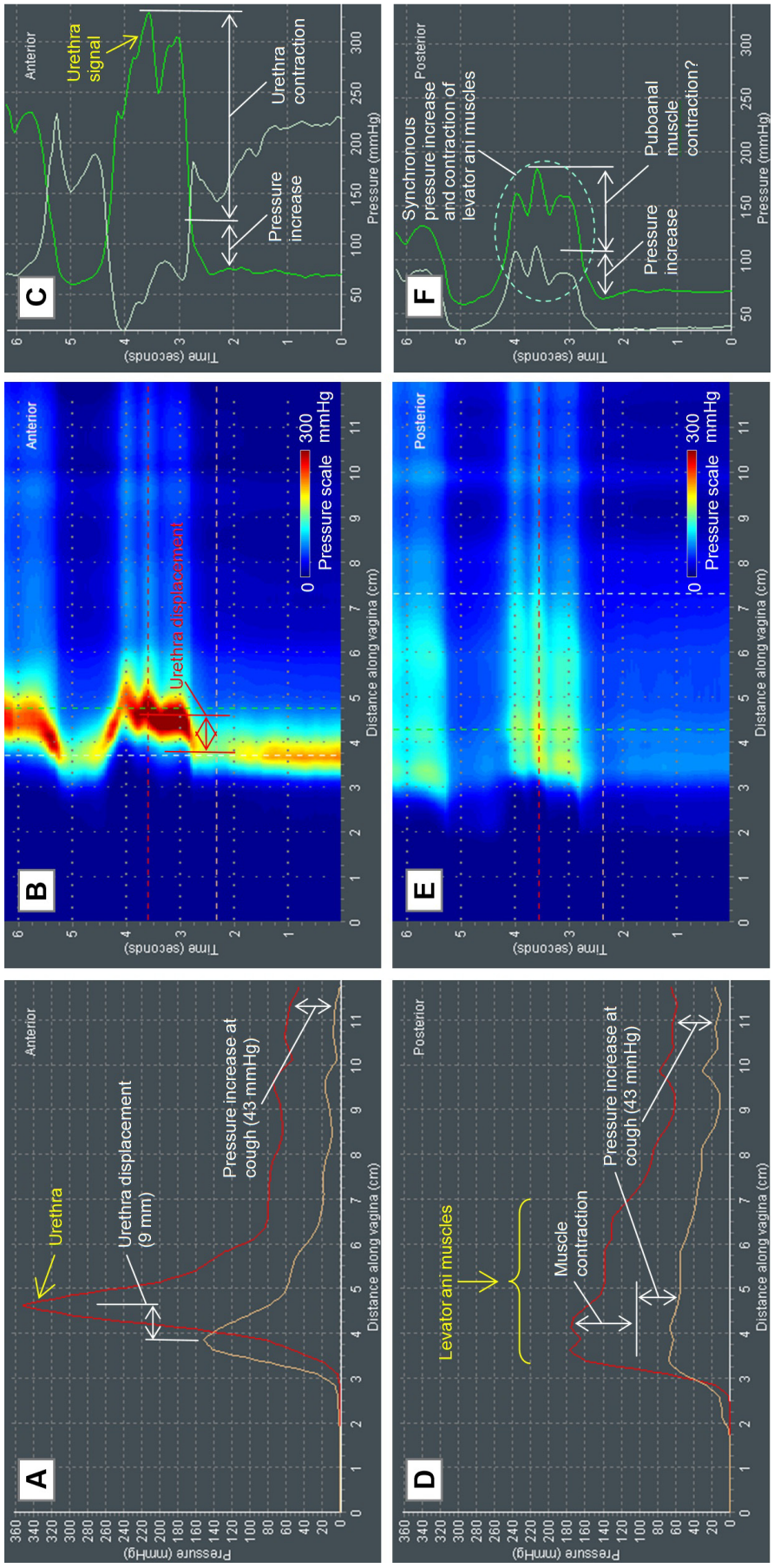

Figure 20 Test 8 (involuntary muscle contraction) results for a 51-year-old patient with normal pelvic floor support.
Notes: (**A**, **D**) Pressure patterns at muscle contraction (red lines) and at rest (light brown lines); (**B**, **E**) anterior and posterior dynamic pressure pattern along the vagina; (**C**, **F**) muscle contraction dynamic at specific locations (see dotted lines in **B**, **E**).

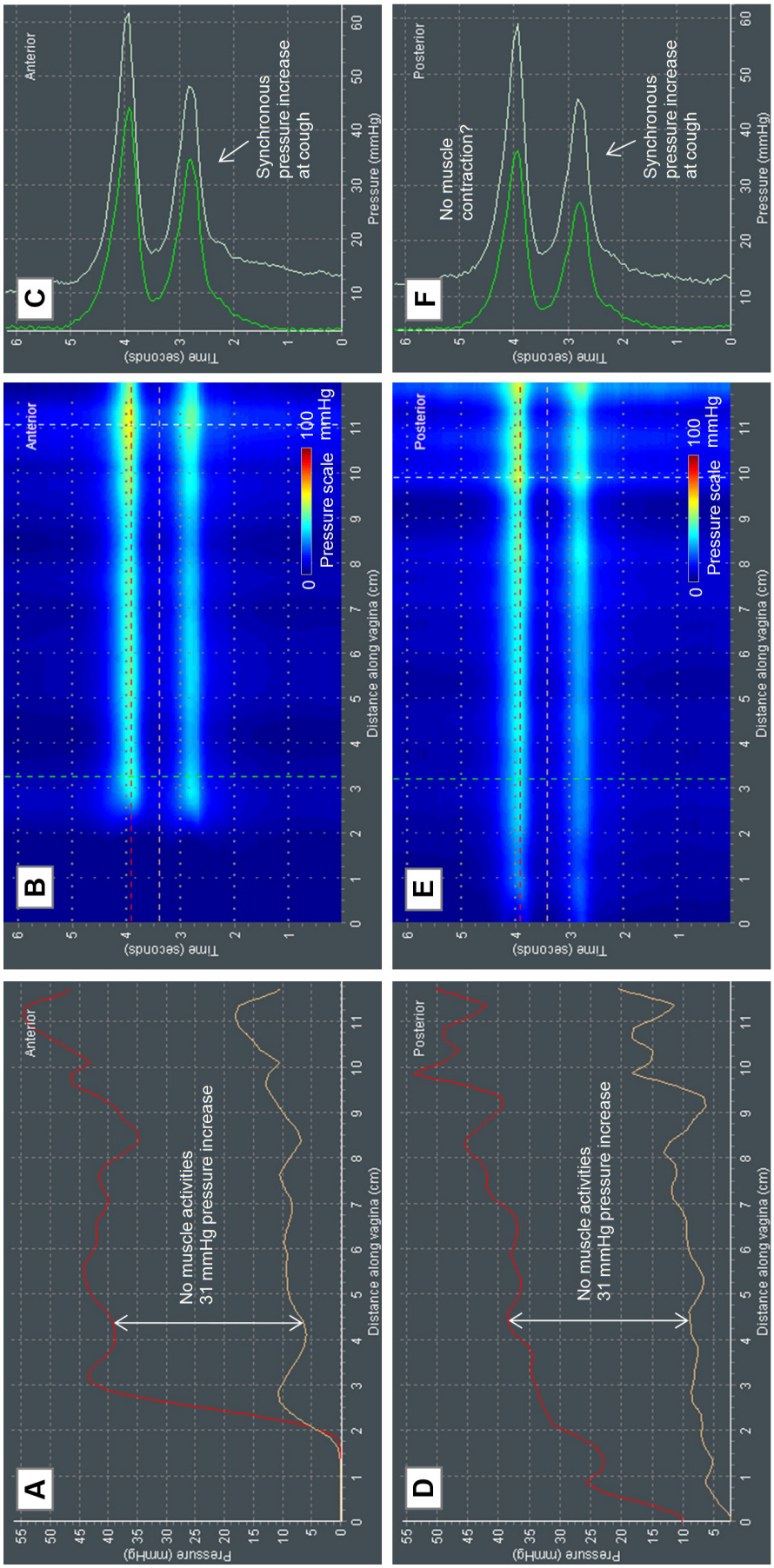

Figure 2 Test 8 (involuntary muscle contraction) results for a 64-year-old patient with Stage IV prolapse.
Notes: (**A**, **D**) Pressure patterns at muscle contraction (red lines) and at rest (light brown lines); (**B**, **E**) right and left side dynamic pressure pattern along the vagina; (**C**, **F**) muscle contraction dynamic at specific locations (see dotted lines in **B**, **E**).

Table 1 VTI parameters, pelvic floor structures, clinical value, and relevant clinical conditions for VTI tests 1–8

VTI test	Test output	VTI parameters and pelvic structures to be characterized	Clinical value
Test 1 Probe insertion	• 2D tactile image of anterior vs posterior • Maximum pressure (*P*) graphs along posterior and anterior • Maximum pressure gradient ($\partial P/\partial y$) graphs along posterior and anterior	• Vaginal tissue elasticity distribution ($\partial P/\partial y$) along anterior and posterior compartments • Strength (*P*) and, possibly, elasticity ($\partial P/\partial y$) of urethra (U) in distal anterior • Strength (*P*) and elasticity ($\partial P/\partial y$) of the ZCE in mid-anterior • Strength (*P*) and elasticity ($\partial P/\partial y$) of the USL/CL in apical anterior • Strength (*P*) and elasticity ($\partial P/\partial y$) of PB in distal posterior • Rest tone (*P*) and elasticity ($\partial P/\partial y$) of levator ani muscles and, possibly, PRM in mid-posterior • Strength (*P*) of LP in apical posterior • Hiatus strength as combined distal anterior and posterior pressure (*P*)	• Detection defects in vaginal wall • PB characterization for diagnosis of defects • PRM characterization for diagnosis of defects • LP characterization for diagnosis of defects • USL/CL characterization for diagnosis of defects • Urethra characterization • Monitoring of vaginal elasticity changes after applied treatment (surgery, physiotherapy, RF, or laser procedures) • Scar detection and characterization of ZCE for UI diagnosis (tethered vagina syndrome) • Characterization of postpartum pelvic floor remodeling • Vaginal elasticity changes with age
Test 2 Probe elevation	• 2D tactile image of anterior and posterior under significant vaginal wall deformation (up to 40 mm) • Pressure (*P*) values at selected locations • Pressure gradients data/image ($\partial P/\partial y$) of anterior and posterior compartments	• Strength (*P*) of pelvic floor support structures along the posterior compartment • Elasticity ($\partial P/\partial y$) of urethra (U) in distal anterior • Elasticity ($\partial P/\partial y$) of the USL/CL in apical anterior • Elasticity ($\partial P/\partial y$) of PRM, PAM, PVM, and ICM at rest • Elasticity of ($\partial P/\partial y$) of LP • PUL and ATFP assessment at maximum posterior deformation is under question	• Detection of defects in pelvic floor support structures including PRM, PAM, PVM, ICM and USL/CL • Comparative analysis of pelvic floor support after applied treatment (surgery, physiotherapy, RF, or laser procedures) • Characterization of postpartum pelvic floor remodeling • Pelvic support changes with age
Test 3 Probe rotation	• 2D tactile image of circumferential vaginal walls • Pressure (*P*) values at selected locations • Integral contact pressure	• Vaginal "tightness" • Irregularities on the vaginal walls along the entire vagina as pressure peak value (*P*) and its size • Asymmetry in pelvic floor structures behind the vaginal walls • Cumulative (integral) contact pressure inside the vagina ("vaginal strength")	• Irregularities detection/characterization on vaginal walls • Monitoring of vaginal wall changes after applied treatment (surgery, physiotherapy, RF, or laser procedures) • Postpartum vaginal wall changes

Tests 5 and 6 Voluntary muscle contraction (anterior vs posterior)	• Dynamic pressure ($P(t)$) signals • Pressure patterns at rest ($P_1(x)$) and at contraction ($P_2(x)$) • MS = $P_2(x) - P_1(x)$ • Structure mobility (Δx) • Contractive desynchronization or not full synchronization • Left $P_l(x)$ vs right $P_r(x)$ side contraction pattern • Phases of contraction	• PPM, PRM, PVM, and ICM strength • Contractive capability (P) of urethra (U) • Contractive desynchronization or not full synchronization among levator ani muscles • Muscle asymmetry (left vs right) in levator ani muscles (weakness or avulsion) • Muscle mobility along the vagina in mid-posterior compartment • Contractive width of levator ani muscles • Multiphase muscle contraction	• Detection of defects in pelvic floor muscle PPM, PRM, PVM, ICM • Contractive capability of urethra (U) • Comparative analysis of pelvic floor MS after pelvic floor treatment • Muscle characterization of postpartum pelvic floor remodeling • Muscle changes with lifestyle: sport, military load influence, and so on • Muscle changes with age
Test 7 Involuntary muscle relaxation (left vs right side)	• Muscle relaxation rate ($\Delta P/\Delta t$) • Uniformity of muscle relaxation • Stages of relaxation	• PVM, PRM, and ICM to keep the load measured as MRR (mmHg/s) • Uniformity/nonuniformity of muscle relaxation • Multistage muscle relaxation	• Detection of muscle relaxation defects in PVM, PRM, ICM • Comparative analysis of pelvic floor MS after pelvic floor treatment • Muscle characterization of postpartum pelvic floor remodeling • Muscle changes with lifestyle: sport, military load influence, and so on • Muscle changes with age
Test 8 Involuntary muscle contraction (cough)	• Dynamic pressure ($P(t)$) signals • Pressure patterns at rest ($P_1(x)$) and at contraction ($P_2(x)$) • Involuntary muscle contractive component IMC = $P_2(x) - P_1(x) - \Delta P$ • Urethra mobility (Δx) • Uniform pressure change (ΔP) at cough	• Contractive capability (P) of urethra (U) • Mobility of the urethra (U) • Uniform pressure increase (P) under along the entire vagina in anterior and posterior compartments • Levator ani muscles IMC	• Detection of defects in urethra (U) • Availability of involuntary component in levator ani muscles • Urethra (U) and levator ani changes with age

Abbreviations: 2D, two-dimensional; ATFP, arcus tendineus fascia pelvis ligament; CL, cardinal ligament; ICM, iliococcygeal muscle; IMC, involuntary muscle contraction components; LP, levator plate; MRR, muscle relaxation rate; MS, muscle strength; PAM, puboanal muscle; PB, perineal body; PPM, puboperineal muscle; PRM, puborectal muscle; PVM, pubovaginal muscle; PUL, pubourethral ligament; RF, radio frequency; UI, urinary incontinence; USL, uterosacral ligament; VTI, vaginal tactile imaging; ZCE, zone of critical elasticity.

raise at cough in the anterior and posterior compartments along the entire vagina, with some pressure elevation at the apical part. Similar to the images obtained in Test 4 (Valsalva), there is a noted widening of the pressure transference along the mid-to-upper vagina.

From these two cases, we may conclude that VTI provides unique quantitative data for involuntary contractive capabilities of the urethra and the levator ani muscles (puboanal). Mobility of urethra can be visualized and estimated.

Test 8 (involuntary muscle contraction) will allow assessment of the following:

- contractive capability (P) of the urethra (U);
- mobility of the urethra (U);
- uniform pressure increase (P) along the entire vagina in the anterior and posterior compartments; and
- levator ani muscles' involuntary contraction components.

The clinical value of Test 8 lies in the following:

- detection of defects in the urethra (U);
- availability of the involuntary component in the levator ani muscles; and
- urethra (U) and levator ani changes with age.

Discussion

In the previous sections, we described VTI examination findings and data interpretation supported by clinical observations. This interpretation is based on a number of widely accepted anatomic and functional assumptions. However, an understanding of the VTI and its interpretation will grow as more clinical experience is gained in pelvic floor research using VTI measurements. Of course, clinical application of VTI data interpretation also requires knowledge of pelvic functional anatomy, physiology, and clinical history for the individual patient.

Among the VTI limitations are image dependence on operator's skill level, contact conditions, and probe size. In general, an examination with a tactile imaging probe is operator dependent, similar to colonoscopy.[37] Operator training is required to improve and standardize operator skills.[38] Minimization or elimination of the operator dependence is also achieved by intentional probe design, data processing algorithms, and real-time feedback to the operator. The VTI intra- and interoperator measurement reproducibility study with 12 subjects demonstrated intraclass correlation coefficients in the range from 0.80 to 0.92 and median tactile image deviations from 6.6% to 15.6%.[24] The lubrication helps to keep contact conditions reproducible. Tactile imaging probes with different size and contact area of 15 μm^2,[39] and 20 cm^2,[22] demonstrate different absolute values of $P(x,y,z)$ acquired for the same tissue. But comparison of the two image data sets reveals a lot of similarity and common features; both probes show close relative distribution within $P(x,y,z)$ and enable similar tissue characterization.[22,39]

The VTI offers an opportunity to assess vaginal tissue elasticity, pelvic floor support, and function. Table 1 summarizes VTI capability in pelvic floor characterization. The pelvic floor conditions can be characterized by at least 31 VTI parameters derived from eight tests (studies). This allows a large body of measurements to evaluate individual variations in support defects as well as identify specific potential markers to measure tissue properties and muscle function in patients' diseased conditions that are accompanied by changes in mechanical properties and often physiologic manifestation. For example, a female patient presents with complaints of increasing vaginal pressure, discomfort, backache, and bulging exacerbated by lifting and straining. The physician performs transvaginal biomechanical mapping with the VTI probe to assess her pelvic floor support status, tissue elasticity, and muscle function and uses the information to determine the best course of treatment. Multiple (up to eight) subprocedures are completed to collect comprehensive biomechanical data for characterization of the vaginal and pelvic floor conditions. The procedure images are visualized in real time on a display to provide feedback to an operator and mapped to produce an examination report, in a form of a computer file and hard-copy record, so that the physician can review and interpret the results, dictate a report, and discuss the results with the patient. Among the clinical conditions when the VTI use can optimize and monitor treatment are POP, stress urinary incontinence, tissue atrophy, and pelvic pain because their etiology includes changes of pelvic tissue biomechanical properties and functions. The proposed approach also may help further differentiate the types of pelvic floor conditions, their underlying severity, and understand how to tailor treatments for the individual patient in the most effective manner.

Abbreviations

2D, two-dimensional; C, cervix; CL, cardinal ligament; ATFP, arcus tendineus fascia pelvis ligament; E, Young's modulus; IMC, involuntary muscle contraction components; ICM, iliococcygeal muscle; kPa, Pa ×1,000; LP, levator plate; m, meter (unit of distance); mmHg, millimeter of mercury (unit of pressure); MS, muscle strength; MRR, muscle relaxation rate; N, Newton (unit of force); P, pressure; Pa, Pascal (unit of pressure); PAM, puboanal muscle; PB, pubic

bone; POP, pelvic organ prolapse; PPM, puboperineal muscle (perineal body); PRM, puborectal muscle; PUL, pubourethral ligament; PVM, pubovaginal muscle; RF, radiofrequency; SUI, stress urinary incontinence; U, urethra; UI, urinary incontinence; USL, uterosacral ligament; VTI, vaginal tactile imager; ZCE, zone of critical elasticity.

Acknowledgments

Research reported in this publication was supported by the National Institute on Aging of the National Institutes of Health under the award numbers R44AG034714 and SB1AG034714. The content is solely the responsibility of the authors and does not necessarily represent the official views of the National Institutes of Health.

Disclosure

Dr Egorov is a co-founder and CEO of Advanced Tactile Imaging, Inc. Dr van Raalte is a co-founder of Advanced Tactile Imaging, Inc. Dr Lucente and Dr Murphy report no conflicts of interest in this work.

References

1. Pizarro-Berdichevsky J, Clifton MM, Goldman HB. Evaluation and management of pelvic organ prolapse in elderly women. *Clin Geriatr Med*. 2015;31(4):507–521.
2. Anderson KM, Davis K, Flynn BJ. Urinary incontinence and pelvic organ prolapse. *Med Clin North Am*. 2015;99(2):405–416.
3. Hendrix SL, Clark A, Nygaard I, Aragaki A, Barnabei V, McTiernan A. Pelvic organ prolapse in the women's health initiative: gravity and gravidity. *Am J Obstet Gynecol*. 2002;186(6):1160–1166.
4. Wu JM, Vaughan CP, Goode PS, et al. Prevalence and trends of symptomatic pelvic floor disorders in U.S. women. *Obstet Gynecol*. 2014; 123(1):141–148.
5. Wood LN, Anger JT. Urinary incontinence in women. *BMJ*. 2014; 349:g4531.
6. DeLancey JO. Pelvic floor anatomy and pathology. In: Hoyte L, Damaser MS, editors. *Biomechanics of the Female Pelvic Floor*. 1st ed. London, UK: Elsevier; 2016:13–51.
7. Dietz HP. *Pelvic Floor Ultrasound. Atlas and Text Book. Creative Commons Attribution License*. Springwood, Australia; 2016:1–127.
8. Petros P. *The Female Pelvic Floor: Function, Dysfunction and Management According to the Integral Theory*. 3rd ed. Berlin, Germany: Springer; 2010:1–330.
9. Walters MD, Karram MM. *Urogynecology and Reconstructive Pelvic Surgery*. 4th ed. Philadelphia, PA: Elsevier; 2015:1–688.
10. Ismail S, Duckett J, Rizk D, et al. Recurrent pelvic organ prolapse: International Urogynecological Association Research and Development Committee opinion. *Int Urogynecol J*. 2016;27(11):1619–1632.
11. Elliott CS, Sokol ER. Might pelvic surgeons be unaware of their surgical failures? Patient reporting and perceptions after failed incontinence or pelvic organ prolapse surgery. *Female Pelvic Med Reconstr Surg*. 2015; 21(5):298–300.
12. Nygaard I, Brubaker L, Zyczynski HM, et al. Long-term outcomes following abdominal sacrocolpopexy for pelvic organ prolapse. *JAMA*. 2013;309(19):2016–2024.
13. Stepp KJ, Walters MD, Karram MM. Anatomy of the lower urinary tract, pelvic floor, and rectum. In: *Urogynecology and Reconstructive Pelvic Surgery*. 4th ed. Philadelphia, PA: Elsevier; 2015:19–31.
14. Timoshenko S, Goodier JN. *Theory of Elasticity*. New York, NY: McGraw-Hill Book Company; 1951:1–508.
15. Landau LD, Lipshitz EM. *Theory of Elasticity*. 3rd ed. Oxford, UK: Elsevier; 1970:1–172.
16. Taber AT. *Nonlinear Theory of Elasticity. Applications in Biomechanics*. London, UK: World Scientific Pub Co Inc; 2004:1–416.
17. Johnston WL. The role of static and motion palpation in structural diagnosis. *J Am Osteopath Assoc*. 1975;75(4):421–424.
18. Duck FA. Physical properties of tissue: a comprehensive reference book. In: *Mechanical Properties of Tissue*. London, UK/San Diego, CA: Academic Press; 1990:137–165. (Chapter 5).
19. Fung YC. *Biomechanics: Mechanical Properties of Living Tissues*. 2nd ed. Ann Arbor, USA: Prentice-Hall, Inc; 1993:1–568.
20. Sarvazyan A. Elastic properties of soft tissues. In: Levy M, Bass HE, Stern RR, editors. *Elastic Properties of Soft Tissues Handbook of Elastic Properties of Solids, Liquids, and Gases*. Vol III. New York, NY: Academic Press; 2001:107–127. (Chapter 5).
21. Egorov V, Ayrapetyan S, Sarvazyan AP. Prostate Mechanical Imaging: 3-D image composition and feature calculations. *IEEE Trans Med Imaging*. 2006;25(10):1329–1340.
22. Egorov V, Sarvazyan AP. Mechanical imaging of the breast. *IEEE Trans Med Imaging*. 2008;27(9):1275–1287.
23. Egorov V, van Raalte H, Lucente V, Sarvazyan A. Biomechanical characterization of the pelvic floor using tactile imaging. In: Hoyte L, Damaser MS, editors. *Biomechanics of the Female Pelvic Floor*, Chapter 17. London, UK: Elsevier; 2016:317–348.
24. van Raalte H, Lucente V, Ephrain S, et al. Intra- and inter-observer reproducibility of vaginal tactile imaging. American Urogynecologic Society 37th Annual Meeting, September 27 – October 1; 2016; Denver, CO.
25. van Raalte H, Lucente V, Ephrain S, Murphy M, Bhatia N, Egorov V. Pelvic organ prolapse surgery characterization by vaginal tactile imaging. *Int Urogynecol J*. 2016;(Suppl 1):S117–S118.
26. van Raalte H, Bhatia N, Egorov V. Is it all just smoke and mirrors? Vaginal laser therapy and its assessment by tactile imaging. *Int Urogynecol J*. 2016;(Suppl 1):S120–S121.
27. van Raalte H, Egorov V. Tactile imaging markers to characterize female pelvic floor conditions. *Open J Obstet Gynecol*. 2015;5(9): 505–515.
28. van Raalte H, Egorov V. Characterizing female pelvic floor conditions by tactile imaging. *Int Urogynecol J*. 2015;26(4):607–609.
29. van Raalte H, Lucente V, Egorov V. High definition pressure mapping of the pelvic floor muscles during Valsalva manever, voluntary muscle contraction and involuntary relaxation. *Female Pelvic Med Reconstr Surg*. 2015;21(5):S149–S150.
30. van Raalte H, Lucente V, Egorov V. Pressure mapping of voluntary and involuntary muscle contraction for assessment of SUI conditions. *Proceedings of International Continence Society 45th Annual Meeting*. Montreal, Canada, October 6–9; 2015:529.
31. van Raalte H, Egorov V. High definition manometry for intravaginal observation of pelvic floor muscle contractions. *Proceedings of International Continence Society 44th Annual Meeting*. Rio De Janeiro, Brazil, October 20–24; 2014.
32. van Raalte H, Egorov V, Lucente V, Murphy M, Saiz C. 3D tactile imaging in early prolapse detection. *Neurourol Urodyn*. 2013; 32(6):704–705.
33. Egorov V, van Raalte H, Lucente V. Quantifying vaginal tissue elasticity under normal and prolapse conditions by tactile imaging. *Int Urogynecol J*. 2012;23(4):459–466.
34. van Raalte H, Lucente V, Egorov V. 3-D imaging and quantifying vaginal tissue elasticity under normal and prolapse conditions. *Int Urogynecol J*. 2011;22(S1):S183–S184.
35. Egorov V, van Raalte H, Sarvazyan A. Vaginal Tactile Imaging. *IEEE Trans Biomed Eng*. 2010;57(7):1736–1744.
36. Bump RC, Mattiasson A, Bo K, et al. The standardization of terminology of female pelvic organ prolapse and pelvic floor dysfunction. *Am J Obstet Gynecol*. 1996;175(1):10–17.

37. Korman LY, Egorov V, Tsuryupa S, et al. Characterization of forces applied by endoscopists during colonoscopy by using a wireless colonoscopy force monitor. *Gastrointest Endosc*. 2010;71(2):327–334.
38. Egorov V, Sarvazyan A. Operator training and performance descriptor for prostate mechanical imaging. *Proceedings of the 7th International Conference on the Ultrasonic Measurement and Imaging of Tissue Elasticity*, Austin, Texas, Oct 27–30; 2008:27.
39. Oie T, Suzuki H, Fukuda T, et al. Tactile mapping system: a novel imaging technology for surface topography and elasticity of tissues or organs. *Innovations (Phila)*. 2009;4(6):345–350.

International Journal of Women's Health

Dovepress

Publish your work in this journal

The International Journal of Women's Health is an international, peer-reviewed open-access journal publishing original research, reports, editorials, reviews and commentaries on all aspects of women's healthcare including gynecology, obstetrics, and breast cancer. The manuscript management system is completely online and includes a very quick and fair peer-review system, which is all easy to use. Visit http://www.dovepress.com/testimonials.php to read real quotes from published authors.

Submit your manuscript here: http://www.dovepress.com/international-journal-of-womens-health-journal

Dr Hichem Bensmail, Bordeaux, France

Biomechanical characterization using tactile imaging and interpretation of female pelvic floor conditions before a treatment

CASE REPORTS

Background

Biomechanical and functional evaluations of vaginal conditions facilitate outcome assessment, leading to improved patient satisfaction. In case of pelvic floor issues, a patient could undergo medical imaging and biomechanical diagnostic tests. The results of these tests may help to analyse options of treatment and suggest the optimal for one patient.

Methods

Vaginal tactile imaging (VTI) allows assessment of the soft tissue of the vaginal walls at rest, with manually applied deflection pressures and with voluntary and involuntary muscle contraction, and relaxation, and Valsalva maneuver. During a patient examination, data collected from the probe sensors are displayed on the VTI computer display in real time. VTI allows acquisition of the pressure patterns along the entire vagina to visualize tissue elasticity, muscle tone and strength at contraction. That provides evaluation of individual variations in tissue elasticity, support defects, as well as pelvic muscle function.

Results

The patients have had normal pelvic support or pelvic organ prolapse. We transposed a set of 31 VTI parameters into a quantitative characterization of pelvic muscles and ligamentous structures. The VTI probe allows compression of vaginal tissues in the orthogonal direction to the tissue surface during probe insertion (Figure 1); pelvic floor tissue displacement

during the probe elevation (Figure 2); vaginal wall deformation and pressure pattern acquisition during the probe rotation (Figure 3); and acquisition of pressure patterns for pelvic muscle contraction along the vagina (Figure 4).

Interpretation of the acquired VTI data for normal pelvic floor support and prolapse conditions is proposed based on biomechanical assessment of the functional anatomy.

Then we processed to VTI data acquisition for four patients with different pelvic floor conditions (Figure 5), Vaginal laxity, Stress Urinary Incontinence (SUI), Pelvic Organ Prolapse (POP).

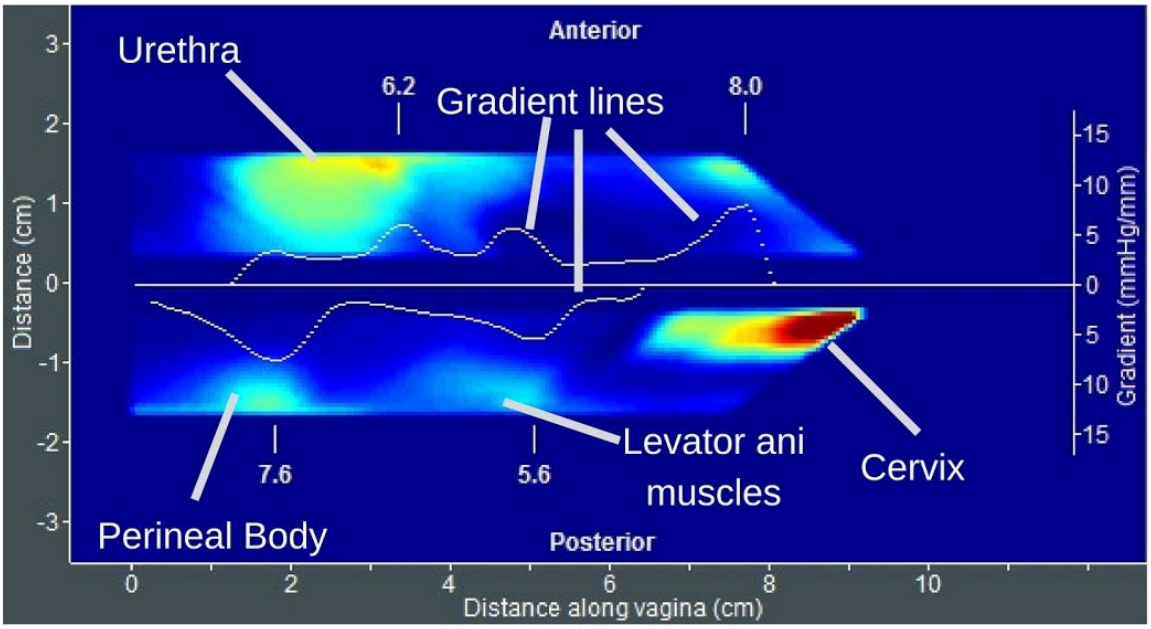

Figure 1 Vaginal Tissue Elasticity

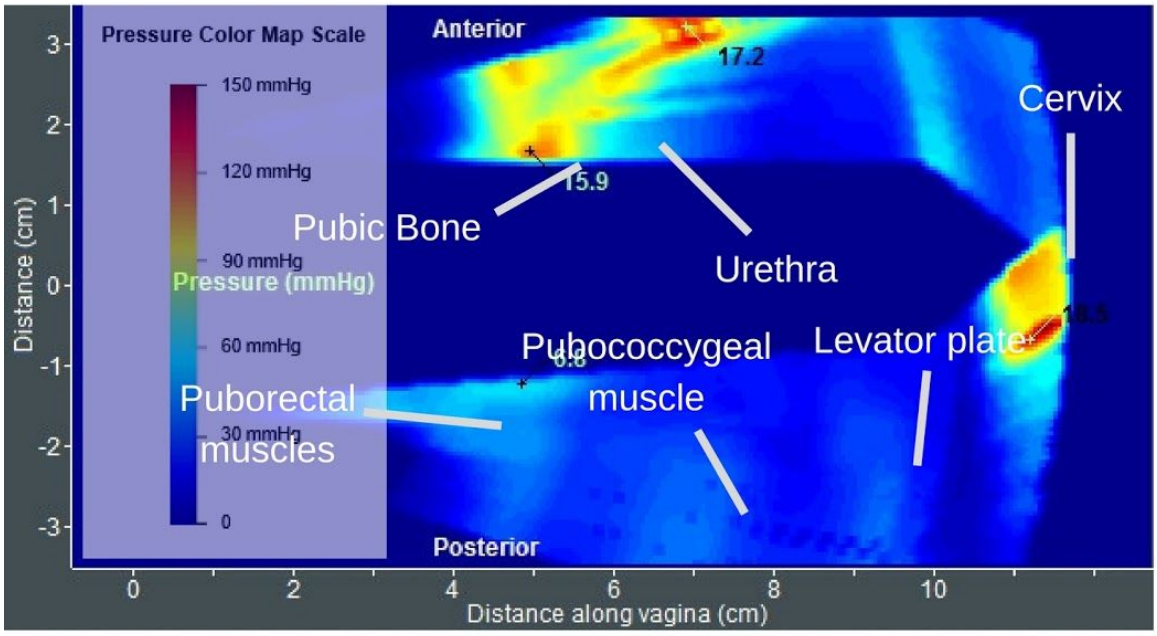

Figure 2 Pelvic Floor Support Conditions

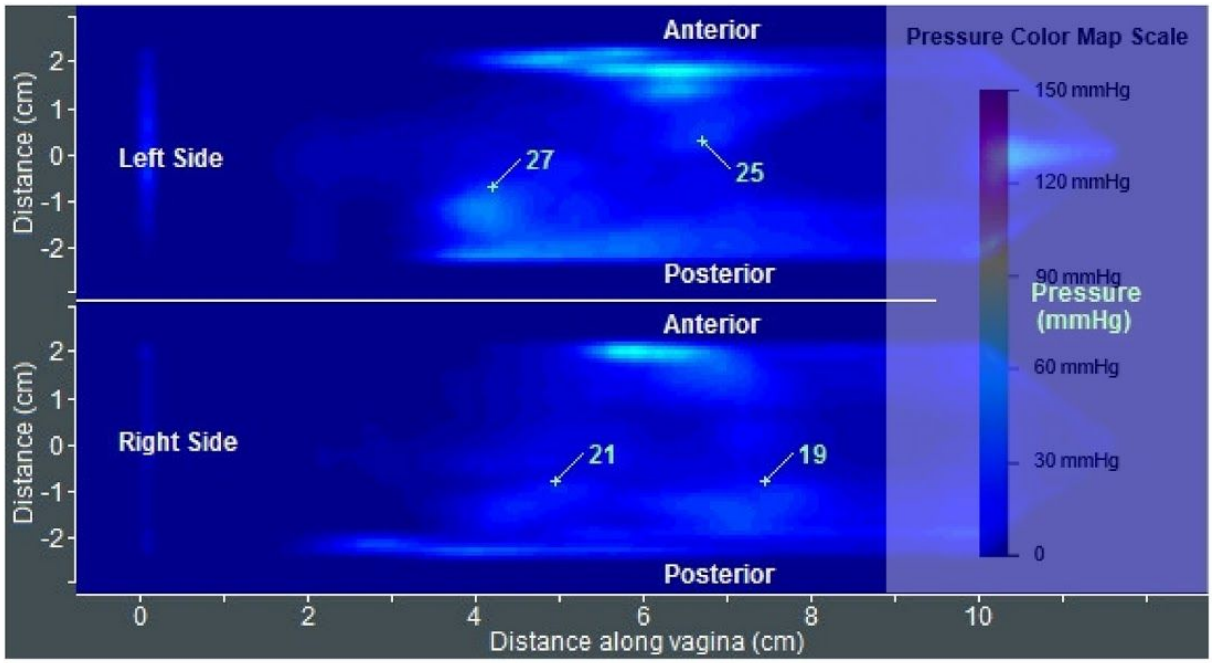

Figure 3 Condition of vaginal walls

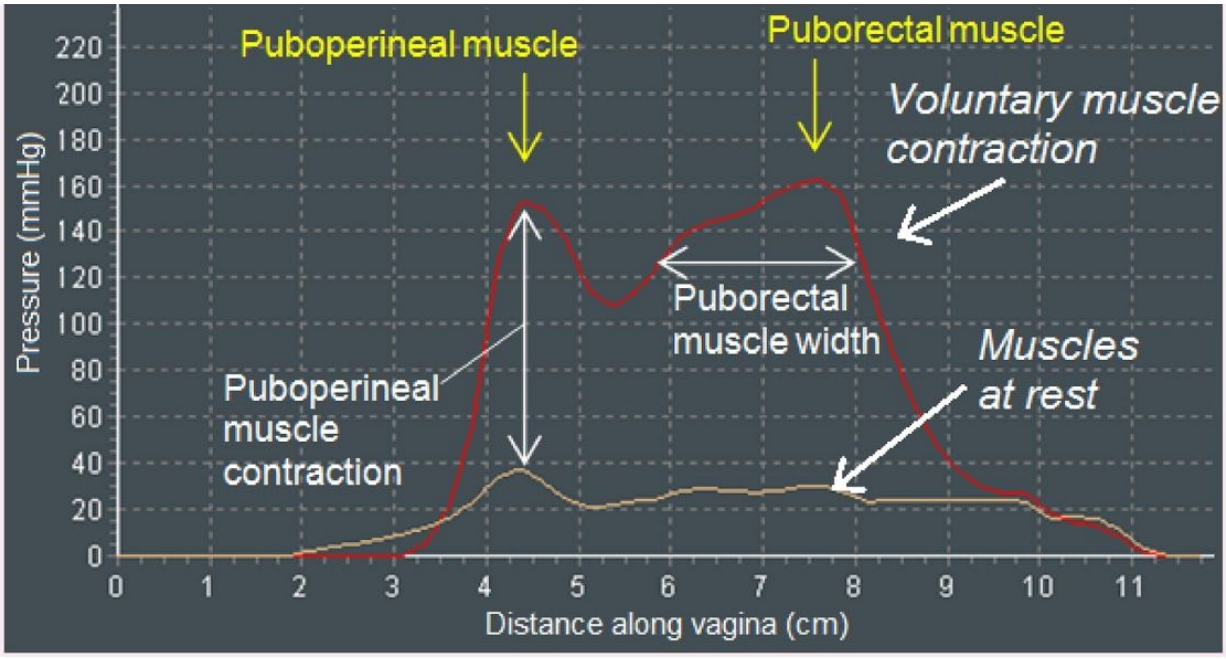

Figure 4 Pelvic Muscle Strength at contraction

Source : Advanced Tactile Imaging

	Patient A SB 40 yo, 3 deliveries Vaginal Laxity No POP, no SUI	Patient B ID 45 yo, 1 delivery 1 C-section Vaginal Laxity Mild SUI No POP	Patient C PN 47 yo, 2 deliveries Vaginal Laxity Surgical Vaginoplasty 3 years before No SUI, No POP	Patient D VK 50 yo, no children Vaginal Laxity Dyspareunia, VVA Light SUI No POP
Test 1	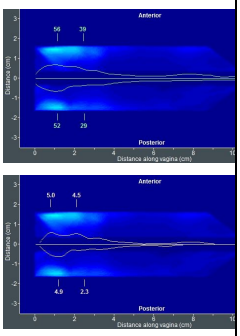	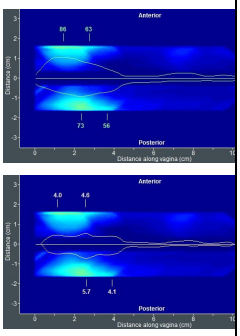	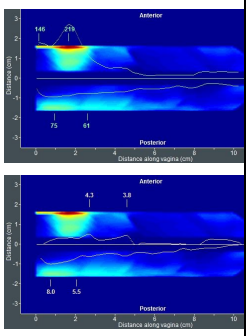	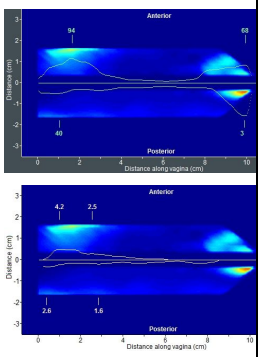
Test 2 Pressure	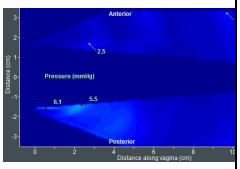	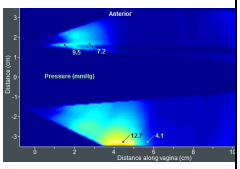	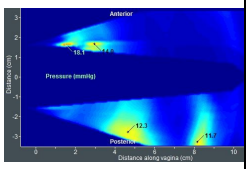	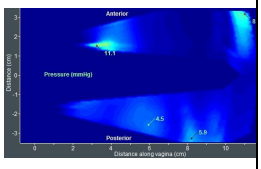
Gradient	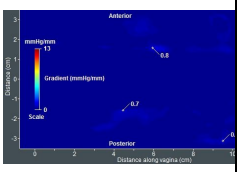	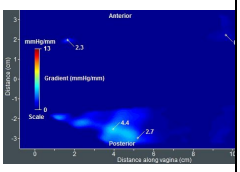	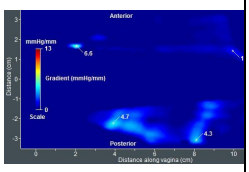	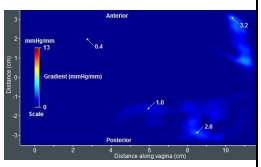
Test 3	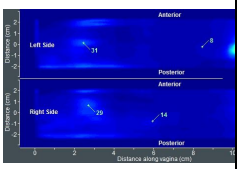	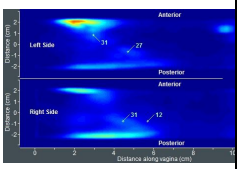	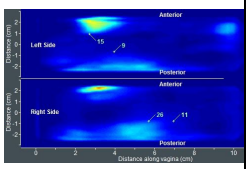	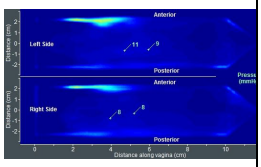
Test 4	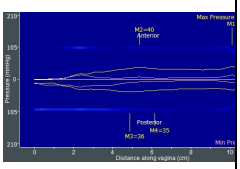	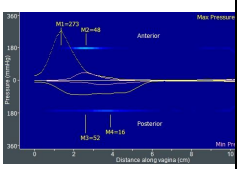	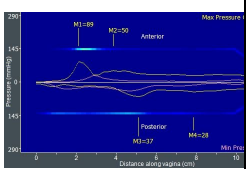	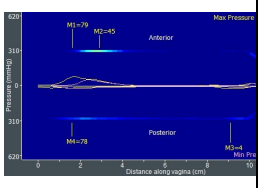

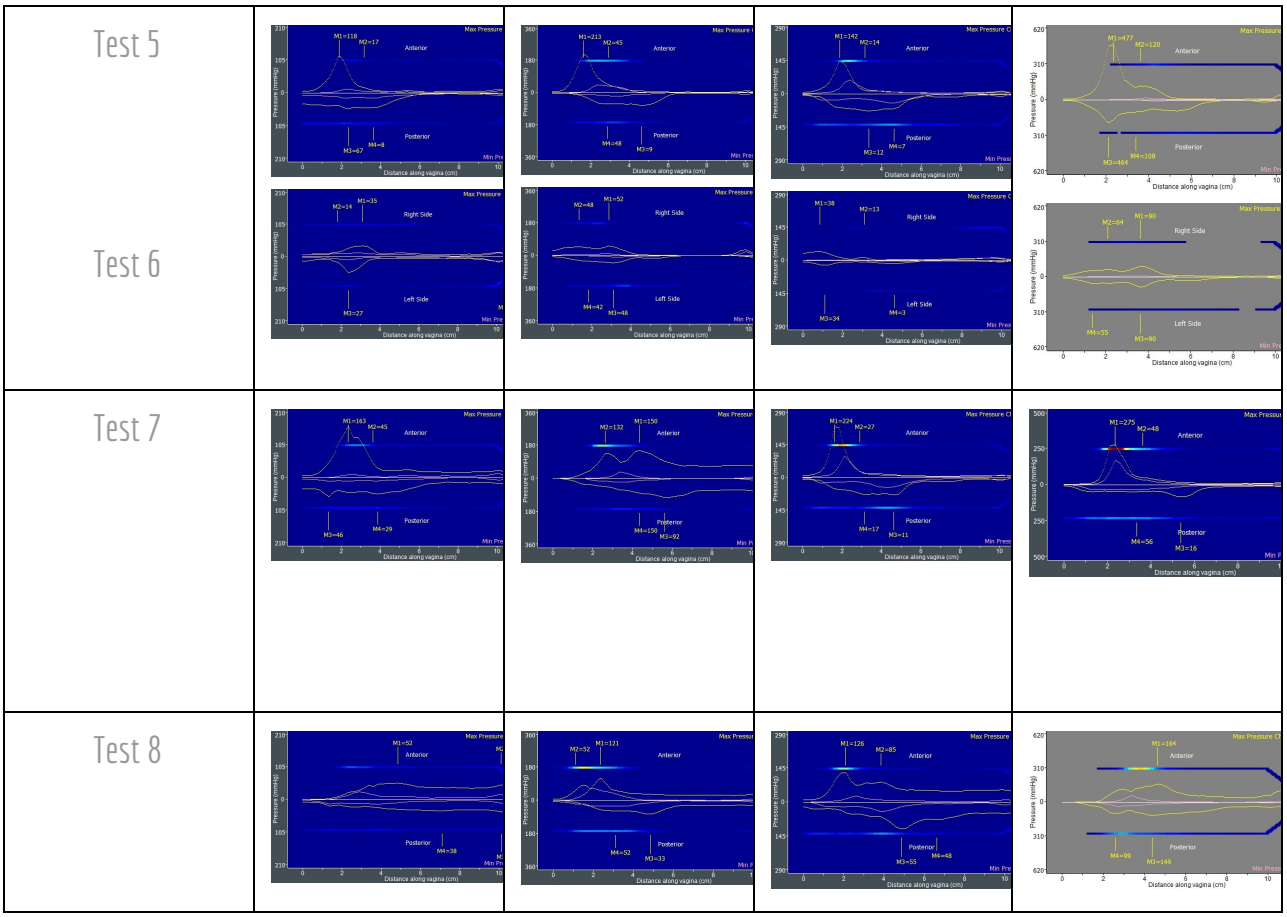

Figure 5 VTI Data acquisition for 4 patients with different pelvic floor conditions

Conclusion

Vaginal tactile imaging allows biomechanical characterization of female pelvic floor structures and tissues in vivo, which may help to optimize treatment of the local conditions such as pelvic organ prolapse, urinary incontinence and atrophy.

References

Dietz, Hans Peter, et al. “Vaginal Laxity: What Does This Symptom Mean?” *International Urogynecology Journal*, 2017, doi:10.1007/s00192-017-3426-0.

Eberhart, Robert, et al. “Exploring Biomechanical Methods to Study the Human Vaginal Wall.” *Neurourology and Urodynamics*, vol. 36, no. 2, Jan. 2016, pp. 499–506., doi:10.1002/nau.22968.

Petros, P.e. Papa. “Symptoms of Defective Emptying and Raised Residual Urine May Arise from Ligamentous Laxity in the Posterior Vaginal Fornix.” *Gynecologic and Obstetric Investigation*, vol. 45, no. 2, 1998, pp. 105–108., doi:10.1159/000009935.

Shindel, A. “Radiofrequency Treatment of Vaginal Laxity after Vaginal Delivery: Nonsurgical Vaginal Tightening.” *Yearbook of Urology*, vol. 2011, 2011, pp. 147–148., doi:10.1016/j.yuro.2010.12.028.